# Development of a Field Deployable Underwater Laser Scanning System

by

Jason Gillham

A thesis

presented to the University of Waterloo

in fulfillment of the

thesis requirement for the degree of

Master of Applied Science

in

Mechanical Engineering

Waterloo, Ontario, Canada, 2011

I hereby declare that I am the sole author of this thesis. This is a true copy of the thesis, including any final required final revisions, as accepted by my examiners.

I understand that my thesis may be made electronically available to the public.

**Abstract**

As humans seek to explore and exploit underwater environments and resources the need for tools and techniques to assist in this is critical. An important component of working in any environment is understanding dimensional information about that environment. The predominant inspection techniques in an underwater environment are sonar and video systems, However, these do not provide fine detail and often critical geometric measurements about small features and defects. Underwater laser scanners have been investigated for underwater measurements and demonstrated to operate with success; however, the current deployment options of these systems are limited. Through this thesis, an easy to deploy underwater laser scanner was developed, overcoming mechanical integration and sensor calibration challenges not previously dealt with. By integrating the laser, sensor and rotary actuator into a single housing, the calibration of the sensor is successfully maintained through multiple deployments of the scanner into a variety of applications. The developed scanner has been successfully deployed for a variety of applications, from Underwater Archeology and Biology in the Dominican Republic and Antarctica to Offshore and Inland asset inspection in the Gulf of Mexico to the Middle East and the Persian Gulf.

**Acknowledgments**

Over the past four years, I have received a generous amount of help and guidance from my academic supervisor, Dr. William Melek and my industrial supervisor Mr. Robert (Bob) Clarke of ASI Group Ltd. Both of these mentors provided insights and access to testing opportunities for the technology that allowed for the creation of a strong final product. The development of this system was done in conjunction with 2G Robotics Inc. where testing facilities, fabricating resources and electronics development skills were provided to complete the system. I look forward to continued work with 2G Robotics Inc. in commercializing the technology. Financial assistance for the completion of this thesis and commercialization of this technology were provided by a number of organizations. I would like to thank IRAP, OCE and Precarn for contributing financially toward the creation of this technology.

Most importantly I would like to recognize both my immediate family, specifically my parents, for their encouragement throughout the past four years and also my girlfriend and her parents for their tremendous support of my ambitions. Without their support my ideas could not have been realized.

# Table of Contents

# List of Figures

# 1 Underwater Technology Background

## 1.1 Introduction

Underwater technology has been developed over the ages, with some of the oldest dating back centuries, as humans ventured to explore the unknown. Some of the oldest technologies are methods to allow humans to propel themselves further with hand and foot webbing. Once further travel was limited by air supply, humans began to create advances through wooden snorkels and wooden diving bells which are basically air-filled inverted buckets used to hold air as someone moves around on the sea floor. Once humanity was able to investigate the sea floor, using what was discovered for food and other purposes was attempted and tools to assist with this started to be developed. With the development of metals and welding, pressure vessels were created allowing for storage of compressed air and the development of SCUBA systems (Self Contained Underwater Breathing Apparatus). In addition, through wars, the use of submarines which allowed people to remain underwater undetected for long periods of time became of significant strategic importance. As humans attempted more and more in the underwater environment the development of additional technologies for working in these environments were necessary. Military has been a significant early driver of marine technology but in today's geopolitical climate, the need for technology to assist in offshore oil production is the driving force behind many modern developments. As humans strive deeper into harsh environments the need for technologies to work in these locations increases. The fabrication of significant structures that deal with water both inland and offshore is a testament to the dependency

that humans have toward water and all we can do with it. The creation of massive ships and hydroelectric dams to major aqueducts and offshore oil infrastructure feed our modern societies' needs. These submerged assets are critical for many industrial applications from municipal potable water to hydroelectric power generation and shipping to offshore oil and gas. Inspection and maintenance of these assets is critical to their longevity and public safety. The inspection of these assets is often challenging and too dangerous for humans to perform due to significant pressures in deep water, or restricted access such as potable water aqueducts. Costs of inspections can also be significant when the asset must be removed from the water such as inspection of ship propellers. The solution has been robotic vehicles equipped with a variety of sensors to allow for control and data transmission to the surface. For example, a SeaEye Falcon ROV can be seen in Figure 1.1 below.

*Figure 1.1: Seaeye Falcon ROV*

Through a combination of visual inspection using cameras and dimensional inspection using sonar, asset owners will make critical decisions regarding allocation of funds for the repair of their asset. These methods are employed in all offshore installation and inspection efforts such as the recent oil spill in the Gulf of Mexico. However, using these methods, decisions are often being made with incomplete information, limited by the quality of data

obtainable with commonly used technologies: Sonar and Video.

## 1.2 Problem Definition

The objective of this thesis is to develop and demonstrate the capabilities of a commercially viable underwater laser scanner capable of obtaining a more complete understanding of the submerged asset than either of the common alternatives (sonar and video). An inspection method that is capable of high precision underwater modeling that can capture measurements unlike video and is not effected by the spreading of sound underwater like sonar would be ideal for measuring small defects. Terrestrial laser scanners provide this solution; however, there is a need for underwater laser scanning that can be easily deployed by underwater robotic vehicles.

## 1.3 Objective

This technology will allow asset owners to have a more complete understanding of their asset when making important decisions. This further level of detail means that owners can be less conservative with their assumptions, resulting in the possibility that the asset can be certified for operation for a longer period of time than it otherwise would have been. Another benefit to this technology is the ability to access a damaged area and fabricate bracing or other means of retrofitting with certainty about the dimensions of the damaged section. An easy to deploy laser scanner for obtaining high precision underwater measurements will provide useful additional information to engineers and asset owners inspecting and assessing underwater assets. With this more complete understanding of their assets, more cost effective decisions can be made.

## 1.4 Thesis Contributions

This thesis addresses the unavailability of an underwater laser scanning system capable of being calibrated once and then being deployed into the field. This is accomplished through the completion of the following novel contributions:

- Developing a single mechanical housing incorporating an actuator, the laser and the sensor.
- Developing a calibration method that is repeatable and does not need to be re-performed in the field.

## 1.5 Thesis Organization

In Chapter 2 a review of existing literature in the area of underwater laser scanners is presented. It is determined that a number of laser scanning systems have been developed. However, the systems that have been developed have deficiencies preventing the technology from being commercially deployable. Design of underwater laser scanning focusing on optical mechanical and processing aspects of the design are presented in Chapter 3. Chapter 4 reviews factors that impact the performance of an Underwater Laser Scanner and demonstrates through a case study how these impact the Underwater Laser Scanner developed through this thesis. Chapter 5 addresses the wide range of applications that the underwater laser scanner can be used for and provides example results from each. The conclusions and future development discussed in Chapter 6 address that the Underwater Laser Scanner that has been developed is a viable tool for easy commercial deployment.

# 2 Underwater Measurement Technologies

Over the last four decades the use of lasers for subsea measuring has been investigated. As early as 1966 lasers were studied in an underwater environment when Angelbeck studied the Application of a Laser Scanning and Imaging System to Underwater Viewing [1].

As infrastructure ages the need for engineers to have an increased level of understanding of the defects in their infrastructure is needed. Three main types of underwater measurement systems have been investigated (sonar, video and laser) to understand the capability of laser for providing an increased level of detail beyond traditional sonar and video techniques.

## 2.1 Existing Common Underwater Inspection Technology

Video and sonar are the most common inspection techniques as they are highly complimentary, as shown in [1 through 5]. Video is a high information bandwidth method allowing people to very quickly and with good detail understand what is right in front of them. Sonar has the benefit of transmitting further in water than light, as shown by [9 through 12], but it does not provide as defined an environment representation as laser nor does it provide the environment representation with as high an update rate. Almost every underwater robotic system is equipped with a video camera for close range navigation and inspection [6] and a sonar for longer range obstacle avoidance and measurement. [8] [9]

### 2.1.1 Video

The most common style of underwater vehicle are Remotely Operated Vehicles (ROVs). These systems consist of a neutrally buoyant and naturally stabilized platform (through

buoyancy distribution) as well as a number of thrusters to control the vehicle as described in [13] [14]. As the name would suggest these vehicles are human controlled from the surface. Power and telemetry is passed through an umbilical linking the vehicle to the control console operated by the pilot. Cameras are incorporated into all commercially available ROVs and the imagery collected with these cameras, or other additional cameras mounted to the vehicle, can be used for vehicle navigation as well as inspection of the objects being observed. A Video Ray ROV can be seen below in Figure 2.1.


*Figure 2.1: VideoRay Pro4 ROV*

Video imagery is very good for quickly conveying a preliminary understanding of underwater assets but without significant additional processing it is incapable of providing meaningful quantitative information regarding the geometry of the objects being observed as presented by [15] and [16]. Even with processing of the imagery into a 3D model, the geometry of the model is not as reliable in all situations compared to data that can be captured with a laser scanner demonstrated by [17].

A benefit of video is the relatively high sample rate. An understanding of an environment can be obtained by a camera far more quickly than a laser or sonar scan can obtain distances measurements over the same region. This speed of acquisition allows cameras to be more reliable on platforms that are susceptible to motion.

A number of problems exist when collecting underwater video. As presented in [18], [19] and [20], these include distortions due to the index of refraction of the water, particles in the water and the non-uniform spectral absorption of light through water. In the next sections these topics are discussed in greater detail.

#### 2.1.1.1 Refraction Distortion

Refraction of light as at travels from one translucent medium to another is described by Snells Law according to the equation defined in equation 2.1 Error: Reference source not found as presented in [21].

$$\frac{\sin(\theta 1)}{\sin(\theta 2)} = \frac{n2}{n1} \quad (2.1)$$

Where n1 and n2 are the index of refraction of air and water respectively and Θ1 and Θ2 are the angles between the ray and the normal of the air-water interface shown in Figure 2.2.

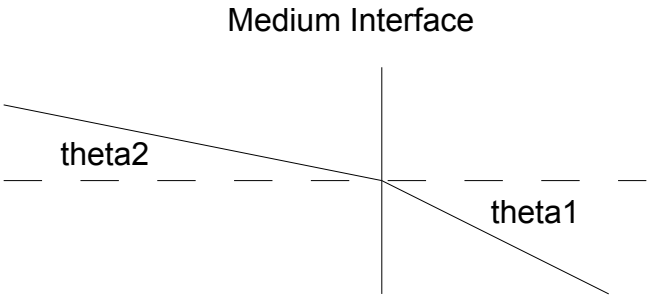


*Figure 2.2: Snells law depicted by the solid line light ray angle changing at the vertical medium interface with respect to the dashed line normal to the interface.*

When imaging underwater, distortions arise due to the air-water interface. The distortion results in the appearance of a zoomed image as the effective focal length of the optical system has been lengthened as shown by [20]. In addition the air-water interface results in a blurred image shown by [18].

#### 2.1.1.2 Effect on Focal Length

The effect on the focal length of the air water interface is the result of a reduction in the field of view of the optical system. The principal rays passing through the camera lens and then through the interface between mediums are bent toward the normal of the interface surface. Thus when viewing through a flat optical port, objects appear closer and larger than they are when viewed in air. One method presented by [20] to overcome this challenge is to use a spherical port where the principal point of the natural lens is located at the center of the sphere. Thus the principal ray for any point on an imaging surface does not observe any refraction as it passes through the interface.

#### 2.1.1.3 Effect on Focus of the Lens

The focus of an imaging system is measured by the size of the circles of confusion. A circle of confusion is the area over which light reflecting from a single point has an influence on an imaging plane. Using a simple pin hole camera model, Figure 2.3 below demonstrates how an imaging surface that is improperly positioned relative to an optical system can result in circles of confusion (observed as fuzzy, out of focus images) as presented in [22].

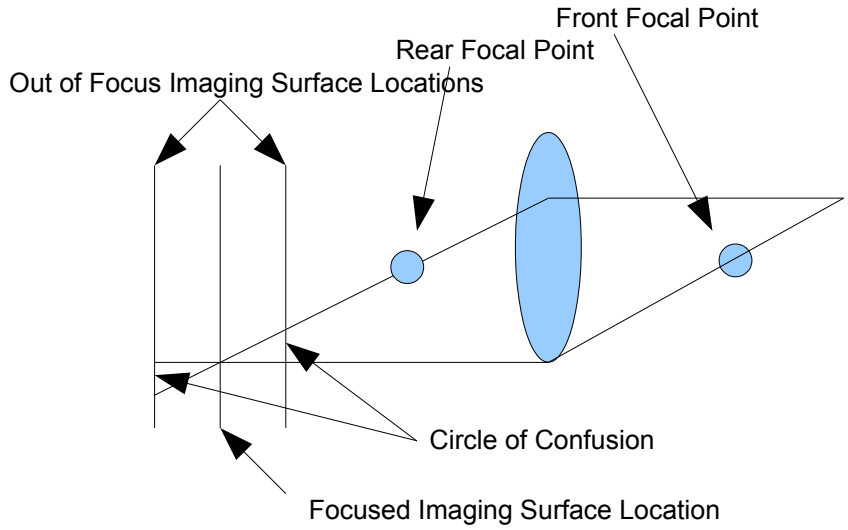


*Figure 2.3: The path of the light through the focal points and the lens should ideally focus on the Focused Imaging Surface. If the imaging sensor is on a plane other than the Focused Imaging Surface then blur is the result of the Circles of Confusion.*

When the light must first pass through a water to air interface before entering the natural lens, the light is refracted by a non-linear magnitude as a function of the angle off the principal direction of the camera. As a result, the points on a planar surface in water being imaged from the air do not focus to a planar imaging surface, as seen in Figure 2.4.

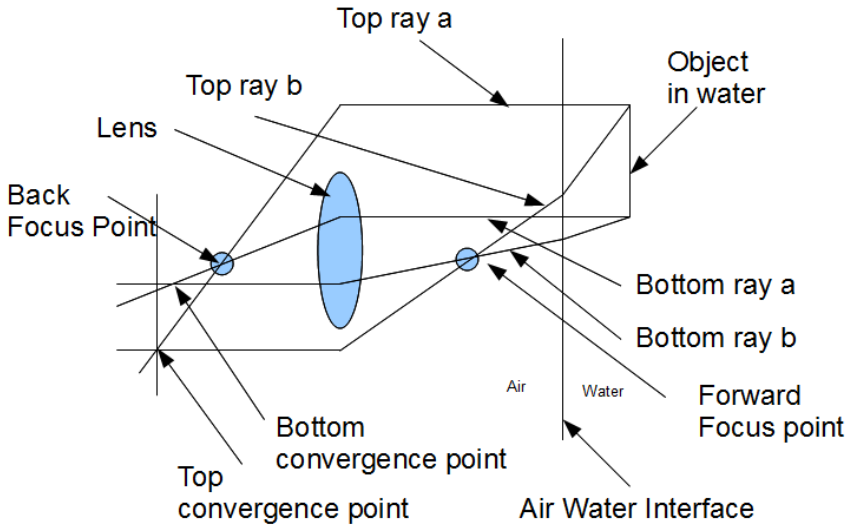


*Figure 2.4: The object in the water represented by a vertical line passes through the air water interface before passing through the lens. It can be seen that due to the distortion of the air-water interface the Top convergence point and Bottom convergence point do not lie on a common plane. This results in a focus error.*

To solve these issues, specially designed lenses presented in [20] are made to counter the effects of the non-linear refraction and the modified focal length.

#### 2.1.1.4 Particles in the Water

Not only is light reflected back from the surface being imaged, it is also reflected back from particles floating in the water. The light reflected back from floating particles is referred to as optical back-scatter and can obscure an image significantly. In many underwater industrial environments where imaging is used, such as inside tunnels, artificial lighting is used. The configuration of this lighting can significantly reduce the amount of back-scatter being observed by the optical sensor as described by [5],[23].Ideally, by configuring the lights to only illuminate the surface that the sensor should be imaging, only light reflecting from that surface will be observed. In reality, the artificial lighting must pass through the water and thus it illuminates these floating particles. To minimize back-scatter when designing an imaging system, the common volume between the field of view of the camera and the field of view of the lights must be minimized as illustrated in Figure 2.5.

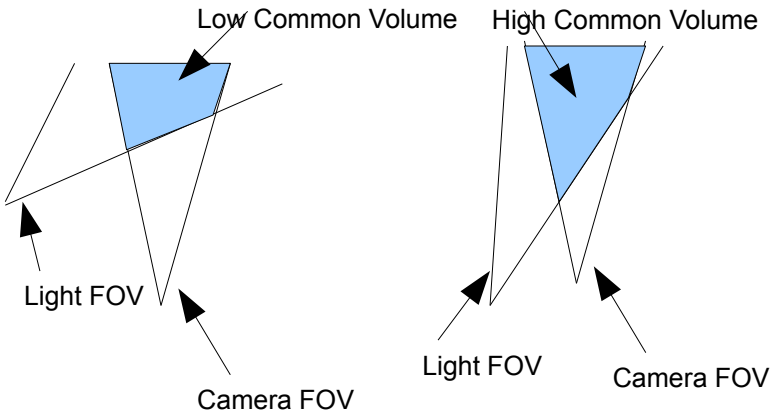


*Figure 2.5: The back-scatter resulting from particles in the water is far smaller when there is a small common volume between the Light Field of View and the Camera Field of View.*

By reducing the common volume between the camera and the light and assuming that there is a uniform distribution of particles in the water, the back-scatter will be reduced as discussed by [39].

#### 2.1.1.5 Light Transitivity Through Water

As electromagnetic waves, including light, travel through any translucent medium the strength of the signal is reduced due to attenuation. Electromagnetic transmisivity is described by the Beer-Lambert law presented in [25].

$$T = I / Io = 10^{(-e \times l \times c)} \quad (2.2)$$

Where I is the end of path intensity, Io is the start of path intensity, e is the Molar Absorptivity, l is the Light Path Length, e is the Molar Absorptivity and c is the Absorption Coefficient.


*Figure 2.6: This plot shows the absorption of light in water as a function of the wavelength of the light. Light around 400nm has the lowest absorption / greatest transmisivity through the water.[28]*

As shown in Figure 2.6, the absorption coefficient for light through water is a function of the wavelength of the light, resulting in less red light and more green and blue light reaching a target relative to the strength of the light at the source. As a result, images are shifted to the blue green spectrum. To correct for this a colour balance and contrast enhancement is performed on underwater images in [23] to allow for higher contrast viewing.

### 2.1.2 Sonar

Both active and passive sonar are used in underwater environments. Passive sonar is utilized for detecting and locating objects underwater that are emitting an acoustic signal. With passive sonar, the detection system does not emit any acoustic signals, as described in [27]. Active sonar systems emit an acoustic signal and then record the amplitude of the return signal as a function of time. The acoustic signal propagates through the water and reflects off of the surrounding environment as discussed in [26]. Based on the time taken for the acoustic signal to propagate from the emitting source to the target and back to the transducer as well as the speed of sound in water, the distance to the reflecting surface can be calculated. Sonars which collect dimensional information in a similar manner to the laser scanner are active.

For underwater sonars the precision of the sensor is based on the size of the acoustic footprint. The acoustic footprint is the area over which an acoustic signal reflects. As described in [12], high precision active sonars use large diameter, high frequency transducers to reduce the beam divergence of the acoustic signal. A large beam divergence results in a greater acoustic footprint on the target surface. A smaller acoustic footprint

allows for higher precision measurements to be taken. Beam divergence in a given direction is inversely proportional to the dimension of the transducer in that same direction. For example relatively small circular transducers will have high beam divergence compared to relatively large transducers. This characteristic is also useful for creating specific beam shapes. A common transducer shape is rectangular, producing a fan shaped acoustic pulse. The four main styles of active sonars are based on the shape of the acoustic beam they emit as described by and how the reflected signal is captured and processed [40].

#### 2.1.2.1 Profiling Sonar

A profiling sonar incorporates a single circular transducer which is mechanically oriented in multiple directions to build a map of the environment. In many cases these system only have a single actuator which rotates the transducer, providing a profile of the environment normal to the axis of rotation. Systems do exist with multiple actuators which can direct the transducer in any direction to build a 3D map of the environment.

#### 2.1.2.2 Imaging Sonar

An imaging sonar is similar to a single axis profiling sonar, however the transducer is rectangular rather than circular. The rectangular transducer is oriented such that the acoustic beam propagates with a far larger beam angle in the vertical direction compared to the horizontal direction and the transducer is rotated about the vertical axis. At a given transducer rotation angle acoustic energy is reflected from all surfaces within the vertical swath. When visualizing the data from this sensor, a polar plot is generated, colorizing the plot at each distance based on the intensity of the return signal. Thus, with measurements at

multiple angles a top down view of the environment is created. This is particularly useful for navigation, as all objects within the vertical swath are sensed with relatively high angular precision.

#### 2.1.2.3 Side Scan Sonar

The transducer of a side scan sonar is similar to that of the imaging sonar in that a fan shaped acoustic pulse is generated. However, the transducer is not mechanically rotated, rather it is linearly translated and each line of data is joined to create the single plot. This style system is typically used for searching for objects on the sea bed.

#### 2.1.2.4 Multi Beam Sonar

A multi beam sonar emits an acoustic pulse and through beam forming focuses the acoustic energy onto receivers. The resulting data is similar to an imaging sonar however no mechanical scanning is required.

#### 2.1.2.5 Acoustic Noise

Acoustic noise from alternate sources can impact the ability to collect quality data. Distance measurements from acoustic sensors are based on the time of flight for an acoustic pulse. In order to accurately determine the location of the sonar contact, the sensor must be able to process the amplitude of the return pulse and identify the time that a peak amplitude is captured. When the acoustic sensor is recording noise from alternate sources it is possible to incorrectly determine the time of the return pulse resulting in incorrect measurements. Methods for accounting for the various sources of noise are presented in [41] [42] and [43].

#### 2.1.2.6 Acoustic Footprints

An acoustic footprint as described by [28], [29] and [30] is the area from which an acoustic pulse is reflected. This footprint can be sizable and result in measurement distortions. A prevalent case is the measurement of curved objects. Acoustic signals will catch the edge of these structures and a return pulse will be obtained at an incorrect angle. This is demonstrated in Figure 2.7 below. In the Figure 2.7 above the dots represent the calculated location for each point. The edge of the wide acoustic signal catches the edge of the corner and a reflection is sent back to the transducer and based on the time of flight and the mean angle of the acoustic pulse the position of the contact is calculated. Since the point of sonar reflection is not in line with the mean angle for the pulse, the contact point location is incorrectly calculated. The incorrectly calculated points result in misinterpretation by sonar at the edges of objects.

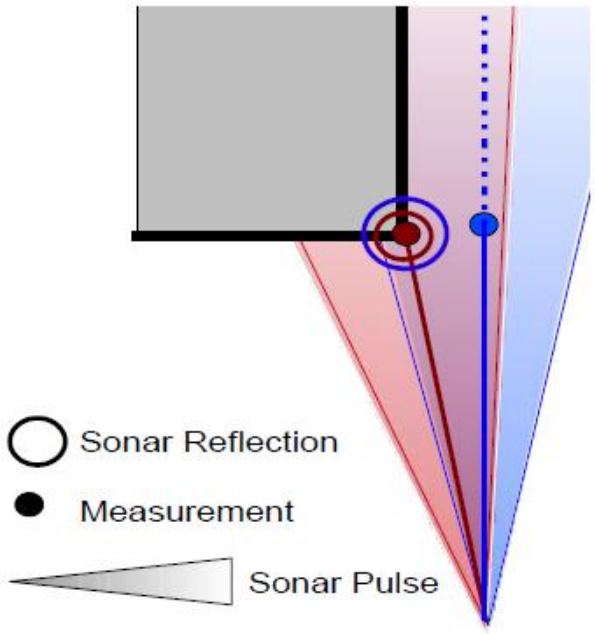


*Figure 2.7: Sonar Footprint*

## 2.2 Underwater Laser Scanners

The use of laser scanning to obtain high resolution dimensional information about an environment is well developed for terrestrial applications. The use of laser scanners in an underwater environment is not new, however, as of yet underwater scanners have not been widely adopted.

Analogous to active sonar ranging, the underwater laser measurement systems reviewed [31 to al] emit an optical signal that is reflected from the target surface and captured by the sensor. The advantage to using laser scanners is the significantly smaller signal footprint contacting the target surface compared to sonar ranging. However, optical signals attenuate far more quickly in water than acoustic signals. Attenuation of optical signals result from three factors: molar factor, transmission distance and absorption coefficient. As a result of this attenuation, the signal to noise ratio at increasing distances and with increasing water turbidity is significantly degraded.

The three main differentiating aspects of the reviewed systems are the housing configuration, the calibration approach and the data transmission protocol.

### 2.2.1 Existing Underwater Laser Scanner Configurations

The laser scanners reviewed in [31 to 38] have a multiple housing design consisting of one or two cameras and one or two laser light sources. As described in [31,33,34] systems can provide a single distance measurement or as described in [36,37,38] the laser scanner can use optics to generate a line of laser light and using a 2D CCD collect a complete profile of points. All of the reviewed systems use a two housing design where the camera and laser

are mounted into separate housings and are attached to the deployment system independently. By mounting each housing independently, for each deployment of the system, a new geometric calibration is required in the field.

### 2.2.2 Existing Underwater Laser Scanner Calibration Methods

Methods based on single point ranging, [36,37,38], are calibrated by taking a variety of readings at known distances and interpolating the results when the scanner is in operation. Presented in [33], a calibration method is described using multiple known points and a radial lens model to undistort the points. The relative positioning between the laser and the sensors are based on the design parameters except for in [32] where a textured surface is used in conjunction with the imaging sensor to accurately model the spacing between the laser and the camera for use in calculating the ultimate contact point.

### 2.2.3 Data Transmission Protocol and Processing

All the laser scanner systems reviewed use analog video, digital video or digital still imagery as the data that is transmitted to the surface for processing. The processing of this data is then performed at the surface in either real time or through post processing.

## 2.3 Summary

Underwater laser scanners have benefits over sonar and video in cases where measurements are required, there is a low level of silt in the water and the ambient light in the environment is minimal. The need for a new system calibration each time the separate laser and camera housing is mounted to the vehicle make it an undesirable solution for regular use outside of the laboratory environment. For commercial acceptance, developing a

system that is easily interfaced with existing ROVs RS-232 or RS-485 communications ports and is easily deployable and robust is critical. To facilitate these criteria, a single housing design is ideal with internal processing circuitry, however, when minimizing the size of the scanner mechanical and sealing constraints arise. This thesis addresses these challenges by packaging the laser and sensor into a single rugged underwater housing

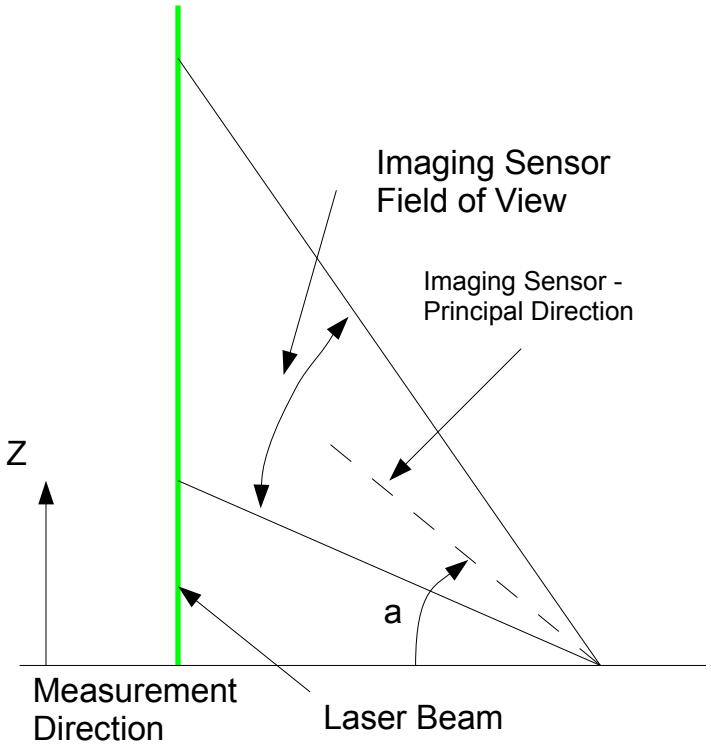


*Figure 2.8: Basic Photogrametric Laser Ranging System showing the camera field of view intersecting the emitted laser line.*

capable of being calibrated once and then deployed into a wide range of environments.

# 3 Design of Laser Scanning System

To create a system that is commercially viable it needs to be easy to operate. A key component of this is the ability to avoid in-field calibration as is required by the systems presented in the literature. To overcome this difficulty, a housing design integrating the actuator, the laser and the optical sensor is developed. In this chapter, the design of the system is discussed. To reach the ultimate design based on photogrametric triangulation of the laser line, a variety of laser ranging techniques are described in greater detail and the benefits and drawbacks of each are discussed. The calibration and data processing method is described outlining how the laser and sensor alignment is determined and how this is then used in conjunction with the rotary actuator to determine the 3D point cloud representation of a target surface. The design and implementation of the scanner is focused on maintaining a compact system contained within a single housing constructed from multiple sealed components. The four key aspects to the laser scanner design are:

- optical design
- mechanical housing design
- electronics circuitry (not covered in the scope of this thesis)
- calibration and processing

The engineering specifications of the system are provided in Appendix D.

## 3.1 Optical Design

The optical design of the laser scanner covers the distortions associated with the air to water interface as the light passes into the optical sensor, and covers the types of available

laser ranging techniques.

### 3.1.1 Types of Laser Ranging

Three laser ranging techniques were considered. These are a time of flight method, a phase shift method and a photogrametric technique as presented in [45].

### 3.1.2 Time of Flight Method

Scanners employing the time of flight method emit a pulse of laser light toward the target surface. A portion of this light is reflected back to the collector and based on half the time of flight divided by the known speed of light, the distance to the object is calculated. This technique works well for longer range measurements and can only capture a single point at a time.

### 3.1.3 Phase Shift Method

Scanners employing the phase shift method emit laser light with a sinusoidal intensity with respect to time. The reflection returns to the sensor with a sinusoidal intensity and for each measurement location the system determines the phase shift between the emitted and reflected signal. Based on the phase shift and the speed of light the distance to the target is calculated.

### 3.1.4 Photographic Method

Scanners employing the photogrametric method emit a beam of laser light onto a surface and, with an imaging sensor, observe the reflected light. Based on the angle at which the light is reflected back to the imaging sensor, the contact point between the laser light beam and the contact surface is calculated.

## 3.2 Laser Ranging Technique Selection

Of the three popular laser ranging techniques, implementation of a system employing a photogrametric measurement technique was selected based on the results of past work. These works outline the benefits of this technique for dealing with turbidity in the water when processing the return signal. The key parameters for the optical design were the angle of the imaging sensor, the baseline distance between the imaging sensor and the laser emitter and the field of view of the optical sensor. A representation of a basic photogrametric laser ranging system is shown below in Figure 2.8.

The green line represents the laser and the angle 'a' represents the principal direction of the optical sensor. The two lines on either side of the principal direction of the optical sensor represent the field of view of the sensor. If the laser light is reflected off of a surface within the sensor's field of view, it will be detected by the sensor. Based on the Z distance of the contact between the target and the laser line, the location at which the reflected light will appear on the CCD will change.

## 3.3 Optical Sensor

A Sony ICX228AL CCD sensor with a 2.7mm M12 lens is used to capture the reflected light. The sensor data sheet is attached in Appendix A. Based on the location of the reflected light on the CCD the angle at which the light entered the sensor can be determined. To properly determine the angle at which the laser light entered the CCD, a number of lens parameters must be accounted for. These include:

### 3.3.1 Radial Distortion

Radial distortion of a lens is a function of the radial position of the pixel on the CCD. The lenses tend to shift pixels radially in a non-linear manner, resulting in barrel or pin-cushion distortion.

### 3.3.2 Tangential Distortion

Tangential distortion is caused by the lens not being completely parallel to the imaging sensor.

From imaging system calibration, a lens model is determined to define the location of the pixels, were an ideal (pin-hole) lens used. The equations representing the model are shown below in equation 3.1 and equation 3.2 for radial and tangential distortion respectively.

$$\begin{aligned} x_{corrected} &= x\left(1 + k_1 r^2 + k_2 r^4 + k_3 r^6\right) \\ y_{corrected} &= y\left(1 + k_1 r^2 + k_2 r^4 + k_3 r^6\right) \end{aligned} \quad (3.1)$$

Where, (x, y) is the original location (on the imager) of the distorted point and (xcorrected,ycorrected) is the new location as a result of the correction. k's are calibration constants and r is the radial distance of a point from the center of the image.

$$x_{corrected} = x + [2\,p_1\,y + p_2(r^2 + 2\,x^2)]$$
$$x_{corrected} = y + [\,p_1(r^2 + 2\mathrm{y}^2) + 2\mathrm{p}_2\,x\,] \quad (3.2)$$

Tangential distortion is minimally characterized by two additional parameters, p1 and p2. Based on the corrected x,y location of the laser contact with the CCD, the angle  at which the laser light entered the CCD is determined using standard image processing algorithms.

## 3.4 Point Locating Algorithm

Using the ray of light at enters at a known angle based on the CCD contact locationand the known origin (principal point of the lens), the ray is traced through 3D space from the air to glass interface of the port and then from the glass to water interface. By calculating the contact point between the laser plane and the ray exiting the port, the location of the contact between the laser beam and the target surface can be calculated.

The system presented uses a complete plane of laser light to illuminate the target surface and thus multiple pixels of laser light are located. The image below in Figure 3.1 is a full image captured by the CCD.

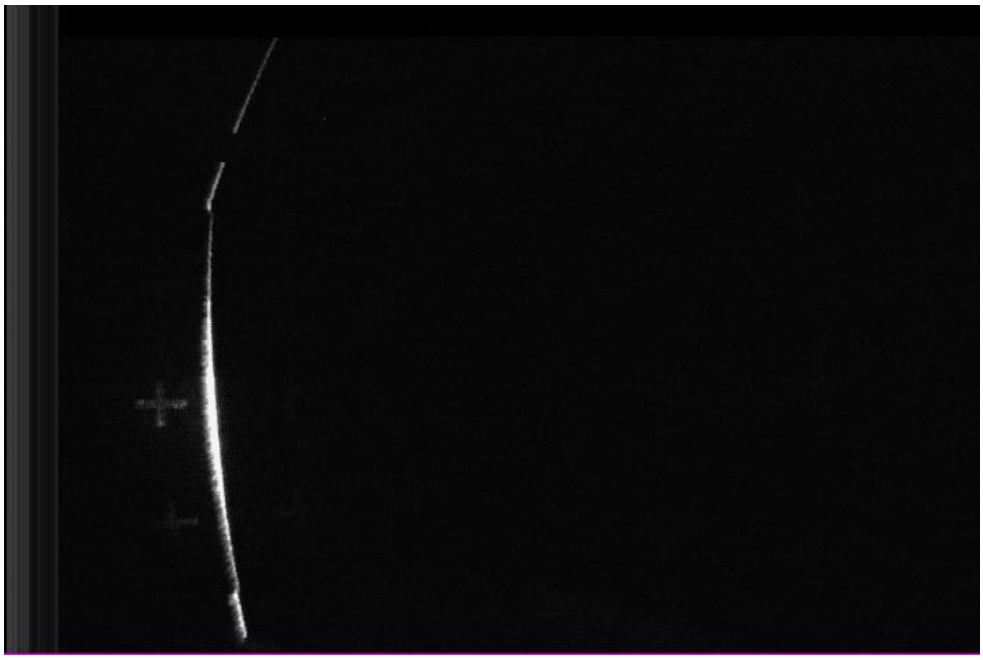

*Figure 3.1: Picture captured with the CCD image senor showing the laser line in the image.*

With the laser fixed in position, a number of points can be processed along the laser plane however only a single profile can be measured. By sweeping the laser plane over multiple angles, a full cloud of distance measurements can be made resulting in a 3D representation of the target surface.

### 3.4.1 Laser Stripe Generator

The laser integrated into the scanner is an unbranded OEM green 5mw diode laser. The wavelength of the laser is 532nm. The principal of the system is for the laser light to be reflected back from the target surface and then returned to the optical sensor. Ideally surfaces should result in a perfectly diffuse reflectance such that regardless of the angle of incidence an equal amount of light is reflected from the contact point in all directions. In reality, a greater percentage of the light energy is reflected in the opposite direction from the source as shown in Figure 3.2.

*Figure 3.2: Graphical comparison between fully diffuse and partially diffuse light scattering surfaces. The left of the graphic has a red incoming ray and shows perfectly diffuse reflection with the green rays. On the right the red ray is not uniformly reflected off the surface and a majority of the light is reflected as if the reflecting surface was a perfect mirror.*

In Figure 3.2 above perfect diffusion is shown on the left and a more realistic reflection is shown on the right.

## 3.5 Drive Design

To rotate the laser plane mechanically, the scanner housing was separated into a stationary and a rotating component. The rotating component contains the laser and optical sensor in a two-part housing containing two separate optical ports. Three static o-ring seals protect the internal electronics from the external water and pressure and a single dynamic seal between the rotating and the static components is used.

Within the static component of the system a ZSS 32 stepper motor with a GPL32 gear head is used to position the rotating head compartment. The datasheet for the motor assembly is attached in Appendix A. The motor is secured to the static housing and coupled to the head of the scanner. A stepper motor was selected to simplify the control of the system and reduce backlash in the system

Ensuring that the internal housing remains water tight while allowing for rotation of the head, passing the electrical connections between the head and the stationary body, making the mechanical connection and mechanically supporting the head with a high degree of

concentricity, all within a small package is a significant challenge.

Of the four functions of the connection between the head and the body, coupling of the motor to the head must be done at the center. To accomplish this, a keyed coupler is concentrically fitted to a hole in the head with a corresponding key way.

To eliminate the need for a slip ring, wires are passed directly through the connection and thus rotation must be limited to 170deg. The wires are passed through slots in the housings past the coupler and then past the motor with a 3mm clearance gap in the direction change between the head and the body. Despite concerns about the wires binding no problems have been encountered during testing.

A standard Parker profile U-cup seal is used between the housing and the head to prevent water from entering at the joint. Seal performance is best when the two surfaces the seal is resting between are held perfectly concentric. An IGUS bushing capable of being submerged is press fit into the body directly beside the seal. Water pressure keeps the two housings together and as an additional method a collar separated by an IGUS thrust bushing holds the flange of the body against the head. The major components or sections of the scanner are indicated in Figure 3.3. A complete drawings package for the system is attached in Appendix B.

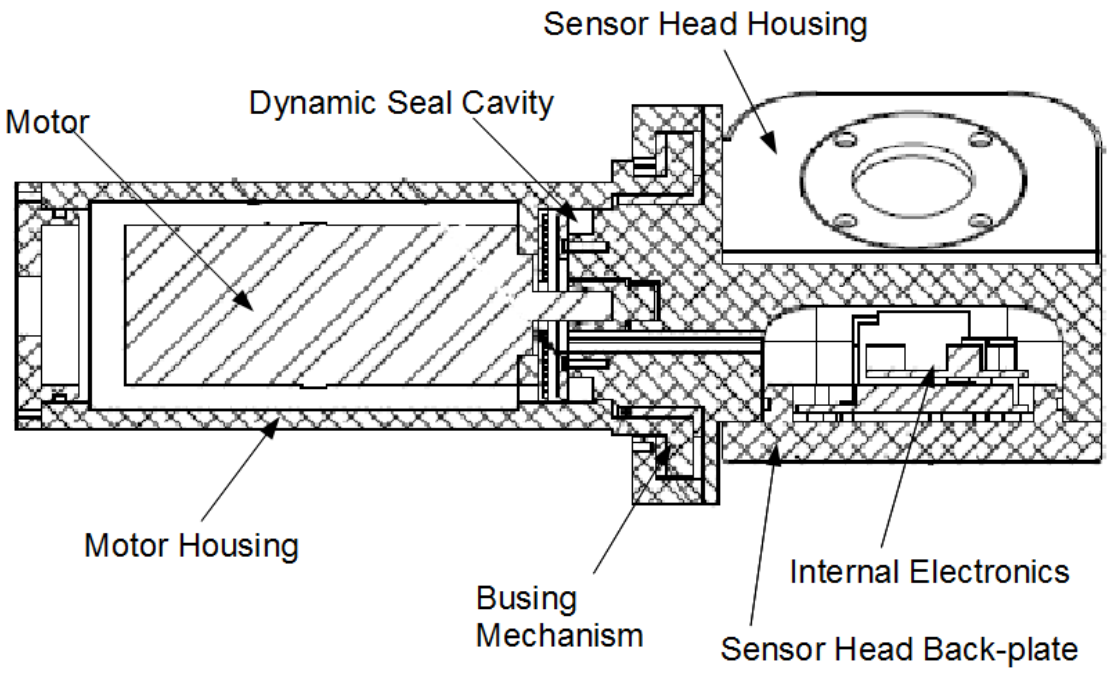


*Figure 3.3: Cross section of the Underwater Laser Scanner with Principal Components of the system indicated.*

### 3.5.1 Electrical System Functionality

The function of the electrical components is to collect the data from the optical sensor, process this data to determine where in the image the laser light is reflecting and then compressing this data to send it to the top side software through an RS-232 or RS-485 communications protocol. Secondary tasks include administering motion of the motor and turning on and off the laser beam.

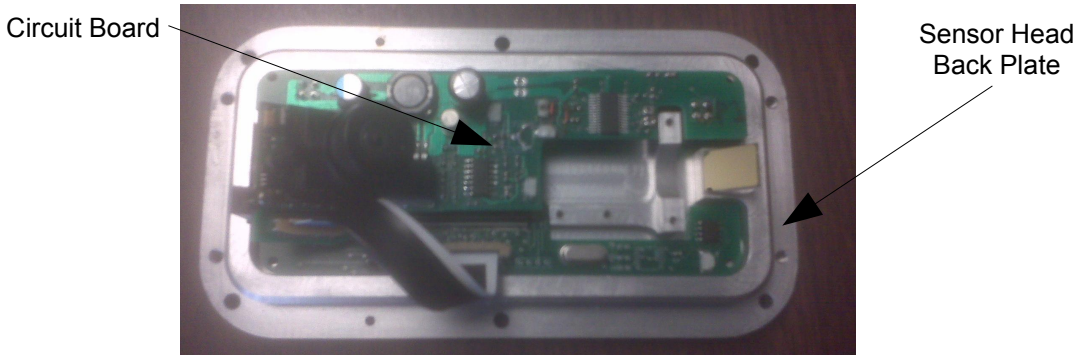


*Figure 3.4: Picture of the internal circuit board used inside the Underwater Laser Scanner*

All electronics are to fit inside of the head of the scanner however, the design of these components is outside of the scope of this project and have been completed by others involved in the work.

## 3.6 Sensor Calibration

Since the system is based on triangulation of the path of the laser light, accurately knowing the relative orientation of the laser and camera is critical for measurement accuracy.

To calibrate the system a calibration jig is used. This jig consists of a number of target vertexes identifiable by the camera. Prior to assembly of the back plate with the head of the scanner, the assembled back plate with all electronics and camera are mounted into the calibration jig. Using the Open Cv image processing library, specifically the cvFindCornerSubPix, the vertexes with known location are found in the image. By knowing the locations of these vertexes, both in the real world and on the imaging plane, the lens model and the location of the camera can be determined.

The test rig has been designed to include points in the region of interest that the laser line is to be seen. This ensures that the system is calibrated for the anticipated operation. A picture of the calibration jig is shown below in Figure 3.5.

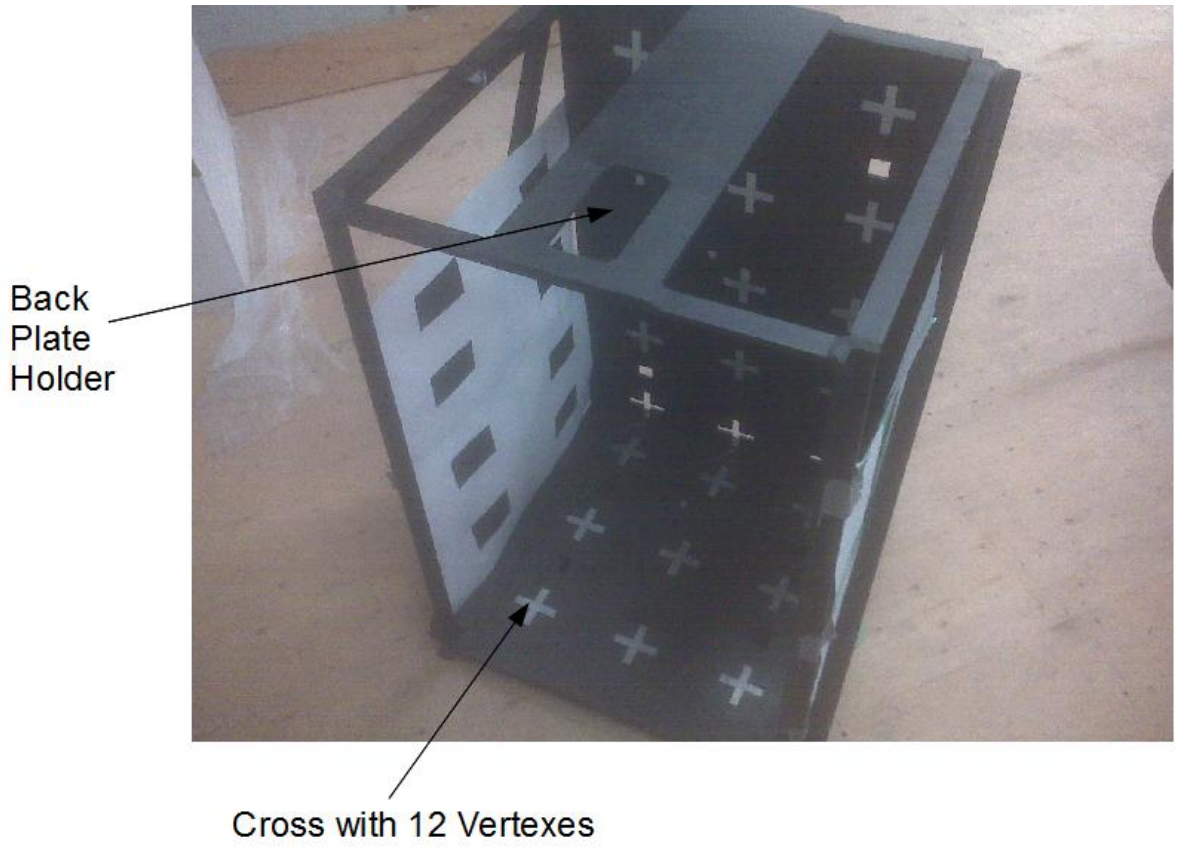


*Figure 3.5: Calibration Jig showing where the back plate is positioned during calibration and the series of crosses and vertexes at known locations for determining the orientation of the sensor and the laser.*

The sensor parameters that are determined during calibration are the intrinsic parameters for the camera and lens (lens model parameters) and the extrinsic matrix for the camera position and the laser plane normal and origin point. A dimensioned drawing of the Calibration jig is located in Appendix C.

## 3.7 Point Location Calculation

As described in the optical design, the location of the laser on the imaging plane must be converted to an X,Y,Z point in 3D space.

Three coordinate systems are used in the calculation process:

1) Camera Frame

2) Head Frame

3) Body Frame

As seen in Figure 3.6, the Camera Frame (Blue) is fixed to the principal point of the camera with the positive Z direction oriented in the direction of the target surface. The X and Y axes are aligned with the (i) and (-j) axes of the CCD respectively.

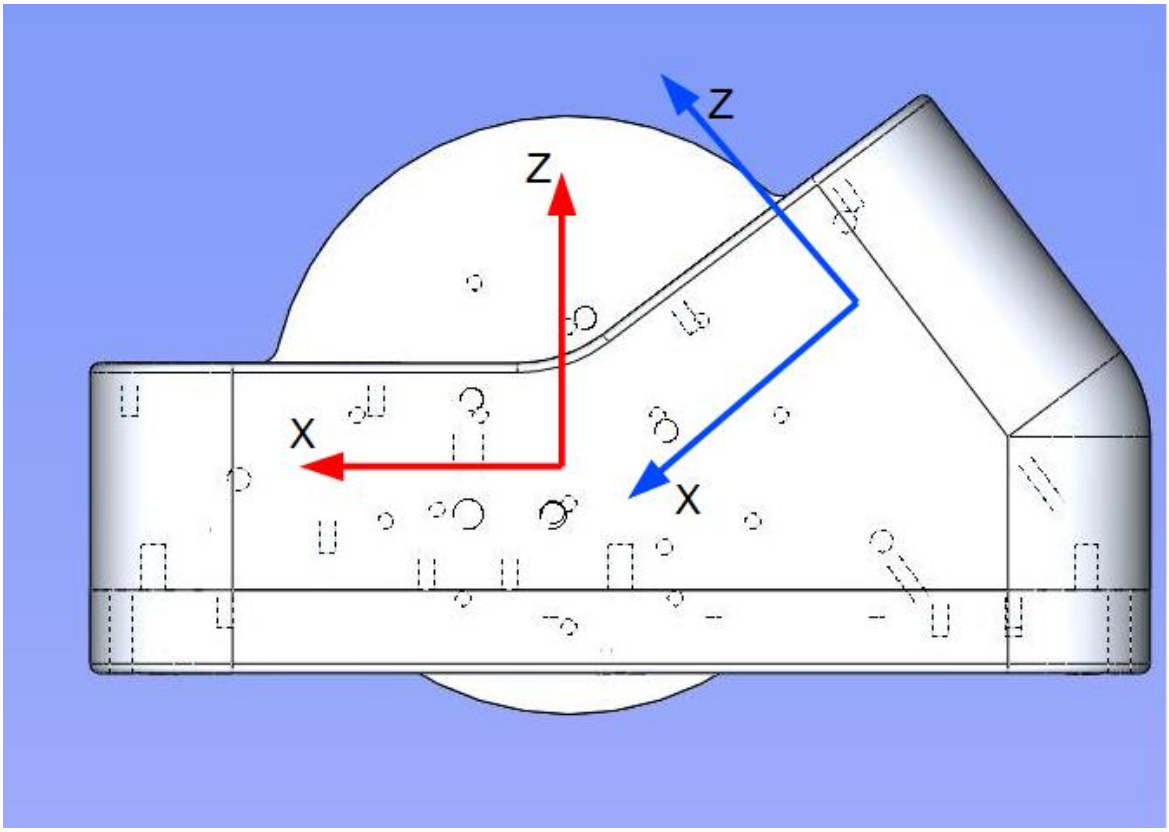


*Figure 3.6: Top view of laser scanner with the camera frame coordinates shown in Blue and the head frame coordinates shown in Red*

The Head Frame (Red), shown in Figure 3.7, is fixed along the center line of the back plate and oriented with positive z axis in the direction of the target surface and the z axis oriented toward the laser side of the system.

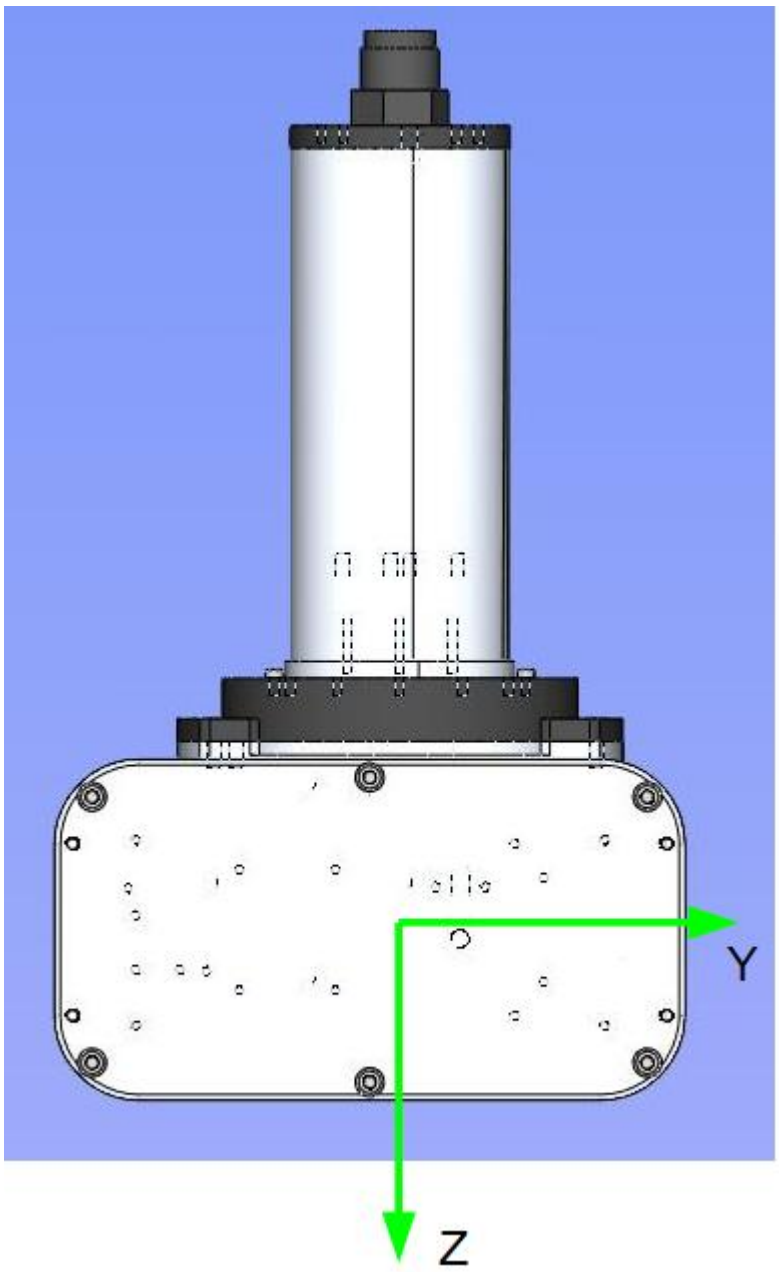


*Figure 3.7: The body frame coordinates of the laser scanner are shown in green*

The body frame (Green) is oriented such that the z axis is up and the y axis is to the left.

### 3.7.1 Converting camera points to XYZ coordinates

When calculating the location of the target, point transformations between these coordinate systems are required. Figure 3.8 contains a pictorial description of the calculation process

to convert the laser pixel location to the location in 3D XYZ space.

#### 3.7.1.1 3D Ray from Camera

The 3D ray is based on the i,j location of a located laser point in the image. Using the calibration data obtained, a focal length of the imaging system is determined. By projecting a line from the contact point of the CCD through the focal point, the ray in camera space is determined.

#### 3.7.1.2 3D Ray Through Optical Port

Remaining in camera space, the ray is refracted through the optical port (air to glass then glass to water interface) using Snells Law. A new point of origin on the glass water interface is also defined from which future ray calculations will originate.

#### 3.7.1.3 3D Ray Transformation to Head Frame

Using a coordinate transformation based on a 4x4 matrix the origin point at the glass water interface and the ray into this point from the contact between the target surface and the laser are calculated.

#### 3.7.1.4 Laser Plane and Ray Intersection

By using the equation of the laser plane determined through calibration and the known ray and origin, the pair of linear equations is solved to provide a point of commonality between the laser plane and the ray of light entering the CCD. This point is calculated in the head frame.

#### 3.7.1.5 Transformation to Body Coordinates

Using a 3x3 rotation matrix with values based on the angle of the motor, the point of contact is transformed from the head frame to the body frame. Once the point is in body frame coordinates, combining it with all adjacent points from other angles will allow for the building of a complete 3D model.

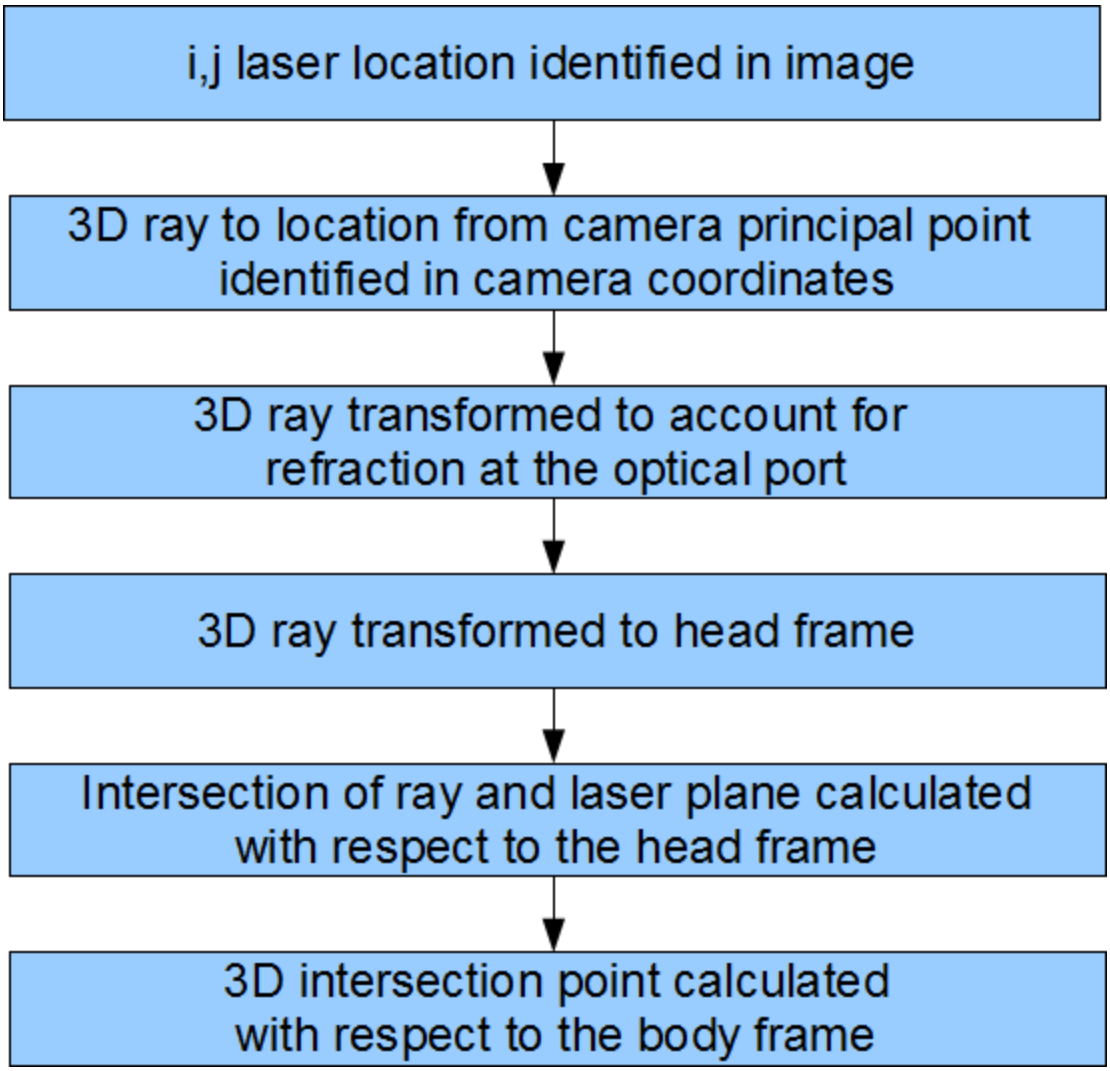


*Figure 3.8: Pictorial View of the Conversion from i,j location to 3D data point*

## 3.8 Conclusions

The design presented meets the criteria set out in Section 2, achieving an underwater laser scanner system capable of being easily deployed and without the need for in-field calibration. A trigonometric/photogrametric laser scanning approach was selected based on success using this method by others. The developed optical calibration approach is successful at determining the location of the reflected laser line. Through a series of transformations the location of the reflections in 3D space are positioned. The mechanical design for the laser scanner provides a single multipart housing allowing the sensor and laser positioning relative to each other to be maintained. Using the internal actuator, the housing very precisely rotates the head containing the laser and sensor to built the complete 3D model of the environment.

# 4 Testing and Experimental Analysis

Validation of the capability of the Underwater Laser Scanner shown in Figure 4.1 is important for understanding the usability of the system. A number of factors impact the accuracy of the system and are discussed in greater detail. Using a testing jig, scan distance measurements are taken and compared with the known values. This section describes a variety of factors that impact quality of the laser scanner data; these are demonstrated using the testing jig.

*Figure 4.1: Underwater Laser Scanner*

## 4.1 Testing Jig

To evaluate the capability of the laser scanner a jig was constructed. The purpose of the jig is to understand the accuracy of the system, and the resolution and limitations on range and

angle of the system.

The test jig was designed for the purpose of mounting the laser scanner to the jig and scanning a set of small and known features. The jig allows for measurements at a range of distances and incident angles between the laser line and the target surface. A picture of the actual test jig in the water is shown below in Figure 4.2.

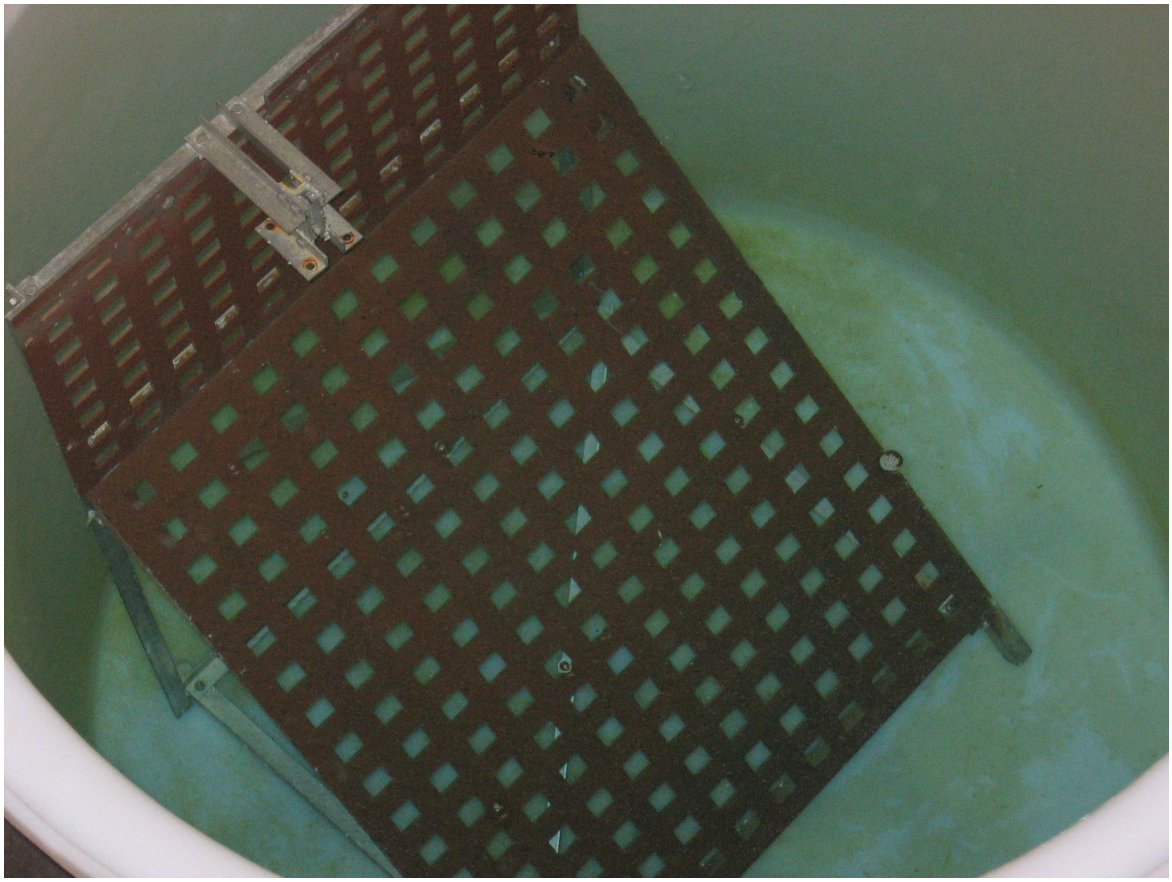

*Figure 4.2: Testing jig in small test tank full of water*

The calibration jig is fabricated using sheets of aluminum that were water jet cut with a set of 3cm by 3cm squares cut into it. By mounting the scanner to the jig an understanding of accuracy as a function of distance can be obtained. The capability of the scanner at high angles of incidence is also calculated using this jig. A dimensioned drawing of the testing

jig is included in Appendix C.

## 4.2 Influence of Range on Resolution and Accuracy

The scanner has greater resolution and accuracy at closer range. The plot below in Figure 4.3 demonstrates how small adjustments in pixel position on the CCD influence the calculated distance.

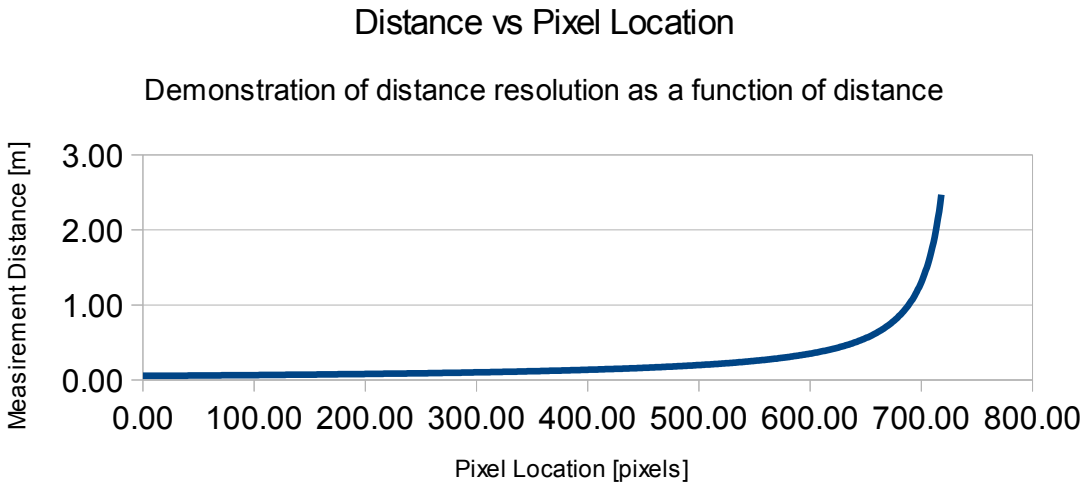


*Figure 4.3: Range vs Pixel Location on the CCD*

## 4.3 Range Limitations

In addition to the geometry of the head, range is also limited by the ability of the system to detect light reflecting from the target surface. Two main factors impact this: angle of incidence and the distance to the target.

### 4.3.1 Angle of Incidence

At low angles of incidence on realistic surfaces (surfaces that are not perfectly diffuse) the amount of light that is reflected back to the optical sensor is less than when the laser beam

has a high angle of incidence with the target surface. As a result, there is a limit to the incidence angle the scanner can make with the target surface. As the angle of incidence increases the ability to detect return signals is diminished.

### 4.3.2 Distance to the Target

The signal attenuates as it travel through the water, preventing the light from reaching the target surface and then returning to the sensor. Once the signal to noise ratio of the reflecting signal is too great it is no longer possible for the sensor to determine the angle This impacts the ability for the sensor to scan objects at a distance.

## 4.4 Test Jig Case Study

To provide some context regarding the operation of the scanner and the performance capability of the scanner the test jig has been scanned using the Underwater Laser Scanner after it has been calibrated. Using this example the performance of the system will be discussed.

### 4.4.1 Overall Scan

With the scanner fixed in place, shown in the upper left of Figure 4.2, a scan was captured. The resulting scan data is shown below with each point colored based on the intensity of the reflected signal.

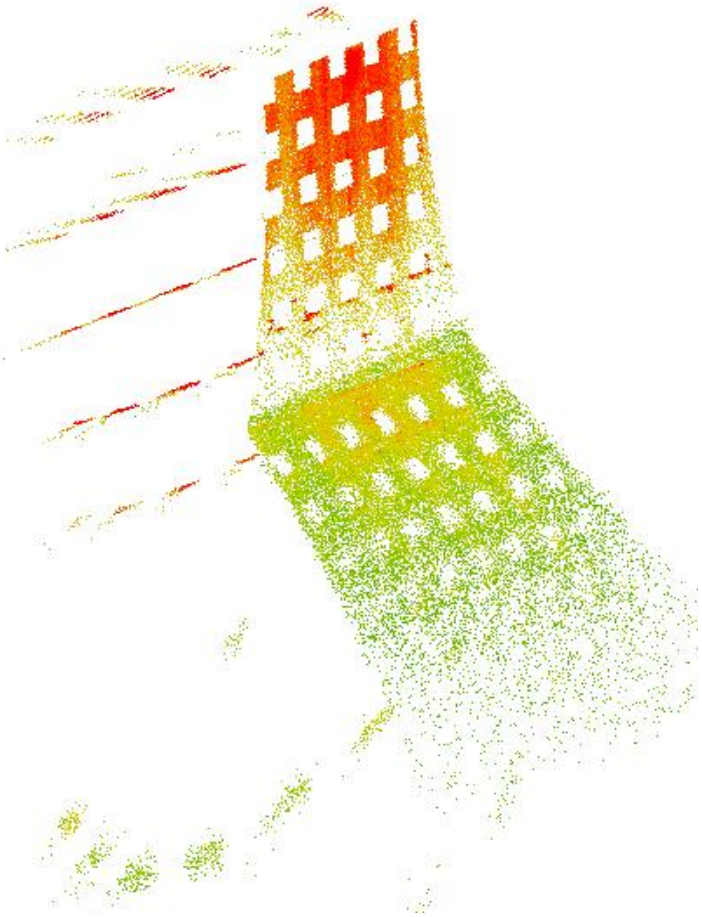

*Figure 4.4: Test Jig Scan with red as high intensity returns and green as low intensity returns*

Using this data, the effect that the distance to the target has on the intensity of the return can be observed.

### 4.4.2 Range vs. Intensity of the Return

As the distance to the target increases, the intensity of the reflected signal decreases. This is due to the increased path length between the laser and the target. This increased distance results in the laser signal spreading and thus having less light per unit line length and more light being absorbed by the water as it travels.

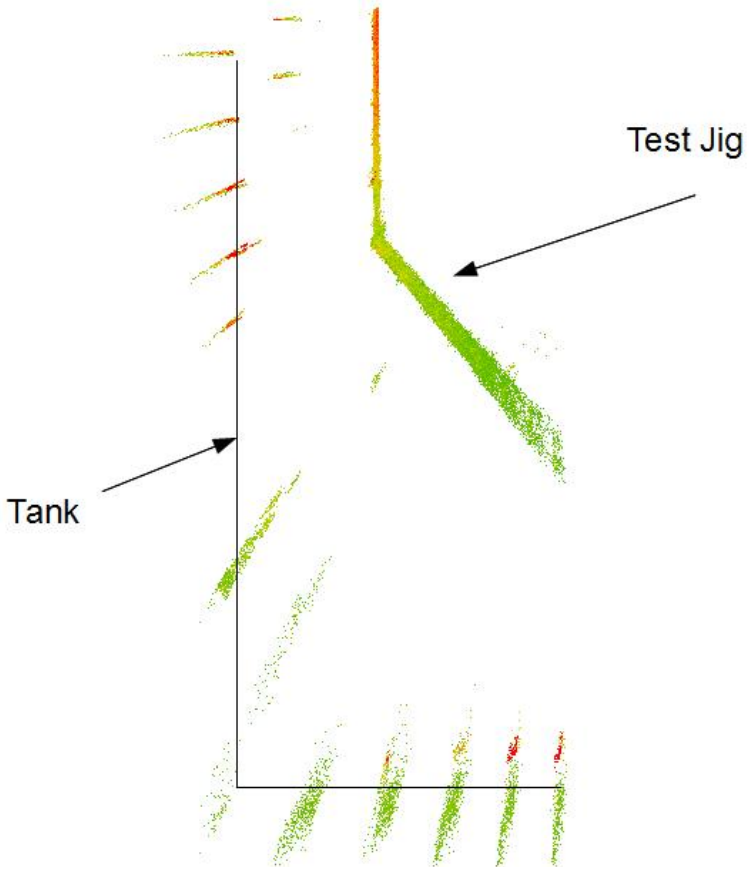


*Figure 4.5: Side View of test Jig Scan in Tank with the tank location indicated*

The intensity of the points reflected from the tank near the top when the scanner is much closer to the tank wall have a far stronger return intensity than the returns at the bottom of the tank where the scanner is approximately twice the distance away. In both cases the laser light is being directed almost normal to the side of the tank.

### 4.4.3 Return Intensity vs. Angle of Incidence

As the angle of incidence between the laser line and the surface of the test jig becomes more shallow, the impact of a surface not being perfectly diffuse becomes apparent. This is highlighted at the top section of the testing jig. Using the bracket mounting position the

angle of incidence is too great for the painted aluminum surface for strong returns to get back to the sensor allowing for distance measurements.

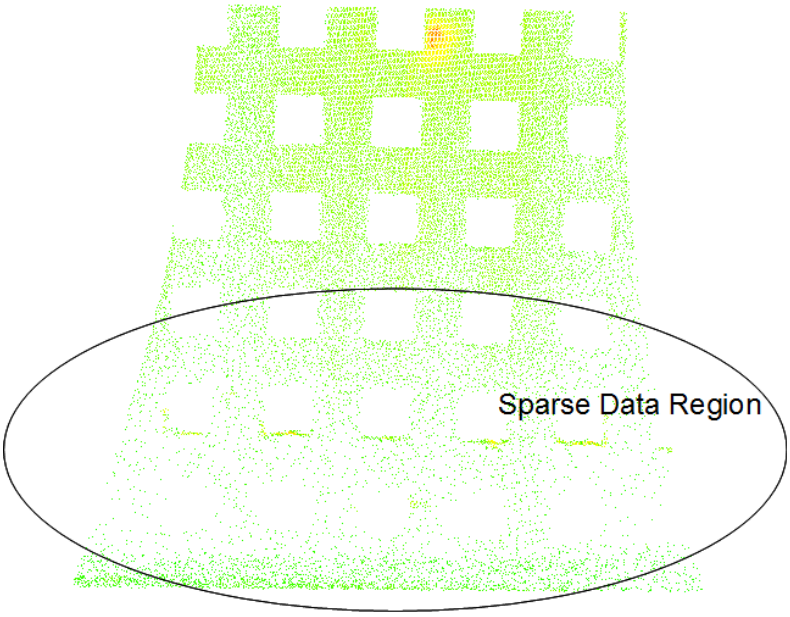


*Figure 4.6: The area toward the bottom of the top plate has sparse data since a high angle of incidence was used for sampling in this region*

The region with a nearly normal angle of incidence toward the top of the plate has a sufficiently dense measurement sampling for accurate measurements to be made using the point cloud. The sparse sampling is insufficient for quality measurements.

### 4.4.4 Range vs. Measurement Accuracy

A single measurement becomes increasingly less accurate with distance from the sensor head. This is observed as increased noise or fuzz defining the target surface. A crisp edge for the test jig is observed toward the top of the vertical plate and toward the bottom of the sloped plate the surface becomes far less clearly defined.

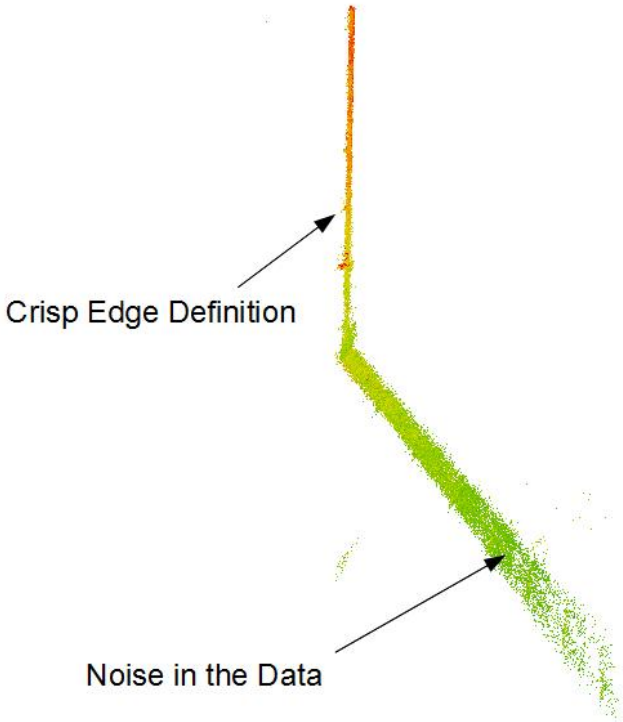


*Figure 4.7: Increasing noise with increasing measurement distance*

To demonstrate the impact this has on the measurements taken, three horizontal and three vertical measurements were taken at each end of the scan as shown in Figure 4.8 and Figure 4.9. The error in each set of measurements is shown in Table 1.

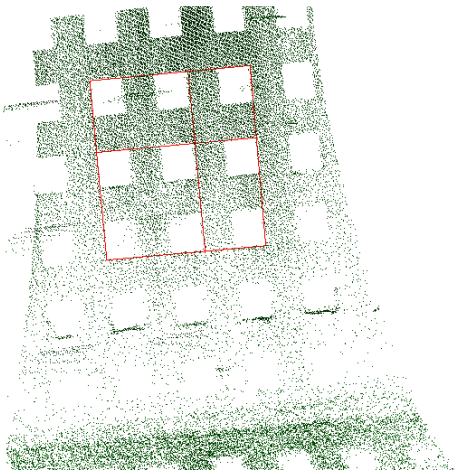

*Figure 4.8: Top Section Measurement Locations*

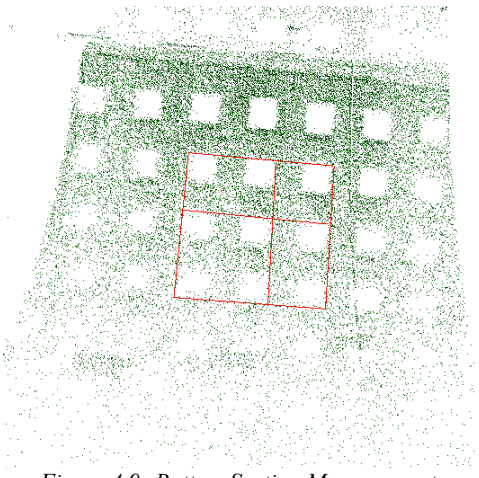

*Figure 4.9: Bottom Section Measurement Locations*

The values in the table are the difference between the actual measurement and the known measurement which for each measurement is 15cm.

| | Close horizontal [cm] | Close vertical [cm] | Further horizontal [cm] | Further vertical [cm] |
|---|---|---|---|---|
| 1 | -0.3 | -0.4 | 0 | -0.6 |
| 2 | -0.2 | -0.3 | 0.1 | -0.8 |
| 3 | -0.2 | -0.3 | 0.5 | -0.9 |

*Table 1: Measurement Errors*

Due to the Gaussian nature of the noise an average of the errors close and far both equal exactly 0.028m. However there is greater variability to the further measurements. The average accuracy of the system is within 2% of the measurement distance.

## 4.5 Discussion

To validate the capability of the developed underwater laser scanner a testing jig was constructed with known dimensions. Using scans of this jig the performance of the scanner

was evaluated. As the range to the target being scanned increases the quality of the data decreases. Similarly as the angle of incidence to the target surface is reduced, the quality of the data degrades. Using the grid test target, the average measurement error over a 15cm distance proved to be on the order of 2%. For best quality data the laser scanner should be operated as close to normal as possible relative to the surface being scanned; minimizing the distance between the scanner and the target surface is also beneficial. The primary deficits of the system was the increasing error with increasing measurement range and the degradation of the data as the angle of incidence between the laser beam and the target surface decreased.

# 5 Industrial Applications and Results

The underwater laser scanner has a number of industrial applications and results of tank and field trials have proven the system to be a viable technology for commercial deployment. In this section a number of applications where the laser scanner has been used and the results of these tests are discussed. In each case, areas of further improvement are identified with specific examples from the scans. All scans presented have results superior to the results expected with sonar. In most cases sonar was not attempted as the results would have been pointless. For the test of the cinder block wall a comparison of both sonar and laser scanner results is made.

## 5.1 Offshore

When operating the laser scanner in the offshore environment, water clarity, salinity of the water and ocean currents are all factors that impact the ability to capture high quality scans. In the offshore environment high detailed measurements are required for a range of assets. One in particular is mooring line ropes used to secure floating drilling and production platforms in place. A high-resolution scan of the ropes can provide a means of more accurately assessing the quality of the lines by quantifying damage to the outer abrasion jacket and by understanding diametric variances indicating damage to the inner core.

The laser scanner was tested offshore in conjunction with a prototype rope inspection vehicle. The intention of the rope inspection vehicle was to drive along the length of the rope capturing imagery of the rope. In addition, profiles of the rope were captured using the laser scanner to understand the diameter of the rope as a function of position. At points of

damage, the vehicle was stopped and the rope was scanned in greater detail. Imagery of the scanned rope can be seen in Figure 5.1,Figure 5.2 and Figure 5.2.

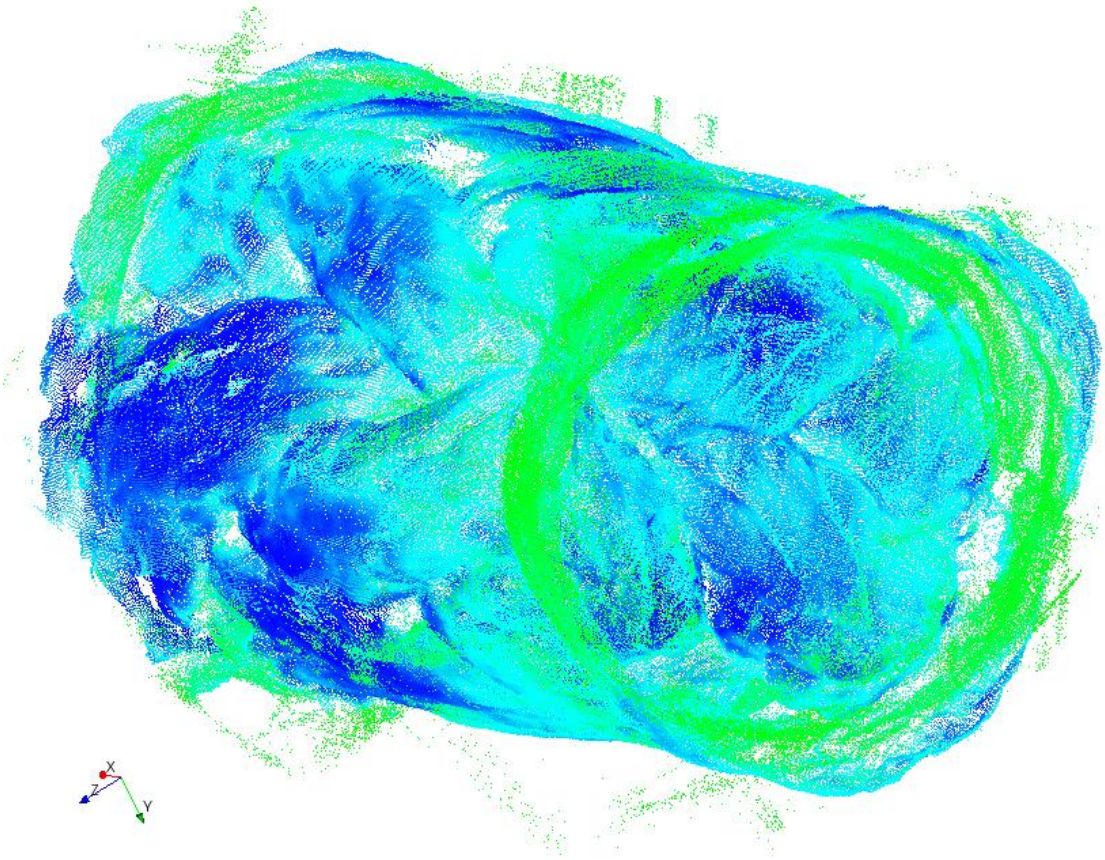


*Figure 5.1: Isometric View of a section of mooring line rope. This rope model was created using 5 separate scans that have been merged.*

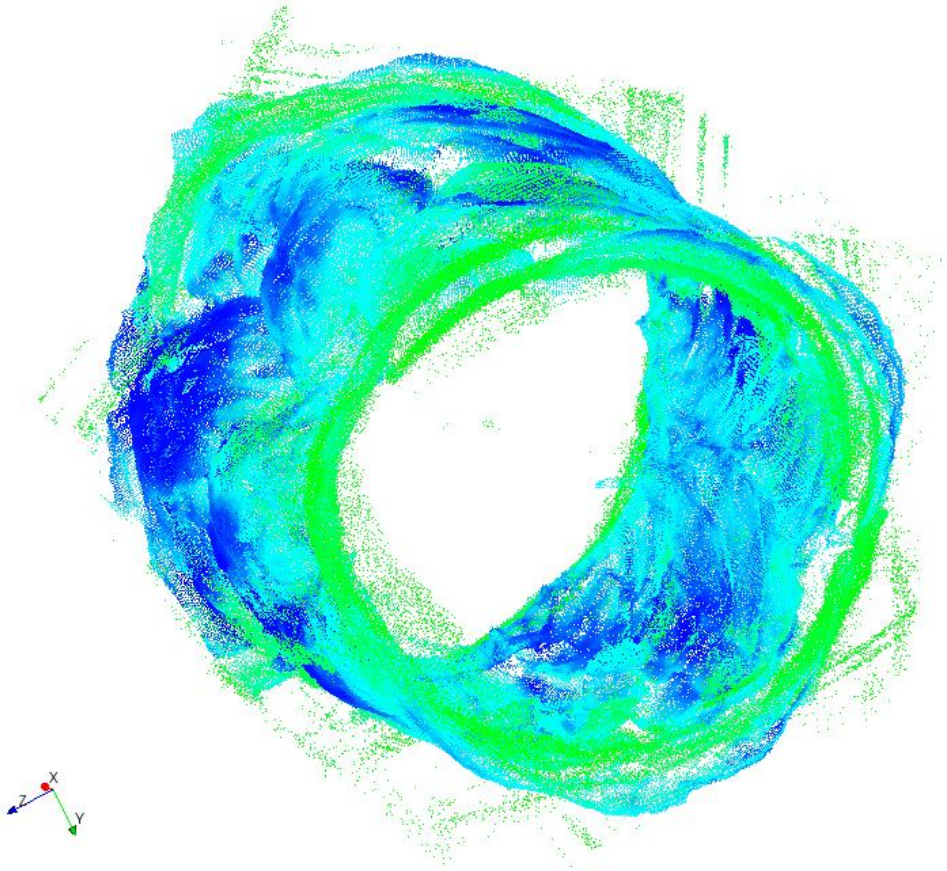


*Figure 5.2: End view of a mooring line showing misalignment between merged scans.*

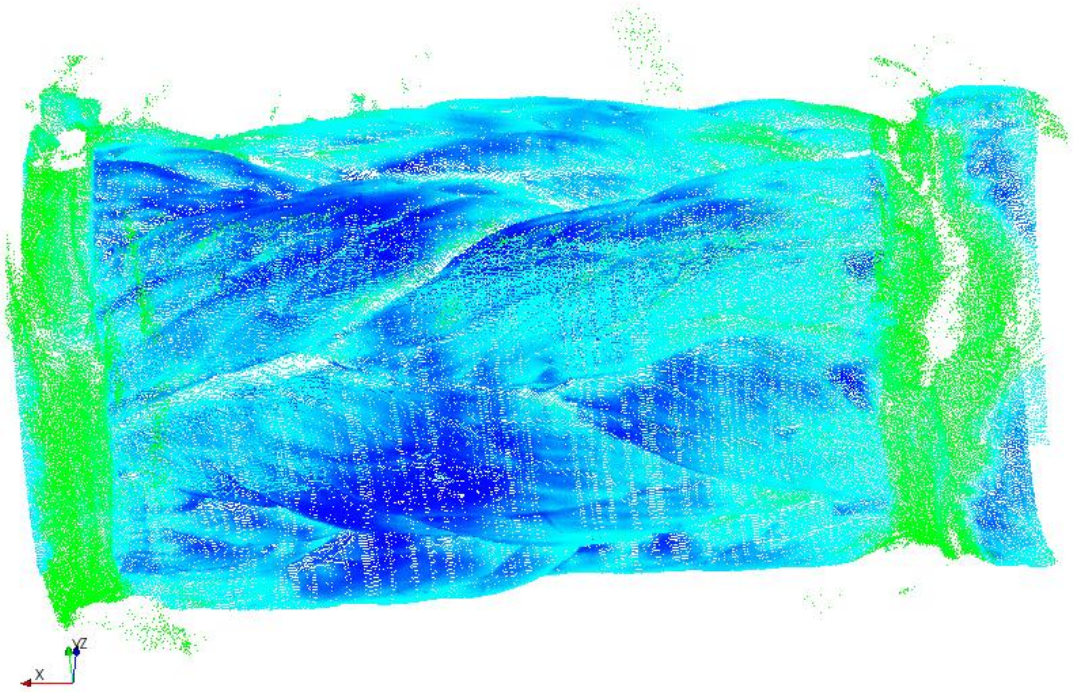


*Figure 5.3: Side View of Rope Scan*

The optical scattering properties of the rope resulted in a number of low intensity points being resolved. This is best seen in Figure 5.2 where there are a number of points that are clearly not part of the rope itself. Additionally, Figure 5.2 shows that one of these scans is not properly registered with the other scans. Improving the methodology to register scans quickly and effectively is a potential improvement.

## 5.2 Archeology

Archeologists need to take hundreds of measurements to classify the artifacts that they find. These measurements are used to assess the age and origin of an artifact. In addition, these

measurements provide a historical record preserving the information found. Taking the measurements is a time consuming process that must often be performed underwater. Bringing the artifacts to the surface and exposing them to the air is an expensive process that has the potential to cause damage. Measurements can sometimes be missed using a manual approach resulting in additional costs.

The laser scanner was used to document a concretion of an Adze. A concretion is an artifact in an encasement of a naturally forming concrete. This concretion forms in salt water near the presence of iron. An Adze is a tool that was used for forming wood on ships. The scan of the artifact can be seen below in Figure 5.4.

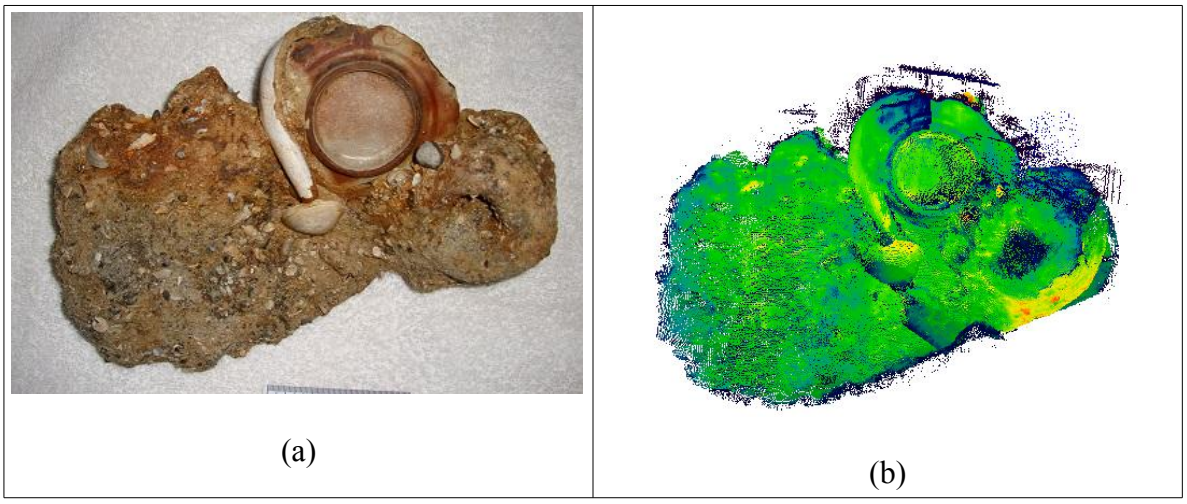

(a) (b)

*Figure 5.4: a) Picture of Adze, b) Scan of Adze in the same view*

An additional archeological application for the system is its use for inspecting native petroglyphs. The Grand Traverse Bay Underwater Preserve has discovered a boulder in 30ft of water that has what appears to be a petroglyph of a mastodon carved on its surface. To validate the origins of the markings a high resolution underwater scan of the carving is being considered. The objective of the scans is to understand the shape profile of the

markings themselves. This will provide an understanding of how the markings were created. To demonstrate the capability of the laser scanner for this application six sample targets were created, three with a marking generated by impacting a chisel with the stone to create a V shaped groove and the remaining three were engraved by impacting a second stone with the target stone to create a U shaped groove. The stones were then scanned from within 15cm and a high detailed model of each stone can be seen and the shape of the groove is clearly identifiable.

Allowing for complete shipwrecks to be scanned by an underwater laser scanner will allow for a greater adoption of this technology in archeology. Currently the technology is not going to help archeologists find an item but it will assist them in quantifying that artifact before removing it for further preservation.

## 5.3 Inshore

Municipal and other inshore assets suffer from damage in the same manner as offshore structures. Damage due to shifting earth around the asset as well as wear from erosion due to the water are two types of damage that can be found. Sonar and video inspection is insufficient to completely characterize the defects and as a result when assessing these assets assumptions must be made. Using the Underwater Laser Scanner can ensure that a complete understanding of the asset is obtained.

To demonstrate the difference between the capability of sonar and laser for measuring inland underwater infrastructure, a cinder block wall was constructed with target features including missing blocks and offset blocks. The wall was scanned with both the 2G Robotics ULS-100 underwater laser scanner and a mechanically scanning 3D sonar using a

2.25Mhz head with an average angular point spacing of one degree. The point cloud data for the two methods has been overlaid, with laser scanner data in red and black, and sonar data in green, in Figure 5.5.

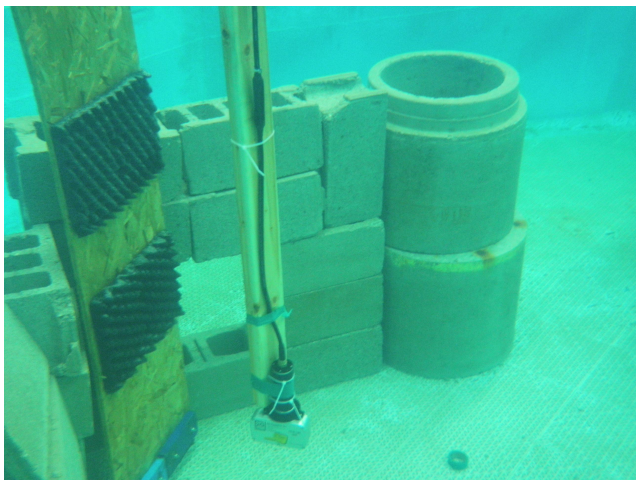

(a)

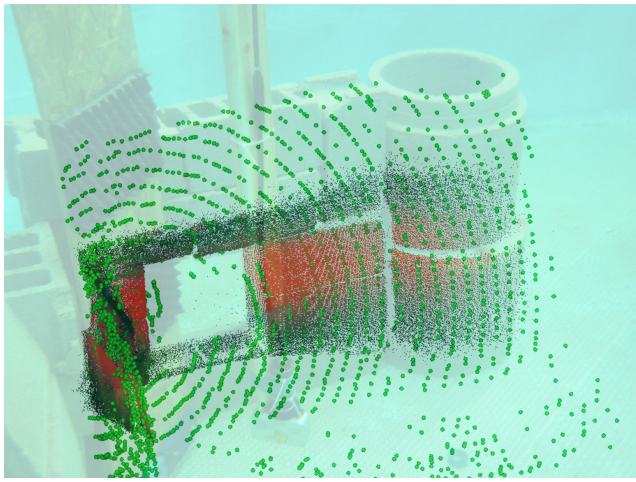

(b)

*Figure 5.5: a) Picture of cinder block wall test target underwater with the Laser Scanner, b) Overlay of the sonar and laser scanner data onto the picture*

As seen in Figure 5.5, the scans generally align well, indicating that both systems are capable of accurately assessing an asset's large-scale structure. However, there is significantly greater variability in the sonar measurements, and the measurement resolution

is much lower. The laser system also resolves edges much more precisely than sonar. The hole in the wall is resolved with very good detail using the laser scanner. While it is possible to identify the presence and general location of the hole in the sonar data, it does not provide a precise understanding of the hole's edges and an accurate position and size for the hole cannot be determined as shown in Figure 5.6. This inaccuracy is due to the size of the sonar system's footprint.

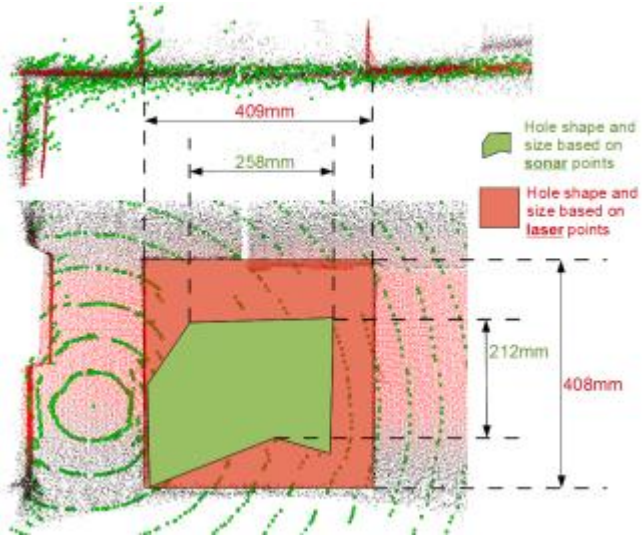


*Figure 5.6: Overlay of the sonar data and laser data demonstrating the superior ability for the laser to resolve a void.*

Very fine details of a chip in the corner of one of the cinder blocks can be measured as shown in Figure 5.7.

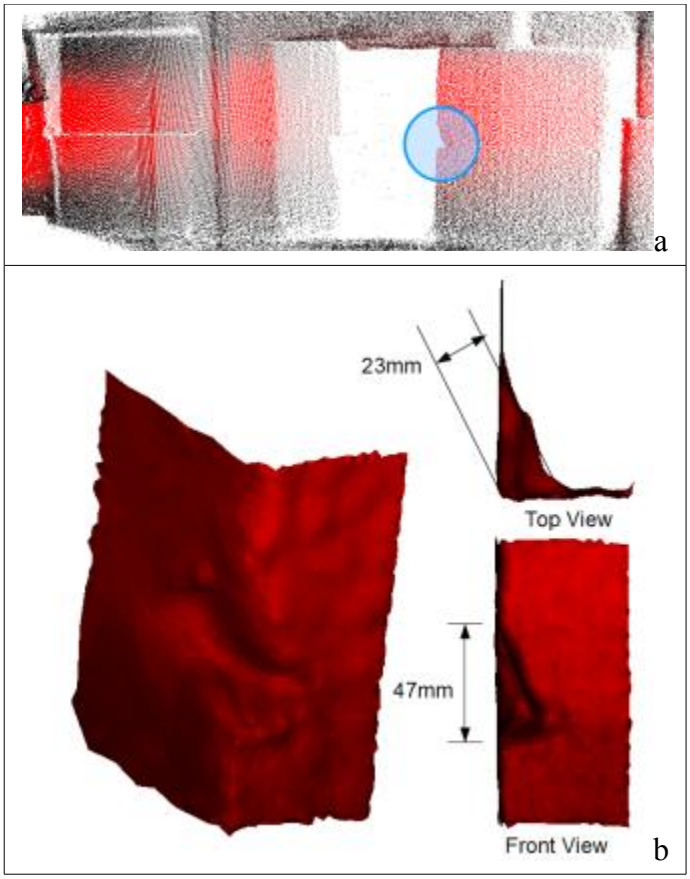


*Figure 5.7: a) location of a chip in one of the cinder blocks, b) surfaced point cloud of just the chip with measurements shown.*

## 5.4 Pipeline Damage

Pipeline inspections typically look for defects such as cracks and spalling or deformations to the pipeline (pipeline ovality). These inspections occur both internal to and external to the pipes themselves. To simulate an internal pipeline inspection a section of sheet metal was rolled and fastened at its edges using 1/4" bolts. To represent small feature defects, a small cut was made in the side wall of the pipe and nuts were glued to the side of the pipe as well. Figure 5.8, Figure 5.9 and Figure 5.10 demonstrate how the size of the nuts can be measured as well as the cut in the pipe.

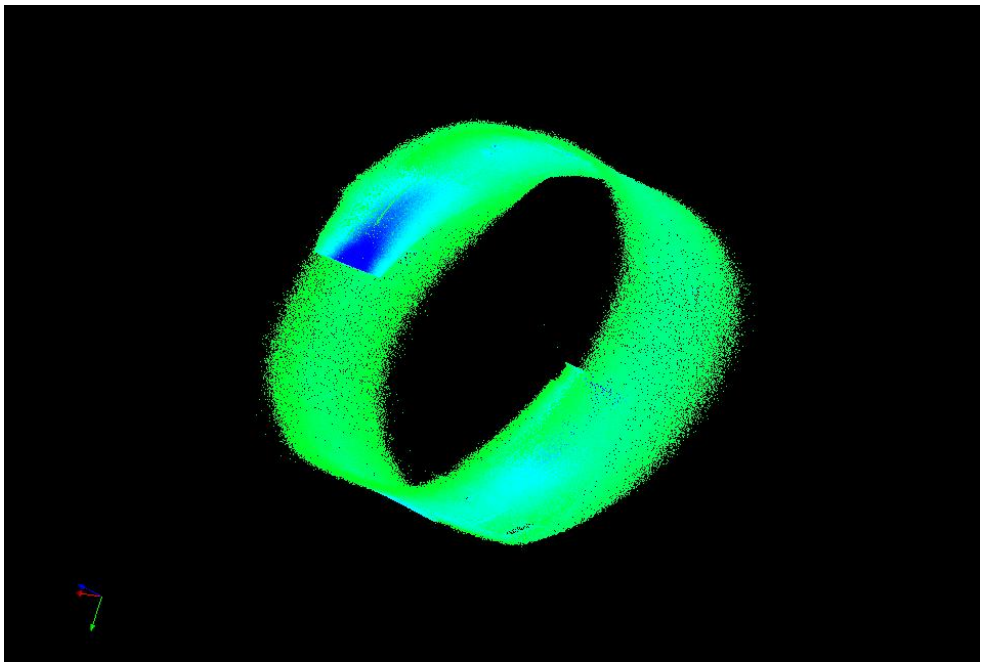

*Figure 5.8: Isometric View of the 3D model representing the scanned pipe*

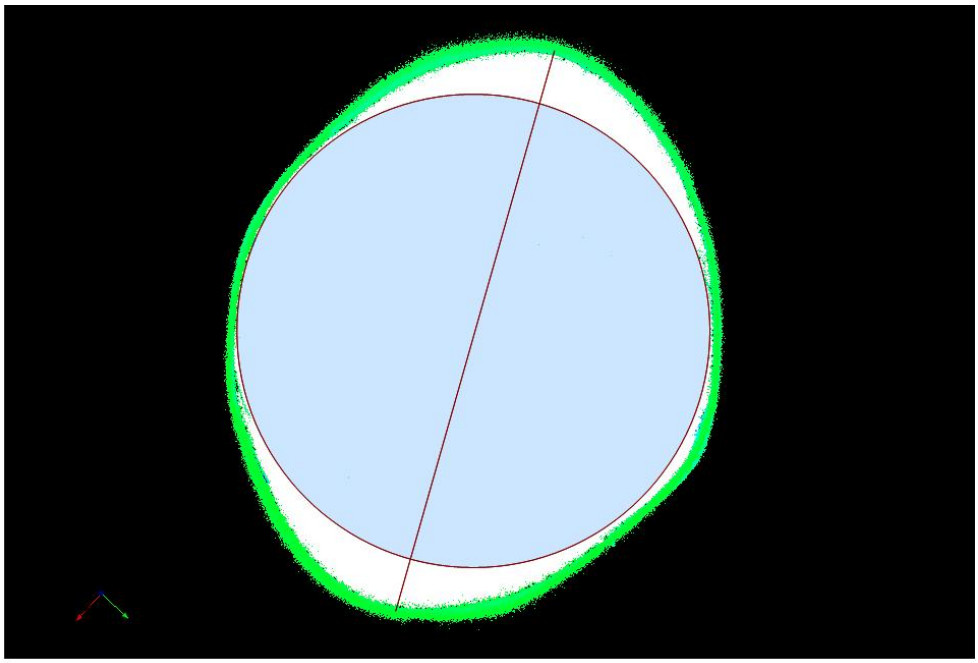

701mm maximum clearance diameter

862mm maximum clear length

0.67m$^2$ clear area

*Figure 5.9: End view of the pipe scan showing the ovality measurements*

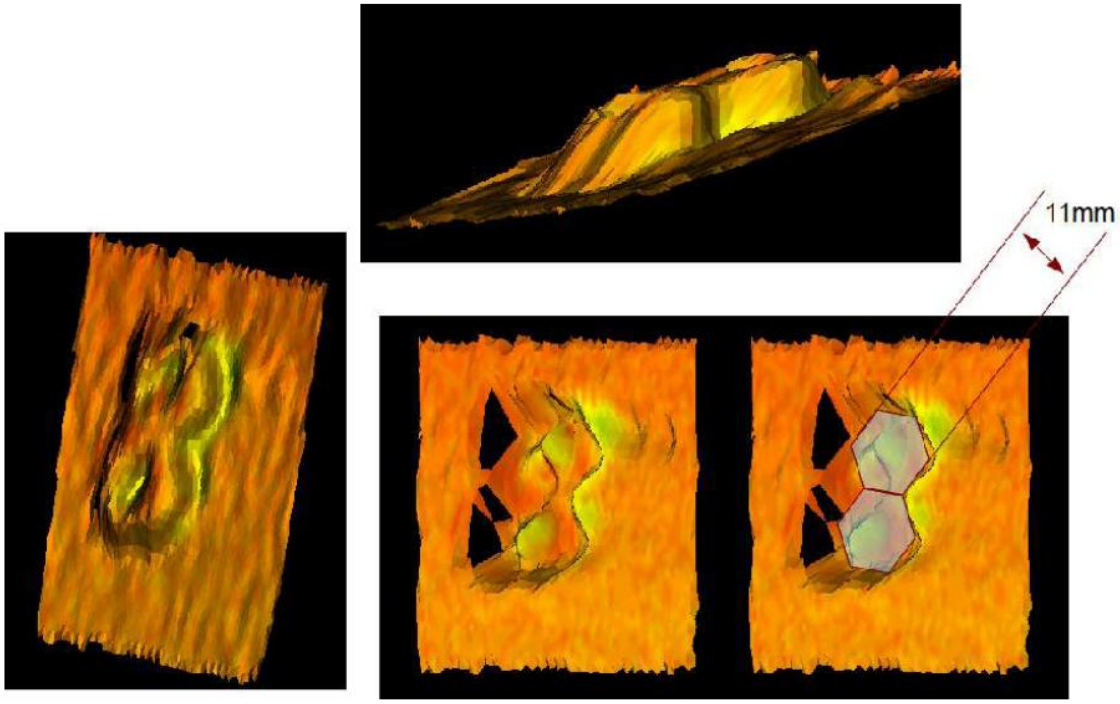


*Figure 5.10: Surfaced point cloud of nuts on the tunnel wall showing the nut measurements*

The depth of very small cracks in concrete structures cannot be measured by the laser scanner, as the laser light cannot penetrate down into the crack and reflect at an angle back to the optical sensor.

To simulate an external pipeline inspection a section of circular steel ducting was deformed. The collected point cloud seen in Figure 5.11 was surfaced and measurements of the size of the dent were successfully obtained. In addition FEA (Finite Element Analysis), Figure 5.12, and CFD (Computational Fluid Dynamic) analysis, Figure 5.13, were performed on the model created using the scanner data.

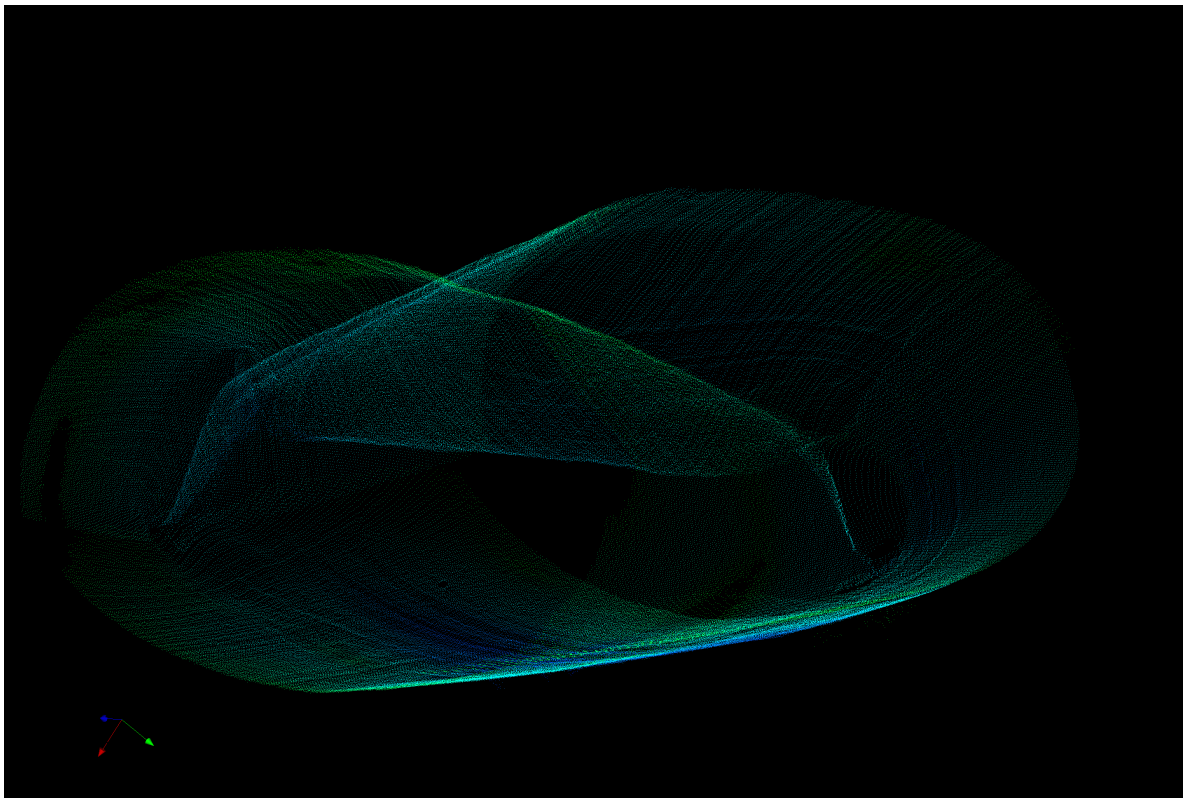

*Figure 5.11: Point cloud of a damaged pipe section*

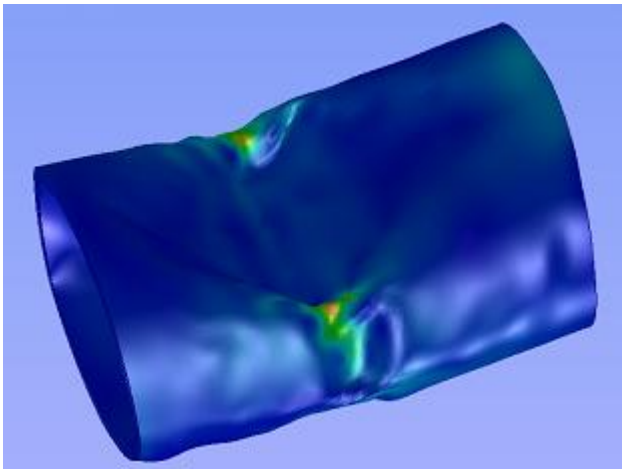

*Figure 5.12: Stress distribution of the damaged pipe section determined through FEA*

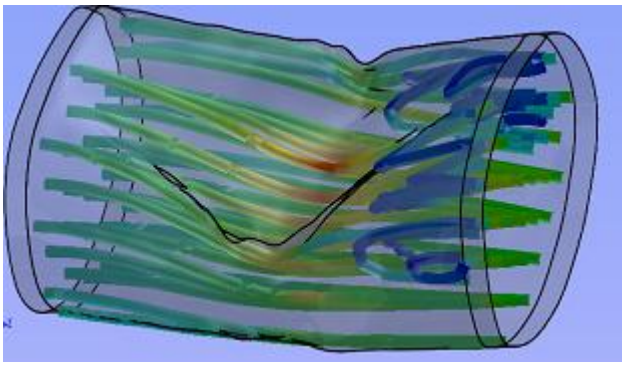

*Figure 5.13: Visualization of flow characteristics through the damaged pipe section based on CFD analysis*

## 5.5 Security

Assessment of the underwater laser scanner for use in evidence collection and mine countermeasures was performed in conjunction with the Niagara Regional Police Dive Team. The scanner was demonstrated to operate successfully when deployed by a diver to a mock evidence site and scans of an inert mine Figure 5.16, a grenade Figure 5.15, and a hand gun Figure 5.14 were performed. Accurate measurements of these items were successfully taken from the scan data, without needing to physically interact with the objects themselves.

*Figure 5.14: Point Cloud Model of a Hand Gun*

*Figure 5.15: Point Cloud Model of a Grenade*

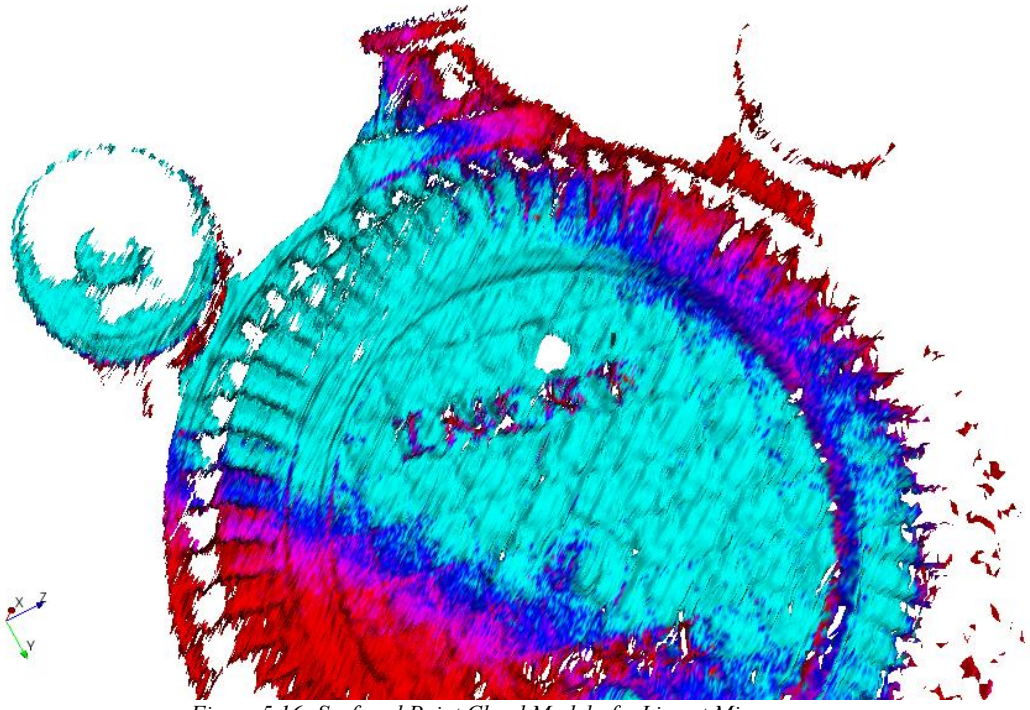


*Figure 5.16: Surfaced Point Cloud Model of a Limpet Mine*

## 5.6 Biological

To assess growth, decay or structure of subsea organics, the laser scanner can very accurately assess changes or variances in size and shape of features. By performing reoccurring scans over a period of time, the change in shape and size can be quantified. One application is mapping and modeling of muscle beds and corral reefs. To simulate these features, parabolic sound canceling foam was submerged and scanned. The fine scale parabolic shapes of each peak of the foam can clearly be identified in the surfaces below.

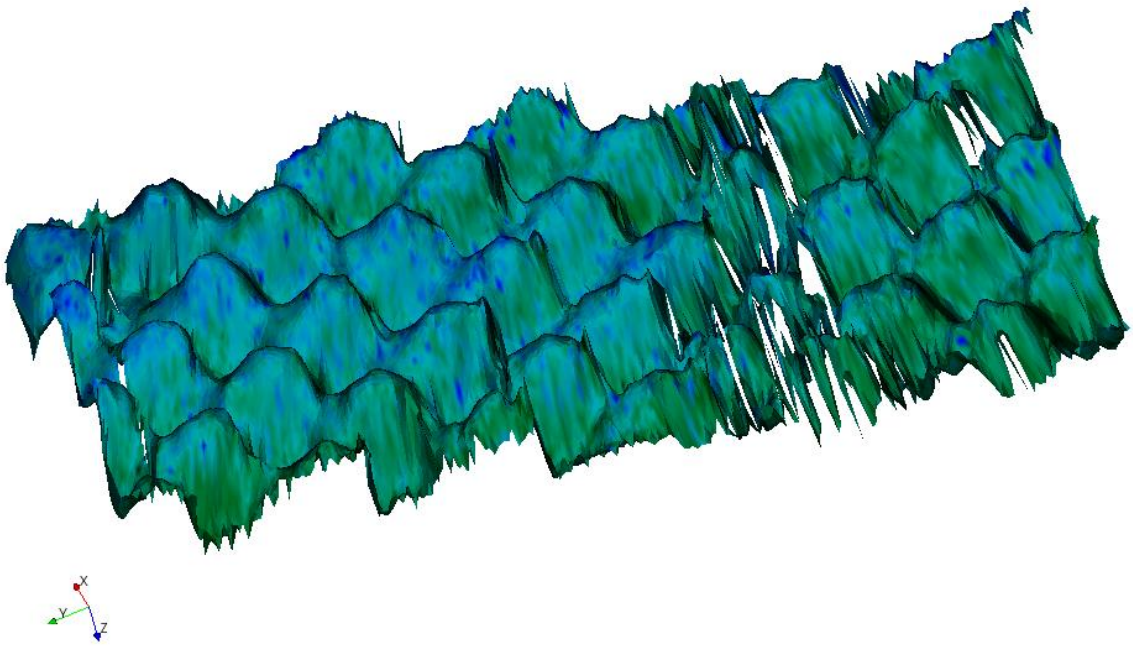


*Figure 5.17: Surfaced Point Cloud Model of sound absorbing foam representing mussels*

The surfacing algorithm used for the foam in Figure 5.17, while not in the scope of this thesis, is an important tool to visualize the collected data. Improvements to this algorithm will help with visualizations.

An additional test of the system was performed in conjunction with Dr. Dawn Sumner of UC Davis. The Geology Department of the University of California Davis is conducting research into the early life on earth through funding from NASA Astrobiology: Exobiology and Evolutionary Biology. The oldest fossils of life consist of stromatolites, which are millimeter to meter high structures created by the growth of bacteria. The shapes of stromatolites reflect both environmental and biological processes. Research is being conducted on the bacterial structures in ice-covered lakes in Antarctica Figure 5.18 because they have similar shapes to fossilized bacterial communities. Using the Underwater Laser Scanner Figure 5.19, Dr. Dawn Sumner and her team from UC Davis and the SETI Institute were able to successfully capture digital 3D models of the structure of these organisms Figure 5.20. With this data her team quantitatively defined the shapes of the living stromatolites. By comparing the scans with fossils of similar prehistoric growths, the team can get a better understanding of how these shapes formed and behaved. Understanding how the structures grow by comparing scans over a period of time on future expeditions will also provide additional incites. This level of analysis was made possible by the high resolution scanning capability of the Underwater Laser Scanner and will allow for new information and comparisons to be performed which were previously impossible.


*Figure 5.18: Base Station on an Antarctic Lake*

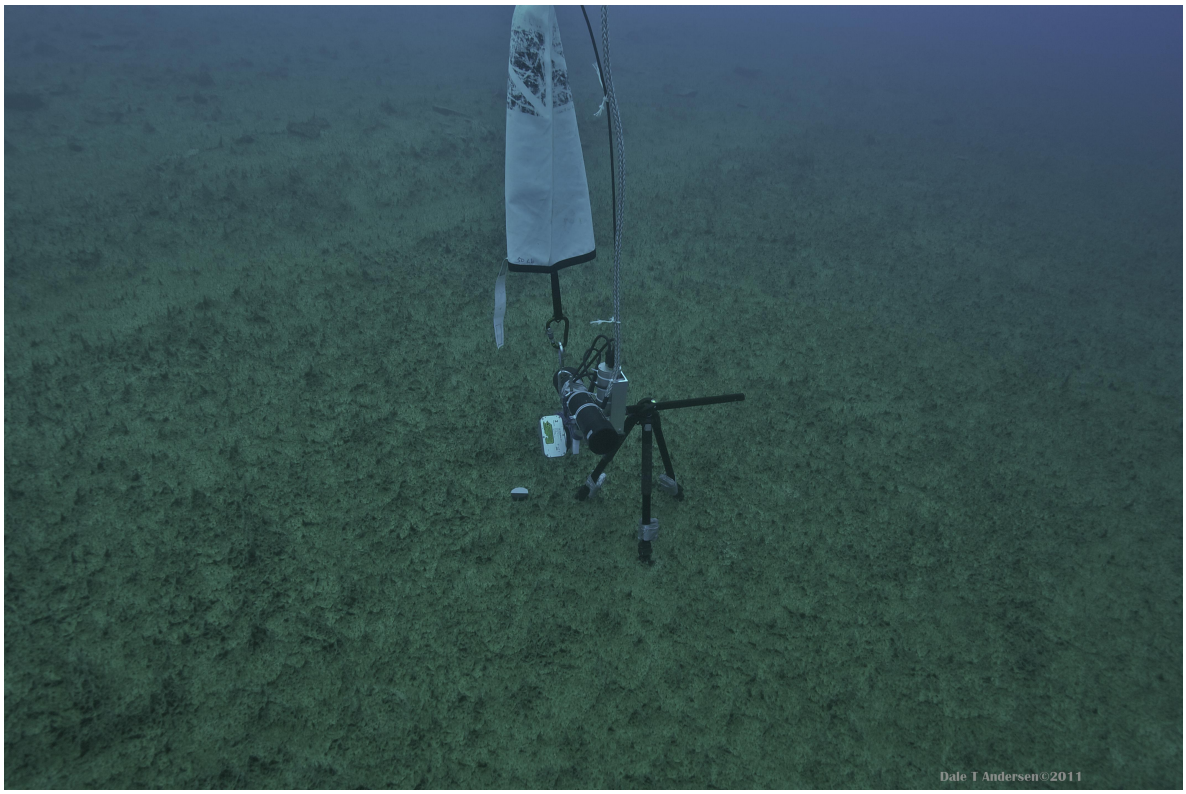


*Figure 5.19: Underwater Laser Scanner Deployed in Antarctica*

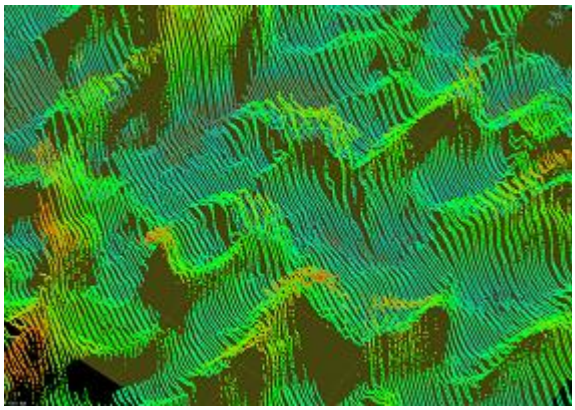

*Figure 5.20: Visualization of Stromatolites Scanned in Antarctica*

## 5.7 Other Applications

The Underwater Laser Scanner can be used in any application where a fine detail measurement is required. There are setup limitations to the system, such as stability, as the body of the scanner must remain stable during a scan. Additionally, low silt and low ambient light conditions are advantageous. If these conditions can be met then the underwater laser scanner is an ideal tool to provide engineers and asset owners with a more complete understanding of their asset than existing technologies such as video and sonar on their own.

It is clear that the underwater laser scanner developed has a wide range of applications and can be used in commercial situations as intended. The sensor can easily be deployed in the field and there is no need for in-field calibration. Using this sensor, results can be obtained that are superior to results obtainable using sonar. In all but one of the presented examples sonar was not attempted as the quality of the data would not have been useful to the industry members investigating the asset.

# 6 Conclusions and Future Work

## 6.1 Conclusions

In Chapter 1 performance limitations of existing technologies (video and sonar) were identified and it was explained how these limitations affect the ability of an asset owner to make informed and proper decisions. Video is good at seeing features but is not capable of providing quantitative assessments that an engineer could act on without significantly conservative assumptions. Sonar is able to provide measurements but the precision of these measurements is limited by the physical nature of sonar; sonar will spread as it travels through the water and there is the potential to incorrectly interpret a surface. A viable solution to these problems was identified to be an Underwater Laser Scanner through the literature review in Chapter 2. A number of laser scanners based on primarily photogrametric triangulation have been developed, however the commercial viability of these systems is limited as there is a need to recalibrate the system before each deployment. In Chapter 3 a new underwater laser scanner was developed allowing focusing on the Optical, Mechanical and Algorithmic designs needed to enable calibration of the system once and have multiple deployments were developed. By using a calibration jig the orientation of the the sensor and the laser were identified in a dry environment and not changed during integration with the rest of the unit. By processing the collected imagery during a scan the incoming ray from the point of contact of the laser can be back calculated to determine the position of the laser contact on a target surface relative to the body of the sensor. Physical characteristics to limit the range and resolution of the scanner were

discussed in Chapter 4 and a demonstration of these limitations were presented using a test jig. The results of the tests were successful, demonstrating an ability to capture accurate measurements. Many applications for the Underwater Laser Scanner exist and have been tested. These applications were discussed and results presented in Chapter 5.

Multiple underwater laser scanners have been developed historically. However, in order for the Underwater Laser Scanners to reach a point of wide scale adoption a small system that is easy to interface both mechanically and electrically was needed. Creating a single small package with all mechanical components in a single housing prevents the need for a re-calibration in the field making it an easy system to use.

Sonar and laser technologies have complimentary features. Long-range sonar scans can be used to assess the general structure of an asset, where high levels of detail are not required. Sonar can accomplish this quickly and at low cost, whereas laser scans of a large area can be time-consuming and more expensive. Once areas of interest have been identified by sonar, however, it is critical for engineers to fully understand the status of these locations. High-resolution laser scans of critical areas can provide the information necessary to ensure safe continued operation of these assets while minimizing unnecessary maintenance expenses. If maintenance is necessary, laser scanner data provides a more complete understanding of repair requirements, reducing risk and lowering the cost of deployment.

The Underwater Laser Scanner was successfully deployed in a range of underwater environments and used for a variety of applications. Results obtained with the scanner demonstrated successful performance of the system in the wide range of applications, validating the ease of deployment and use of the sensor and the ability for wide scale adoption.

## 6.2 Future Work

Further development of the technology to increase the scanning range and improved algorithms for creating visualizations of the data will further enhance the capability and useability of the sensor. The increased range can be achieved through the use of lasers with increased power and laser focusing optics with improved light transmisivity. Improved data visualization through the use of 3D viewing technologies will improve the ability to understand a scanned object, compared to simply viewing the object as flat imagery.

A key limitation of the technology that have been identified is the reduced performance of the system at high angles of incidence. By improving the performance of the laser scanner at higher angles of incidence, the system will be able to obtain measurements over greater areas, resulting in less time to obtain scans of complete areas. Additionally, the stability of the system is critical for high quality data. Integrating the scanner into specific deployment systems, specially designed for deployment of the sensor into specific environments, will increase the versatility of the device. Specifically, for assets where multiple setups are required to obtain a complete understanding of the environment, such as bridges and dams, an automated robotic system capable of incrementally traversing the structure and obtaining many scans with the sensor will expand the applications that the sensor can be easily deployed into. Currently the technology is not the right tool for locating an object of interest it is however the right technology for quantifying the object that has been found. By automating complete coverage of the area of interest using a robotic system it may become suited to finding items of interest as well.

# References

[1] Xu, Chunhui; Asada, Akira; Abukawa, Kazuki “A Method of generating 3D views of aquatic plants with DIDSON” 2011 IEEE Symposium on Underwater Technology, UT'11 and Workshop on Scientific Use of Submarine Cables and Related Technologies, SSC'11, 2011.

[2] Dai, Wei “Development of deepwater riser monitoring systems” Proceedings - 3rd International Conference on Measuring Technology and Mechatronics Automation, ICMTMA 2011, v 1, p 1050-1055, 2011.

[3] Robert Clarke, P. Eng. and Jason Gillham, ASI Group Ltd. “Advanced sonar revolutionizes underwater structure inspections” Power magazine, January 15 2007.

[4] Reed, Scott ; Wood, Jon; Vazquez, Jose; Mignotte, Pierre-Yves; Privat, Benjamin “ A smart ROV solution for ship hull and harbor inspection” Proceedings of SPIE - The International Society for Optical Engineering, v 7666, 2010, Sensors, and Command, Control, Communications, and Intelligence (C3I) Technologies for Homeland Security and Homeland Defense IX.

[5] Poissonnet, Cyril “High definition video systems for underwater inspection” MTS/IEEE Seattle, OCEANS 2010, 2010, MTS/IEEE Seattle, OCEANS 2010.

[6] Walther, Dirk; Edgington, Duane R.; Koch, Christof “Detection and tracking of objects in underwater video” Proceedings of the IEEE Computer Society Conference on Computer Vision and Pattern Recognition, v 1, p I544-I549, 2004.

[7] Ruiz, Ioseba Tena; Petillot, Yvan; Lane, David; Bell, Judith “ Tracking objects in underwater multibeam sonar images” IEE Colloquium (Digest), n 103, p 69-75, May 10, 1999.

[8] Lane, David M.; Chantler, Mike J.; Dai, Dongyong “Robust tracking of multiple objects in sector-scan sonar image sequences using optical flow motion estimation” IEEE Journal of Oceanic Engineering, v 23, n 1, p 31-46, Jan 1998.

[9] Daraigan, Sami Gumaan; Hashim, Syahril Amin; Jafri, Mohd. Zubir Mat; Abdullah, Khiruddin; Jena, Wong Chow; Saleh, Nasirun Mohd. “Multispectral absorption algorithm for retrieving TSS concentrations in water” International Geoscience and Remote Sensing Symposium (IGARSS), p 2848-2851, 2008, 2007 IEEE International Geoscience and Remote Sensing Symposium, IGARSS 2007.

[10] Giles, John W. ; Bankman, Isaac N. " Underwater optical communications systems part 2: Basic design considerations" Proceedings - IEEE Military Communications Conference MILCOM, v 2005, 2005, MILCOM 2005: Military Communications Conference 2005.

[11] David Gorda Tucker "Underwater observation using sonar" 1st edition, Fishing News (Books) Limited, Michigan, 1966.

[12] Urick. Robert J. "Principles of underwater sound 3rd ed." McGraw-Hill, Inc. 1983.

[13] Fabekovic, Zoran; Eškinja, Zdravko; Vukic, Zoran "Micro ROV Simulator" Proceedings Elmar - International Symposium Electronics in Marine, p 97-101.

[14] Dunnigan, M.W.; Lane, D.M.; , "Evaluation and reduction of the dynamic coupling between an ROV and manipulator," Control and Guidance of Underwater Vehicles, IEE Colloquium, vol., no., pp.4/1-4/4, 1993.

[15] Negahdaripour, S.; Taatian, A.; , "3-D motion and structure estimation for arbitrary scenes from 2-D optical and sonar video," OCEANS 2008 , vol., no., pp.1-8, 15-18 Sept. 2008.

[16] Leach, J.H.J.; , "The development of a towed vehicle for optical mapping in shallow water," OCEANS '98 Conference Proceedings , vol.3, no., pp.1455-1458 vol.3, 28 Sep-1 Oct 1998.

[17] P. Grussenmeyer; T. Landes; T. Voegtle; K. Ringle; "COMPARISON METHODS OF TERRESTRIAL LASER SCANNING, PHOTOGRAMMETRY AND TACHEOMETRY DATA FOR RECORDING OF CULTURAL HERITAGE BUILDINGS" The International Archives of the Photogrammetry, Remote Sensing and Spatial Information Sciences. Vol. XXXVII. Part B5. pp.213-218 Beijing 2008.

[18] Smith, P.F.; "Underwater photography: scientific and engineering applications", Van Nostrand Reinhold Co., 1984.

[19] Heinz-Gert De Couet; Andrew Green;, "The Manual of Underwater Photography", Best Pub Co , December 1989.

[20] Rebikoff, D.; Cherney, P; "Underwater Photography", New York, Amphoto, 1965.

[21] Wolfson, R; "Essential University Physics" Addison Wesley, 2006.

[22] Kraus, K.; "Photogrammetry: geometry from images and laser scans, Volume 1", Walter de Gruyter, 2007.

[23] Trucco, E.; Olmos-Antillon, A.T.; , "Self-Tuning Underwater Image Restoration," Oceanic Engineering,

IEEE Journal of , vol.31, no.2, pp.511-519, April 2006.

[24] Yan Fuli; Jiao Yunqing; Liu Jing; Xiong Jin'guo; Fu Qinghua; , "Inherent Optical Properties of Highly Turbid Eutrophic Waters, Taihu Lake, China," Geoscience and Remote Sensing Symposium, 2006. IGARSS 2006. IEEE International Conference on , vol., no., pp.1060-1062, July 31 2006-Aug. 4 2006.

[25] Gore, M. G.; “Spectrophotometry and spectrofluorimetry: a practical approach”, Oxford University Press, 2000.

[26] Siciliano, Khatib; “Springer Handbook of Robotics” Springer, 2008.

[27] Marriott, J. “Detecting the lone submarine” New Scientist, 3 Jun 1971 pp567-596.

[28] Guo, J.; Wang, W.H.; Huang, S.W.; Chen, E.; Chiu, F.C.; , "Map uncertainties for unmanned underwater vehicle navigation using sidescan sonar," OCEANS 2010 IEEE - Sydney , vol., no., pp.1-10, 24-27 May 2010.

[29] Hegrenaes, O.; Sabo, T.O.; Hagen, P.E.; Jalving, B.; , "Horizontal mapping accuracy in hydrographic AUV surveys," Autonomous Underwater Vehicles (AUV), 2010 IEEE/OES , vol., no., pp.1-13, 1-3 Sept. 2010.

[30] Kraeutner, P.H.; Bird, J.S.; Charbonneau, B.; Bishop, D.; Hegg, F.; , "Multiangle Swath Bathymetry Sidescan quantitative performance analysis," OCEANS '02 MTS/IEEE , vol.4, no., pp. 2253- 2263 vol.4, 29-31 Oct. 2002.

[31] Caimi, F.M.; Smith, D.C.; Kocak, D.M.; , "Underwater Laser Systems For Rangin, Size Estimation, And 3-D Measurement," OCEANS '92. 'Mastering the Oceans Through Technology'. Proceedings. , vol.2, no., pp.722, 26-29 Oct 1992.

[32] Wang, C.C.; Lee, J.M.; , "A 2D rough surface to be used to calibrate underwater laser scanner," OCEANS '04. MTTS/IEEE TECHNO-OCEAN '04 , vol.3, no., pp.1235-1239 Vol.3, 9-12 Nov. 2004.

[33] Crawford, A.M.; Hay, A.E.; , "A simple system for laser-illuminated video imaging of sediment suspension and bed topography," Oceanic Engineering, IEEE Journal of , vol.23, no.1, pp.12-19, Jan 1998.

[34] Kondo, H.; Ura, T.; , "Underwater structure observation by the AUV with laser pointing device," Underwater Technology, 2002. Proceedings of the 2002 International Symposium on , vol., no., pp. 178- 183, 2002.

[35] Jasinski, M.E.; Sortland, B.; Soreide, F.; , "Applications of remotely controlled equipment in Norwegian marine archaeology," OCEANS '95. MTS/IEEE. Challenges of Our Changing Global Environment. Conference Proceedings. , vol.1, no., pp.566-572 vol.1, 9-12 Oct 1995.

[36] Chau-Chang Wang; Shiahn-Wern Shyue; Shi-Her Cheng; , "Underwater structure inspection with laser light stripes," Underwater Technology, 2000. UT 00. Proceedings of the 2000 International Symposium on , vol., no., pp.201-205, 2000.

[37] Poupart, M.; Benefice, P.; Plutarque, M.; , "Subaquatic inspections of EDF (Electricite de France) dams," OCEANS 2000 MTS/IEEE Conference and Exhibition , vol.2, no., pp.939-942 vol.2, 2000.

[38] Nakatani, T.; Shuhao Li; Ura, T.; Bodenmann, A.; Sakamaki, T.; , "3D visual modeling of hydrothermal chimneys using a rotary laser scanning system," Underwater Technology (UT), 2011 IEEE Symposium on and 2011 Workshop on Scientific Use of Submarine Cables and Related Technologies (SSC) , vol., no., pp.1-5, 5-8 April 2011.

[39] Jaffe, J.S. “Underwater Optical Imaging The Design of Optimal Systems” Available: http://www.tos.org/oceanography/issues/issue_archive/issue_pdfs/1_2/1.2_jaffe.pdf.

[40] Gross, P.; Andrew, P.; , "The application of sector scanning sonar and multibeam imaging sonar for underwater security," OCEANS 2007 , vol., no., pp.1-7, Sept. 29 2007-Oct. 4 2007.

[41] Sintes, C.; Solaiman, B.; , "Side scan sonar and interferometric noise," OCEANS '99 MTS/IEEE. Riding the Crest into the 21st Century , vol.3, no., pp.1591-1596 vol.3, 1999.

[42]Hsiang-Chih Chan; Chi-Fang Chen; Ruey-Chang Wei; , "Analysis of the significantly statistical duration to clarify the uncertainty of ambient noises due to environmental changes," OCEANS 2008 - MTS/IEEE Kobe Techno-Ocean , vol., no., pp.1-5, 8-11 April 2008.

[43] Sintes, C.; Solaiman, B.; , "Strategies for unwrapping multisensors interferometric side scan sonar phase," OCEANS 2000 MTS/IEEE Conference and Exhibition , vol.3, no., pp.2059-2065 vol.3, 2000.

[44] Bradski, G; Kaehler, A; “Learning OpenCV” O’Reilly Media, Inc., 2008.

[45] Grussenmeyer, P.; Guillemin S. “PHOTOGRAMMETRY AND LASER SCANNING IN CULTURAL HERITAGE - DOCUMENTATION: AN OVERVIEW OF PROJECTS FROM INSA STRASBOURG” Available: http://geomaticsksa.com/GTC2011/S4/PDF/21.pdf.

# Appendix A

# Stepper Motor
## with GPL Planetary Gear

**Stepper motor with GPL 22 – 26 gear**

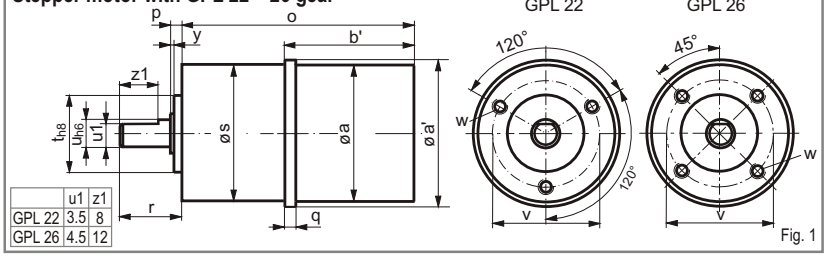


| | u1 | z1 |
|---|---|---|
| GPL 22 | 3.5 | 8 |
| GPL 26 | 4.5 | 12 |

Fig. 1

**Stepper motor with GPL 32 – 80 gear**

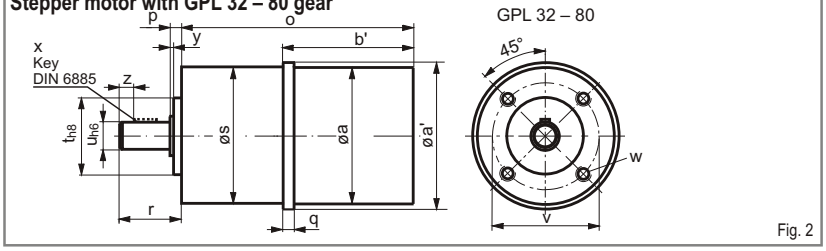


Fig. 2

| Gear | Stepper motor | Dimensions in mm | | | | | | | | | | | | | | | | |
|---|---|---|---|---|---|---|---|---|---|---|---|---|---|---|---|---|---|---|
| | | | | | 1 stage | 2 stages | 3 stages | | | | | | | | | | | |
| | | a | a' | b' | | o | | p | q | r | s | t | u | v | w | x | y | z |
| 22 | ZSS 19<br>ZSS 20 | 19 | 22 | 29<br>45.5 | 50<br>66.5 | 57<br>73.5 | 64<br>80.5 | 2.5 | 4.5 | 15 | 22 | 12 | 4 | 16 | M2.5x4 | – | 0.5 | – |
| | ZSS 25<br>ZSS 26 | 25 | 25.5 | 33.5<br>49.5 | 54.5<br>70.5 | 61.5<br>77.5 | 68.5<br>84.5 | | 5 | | | | | | | | | |
| 26 | ZSS 25<br>ZSS 26 | 25 | 26 | 33.5<br>49.5 | 59<br>75 | 67<br>83 | 75<br>91 | 2.5 | 5 | 17 | 26 | 14 | 5 | 20 | M3x4 | – | 0.5 | – |
| 32 | ZSS 32<br>ZSS 33 | 32 | 33 | 40.5<br>59.5 | 69.5<br>88.5 | 78.5<br>97.5 | 87.5<br>106.5 | 4 | 5 | 20 | 32 | 20 | 6 | 26 | M3x5 | – | 1 | – |
| 42 | ZSS 41<br>ZSS 42<br>ZSS 43 | 42 | 43 | 53<br>68<br>83 | 88<br>103<br>118 | 100.5<br>115.5<br>130.5 | 113<br>128<br>143 | 4 | 7 | 22.5 | 42 | 25 | 8 | 32 | M4x8 | 3x3x14 | 1 | 2.25 |
| 52 | ZSS 52 | 52 | 53 | 82.5 | 123.5 | 138 | 152.5 | 4 | 9 | 24 | 52 | 32 | 12 | 40 | M5x8 | 4x4x16 | 1 | 2 |
| | ZSS 56<br>ZSS 57 | 56.4 | 57 | 74<br>90 | 115<br>131 | 130<br>145 | 144<br>160 | | | | | | | | | | | |
| 80 | RSS 79<br>RSH 79 | 80 | 80 | 125 | 168.5 | 186.5 | 204.5 | 5 | 23.1 | 35 | 80 | 50 | 14 | 65 | M6x12 | 5x5x20 | 2.5 | 5 |
| | RSS 80<br>RSH 80 | 80 | 80 | 147 | 190.5 | 208.5 | 226.5 | | | | | | | | | | | |

| Gear | Weight without motor | | | perm. radial load (center of shaft) | Permissible axial load | Protection class Gear | Protection class Gear + Motor | |
|---|---|---|---|---|---|---|---|---|
| | 1-stage | 2-stage | 3-stage | | | | | |
| GPL 22 | 50 g | 75 g | 100 g | 30 N | 24 N | IP 44 | **IP 40** | IP 44 |
| GPL 26 | 70 g | 90 g | 115 g | 50 N | 40 N | IP 44 | **IP 40** | IP 44 |
| GPL 32 | 135 g | 180 g | 250 g | 80 N | 65 N | IP 54 | **IP 40** | IP 44 |
| GPL 42 | 275 g | 350 g | 425 g | 150 N | 120 N | IP 54 | **IP 43** | IP 65 |
| GPL 52 | 475 g | 600 g | 725 g | 250 N | 200 N | IP 54 | **IP 43** | IP 65 |
| GPL 80 | 1.5 kg | 2.1 kg | 2.75 kg | 400 N | 320 N | IP 54 | **IP 54** | IP 65 |

**IP xx = Standard**
IP xx = optional
(dimensions on request)

## Technical Information

- Stepper motor mounted gear
- 200-step
  2-phase powerful stepper motor
- 1- to 3-stage planetary gear
- Low gear backlash
  – Standard: 20 to 50 angular minutes
  – Low-backlash: 6 to 15 angular minutes
- Maximum permanent torque 0.1 to 38 Nm
- 100% permissible short-term overload
- Adapted for permanent, alternate or intermittent operation
- Ideal for combination with toothed belt modules
- 4:1 to 256:1 reduction ratios
  (depending on the gear type)
- High efficiency
- Low gear inertia
- Permissible temperature range
  –30 to +90 °C

customized solutions *in motion*

## Mechanical Characteristics

| Gear | Stepper motor | Mechanical Gear Characteristics | | | | | | | | | | | |
|---|---|---|---|---|---|---|---|---|---|---|---|---|---|
| | | | | | standard | | | low-backlash | | | | | |
| | | Stages | Reduction ratios | | No-load backlash | Nominal torque (S1) | Emergency stop torque (S1) | No-load backlash | Nominal torque (S5) | Emergency stop torque (S5) | Torsional stiffness | Average mass inertia at drive | Efficiency |
| | | | | | | Nm | | | Nm | | Nm/arcmin | kgcm² | % |
| GPL 22 | ZSS 19<br>ZSS 20<br>ZSS 25<br>ZSS 26 | 1 | 4:1<br>5:1 | 7:1 | 20' | 0.1 | 0.2 | – | – | – | 0.19 | 0.008 | 96 |
| | | 2 | 16:1<br>20:1<br>28:1 | 35:1<br>49:1 | 35' | 0.5 | 1 | – | – | – | 0.21 | 0.006 | 90 |
| | | 3 | 64:1<br>80:1<br>112:1 | 140:1<br>196:1<br>245:1 | 50' | 1.5 | 3 | – | – | – | 0.2 | 0.004 | 85 |
| GPL 26 | ZSS 25<br>ZSS 26 | 1 | 3.5:1<br>4.33:1 | 6:1<br>7.67:1 | 20' | 0.3 | 0.6 | – | – | – | 0.24 | 0.012 | 96 |
| | | 2 | 12.25:1<br>18.78:1<br>26:1 | 33.22:1<br>46:1 | 35' | 1 | 2 | – | – | – | 0.26 | 0.010 | 90 |
| | | 3 | 81.37:1<br>112.67:1<br>143.96:1 | 199.33:1<br>276:1 | 50' | 3 | 6 | – | – | – | 0.25 | 0.0095 | 85 |
| GPL 32 | ZSS 32<br>ZSS 33 | 1 | 4:1<br>4.5:1<br>5.2:1 | 6.25:1<br>8:1 | 20' | 0.4 | 0.8 | 6' | 0.8 | 1.6 | 0.3 | 0.015 | 96 |
| | | 2 | 16:1<br>18:1<br>20.8:1<br>25:1<br>29:1 | 32:1<br>36:1<br>41.6:1<br>50:1 | 35' | 2 | 4 | 10' | 4 | 6 | 0.32 | 0.012 | 90 |
| | | 3 | 72:1<br>81:1<br>100:1<br>130:1 | 144:1<br>200:1<br>225:1<br>256:1 | 50' | 6 | 12 | 15' | 6 | 12 | 0.3 | 0.011 | 85 |
| GPL 42 | ZSS 41<br>ZSS 42<br>ZSS 43 | 1 | 4:1<br>5:1 | 6:1 | 20' | 0.7 | 1.4 | 6' | 1.4 | 3 | 0.4 | 0.03 | 96 |
| | | 2 | 14:1<br>16:1 | 20:1 | 35' | 4 | 8 | 10' | 8 | 12 | 0.42 | 0.024 | 90 |
| | | 3 | 56:1<br>64:1<br>80:1<br>100:1 | 120:1<br>144:1<br>184:1 | 50' | 12 | 24 | 15' | 12 | 24 | 0.4 | 0.024 | 85 |
| GPL 52 | ZSS 52<br>ZSS 56<br>ZSS 57 | 1 | 4:1<br>4.5:1<br>5.2:1 | 6.25:1<br>8:1 | 20' | 1.5 | 3 | 6' | 3 | 6 | 1.2 | 0.06 | 96 |
| | | 2 | 16:1<br>18:1<br>20.8:1<br>25:1<br>29:1 | 32:1<br>36:1<br>41.6:1<br>50.1:1 | 35' | 10 | 20 | 10' | 20 | 30 | 1.3 | 0.055 | 90 |
| | | 3 | 72:1<br>81:1<br>100:1<br>130:1 | 144:1<br>200:1<br>225:1<br>256:1 | 50' | 30 | 60 | 15' | 30 | 60 | 1.35 | 0.05 | 85 |
| GPL 80 | RSS 79 | 1 | 4:1 | | 20' | 3 | 6 | 6' | 6 | 12 | 1.5 | 0.12 | 96 |
| | RSH 79<br>RSS 80 | 2 | 14:1<br>16:1 | 20:1<br>24:1 | 35' | 15 | 30 | 10' | 30 | 38 | 1.5 | 0.08 | 90 |
| | RSH 80 | 3 | 56:1 | 64:1 | 50' | 38 | 75 | 15' | 38 | 75 | 1.4 | 0.075 | 85 |

### Material

Gear housing:

GPL 22: stainless steel

GPL 26 – 80: rustproof for normal environmental conditions

Output shaft bearing: 2 deep groove ball bearings

### Grease Lubrication

Maintenance-free permanent lubrication with grease of the highest quality.

After three years or every 10,000 hours of operation we recommend servicing.

## Operating Modes

### S1: Continuous operation

The gear box's operating time exceeds 15 minutes without a break or the duty cycle is more than 60%. In no case the gear box housing temperature may exceed 70 °C.

### S5: Cyclical operation

The gear box's duty cycle is less than 60%. The number of operations per hour can range anywhere from a few to several thousand.

If the number of operations exceeds 1000 per hour, the maximum torque occuring has to be multiplied by a shock factor (fig. 3) to take into account the additional dynamic load.

The data in this publication are based on software models and empirical values for the S1 and S5 modes and on a shock factor of 1.25.

## Shock Factor

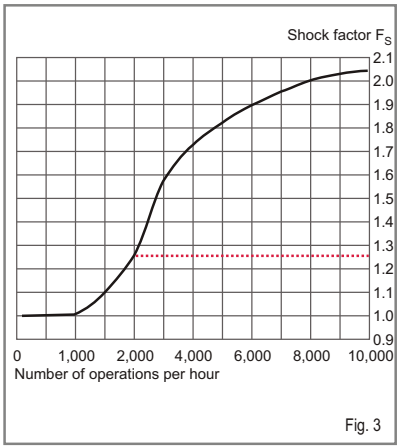


Fig. 3

## Ordering Data

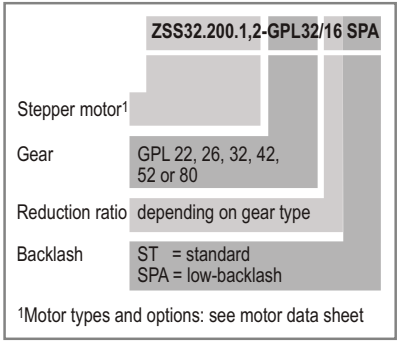


[1]Motor types and options: see motor data sheet



**Phytron, Inc.**
600 Blair Park Rd, Suite 220, Williston, VT 05495 USA
Tel 802-872-1600 Fax 802-872-0311 info@phytron.com www.phytron.com



customized solutions in motion

# Appendix B

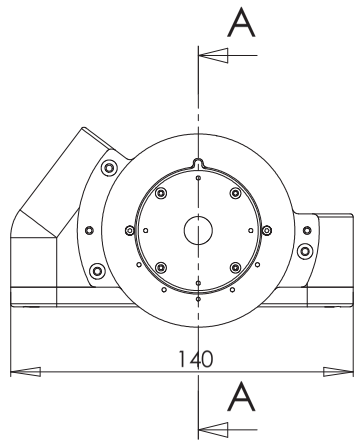


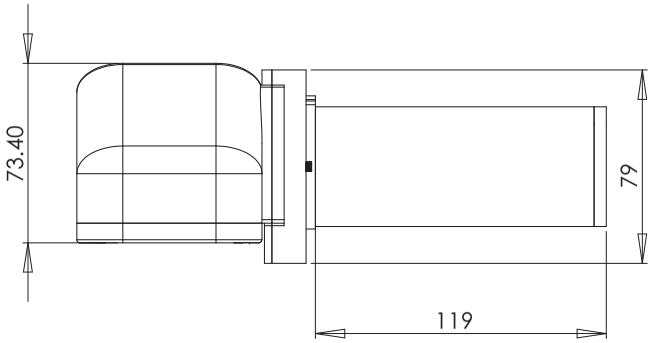


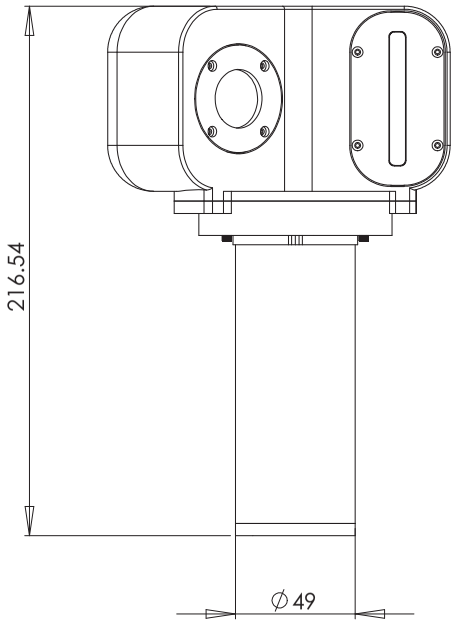


74

| UNLESS OTHERWISE SPECIFIED: | | NAME | DATE |
|---|---|---|---|
| DIMENSIONS ARE IN mm | MODEL | G. Dijkema | 10/15/09 |
| TOLERANCES:<br>0.x = +/- 0.03<br>0.xx = +/- 0.01<br>0.xxx = +/- 0.005<br>x/x = +/- 1/32 | DRAWING | G. Dijkema | 10/15/09 |
| MATERIAL | COMMENTS: | | |
| STOCK | | | |
| FINISH | | | |



2G Robotics Inc.
2-614 Colby Dr., Waterloo ON. Canada, N2V 1A2

TITLE: Single Axis Scanner

| SIZE | DWG. NO. | REV |
|---|---|---|
| B | BP008-000-000-00 | A2 |

SHEET 1 OF 3

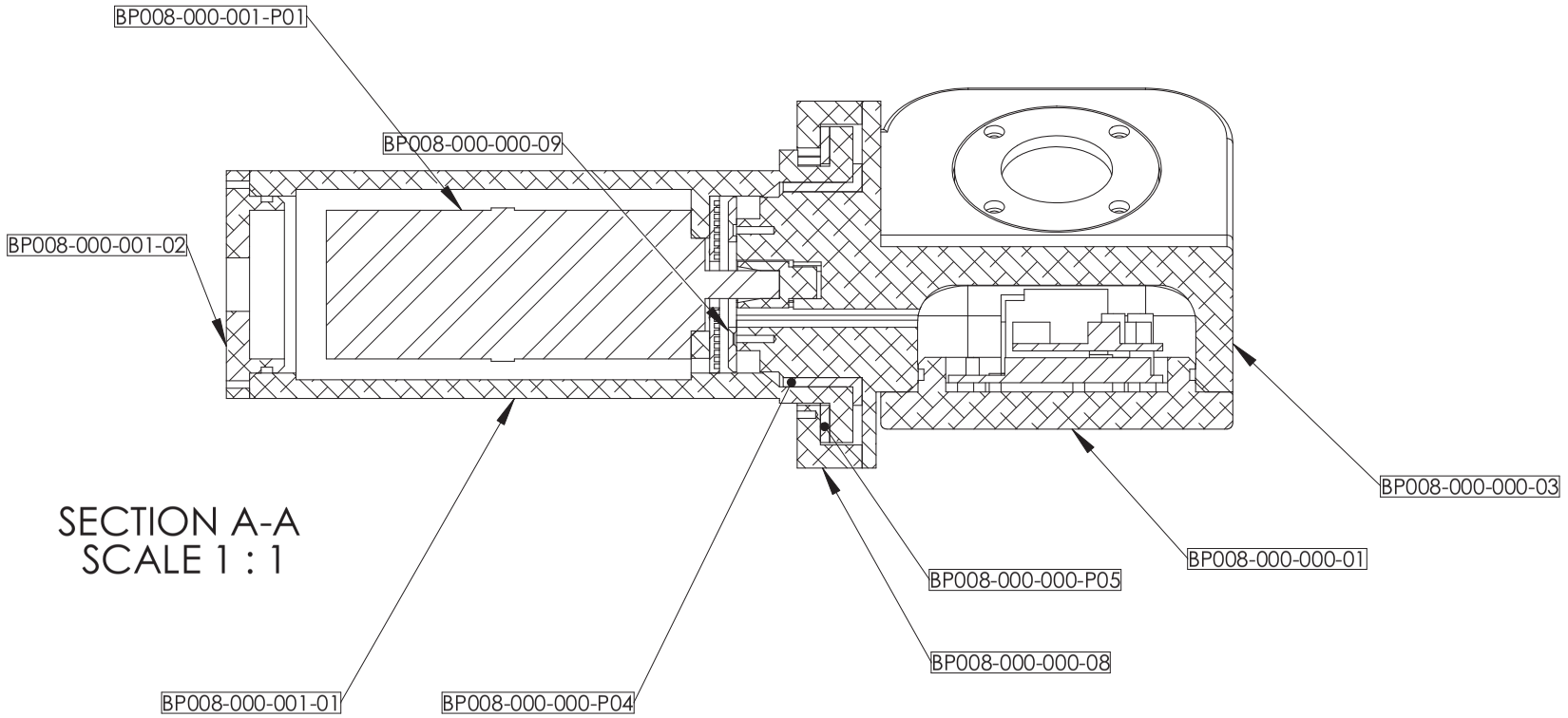


75

SECTION A-A
SCALE 1 : 1

| UNLESS OTHERWISE SPECIFIED: | | NAME | DATE |
|---|---|---|---|
| DIMENSIONS ARE IN mm | MODEL | G. Dijkema | 10/15/09 |
| TOLERANCES:<br>0.x = +/- 0.03<br>0.xx = +/- 0.01<br>0.xxx = +/- 0.005<br>x/x = +/- 1/32 | DRAWING | G. Dijkema | 10/15/09 |
| MATERIAL | COMMENTS: | | |
| STOCK | | | |
| FINISH | | | |



2G Robotics Inc.
2-614 Colby Dr., Waterloo ON. Canada, N2V 1A2

TITLE: Single Axis Scanner

| SIZE | DWG. NO. | REV |
|---|---|---|
| B | BP008-000-000-00 | A2 |

SHEET 2 OF 3

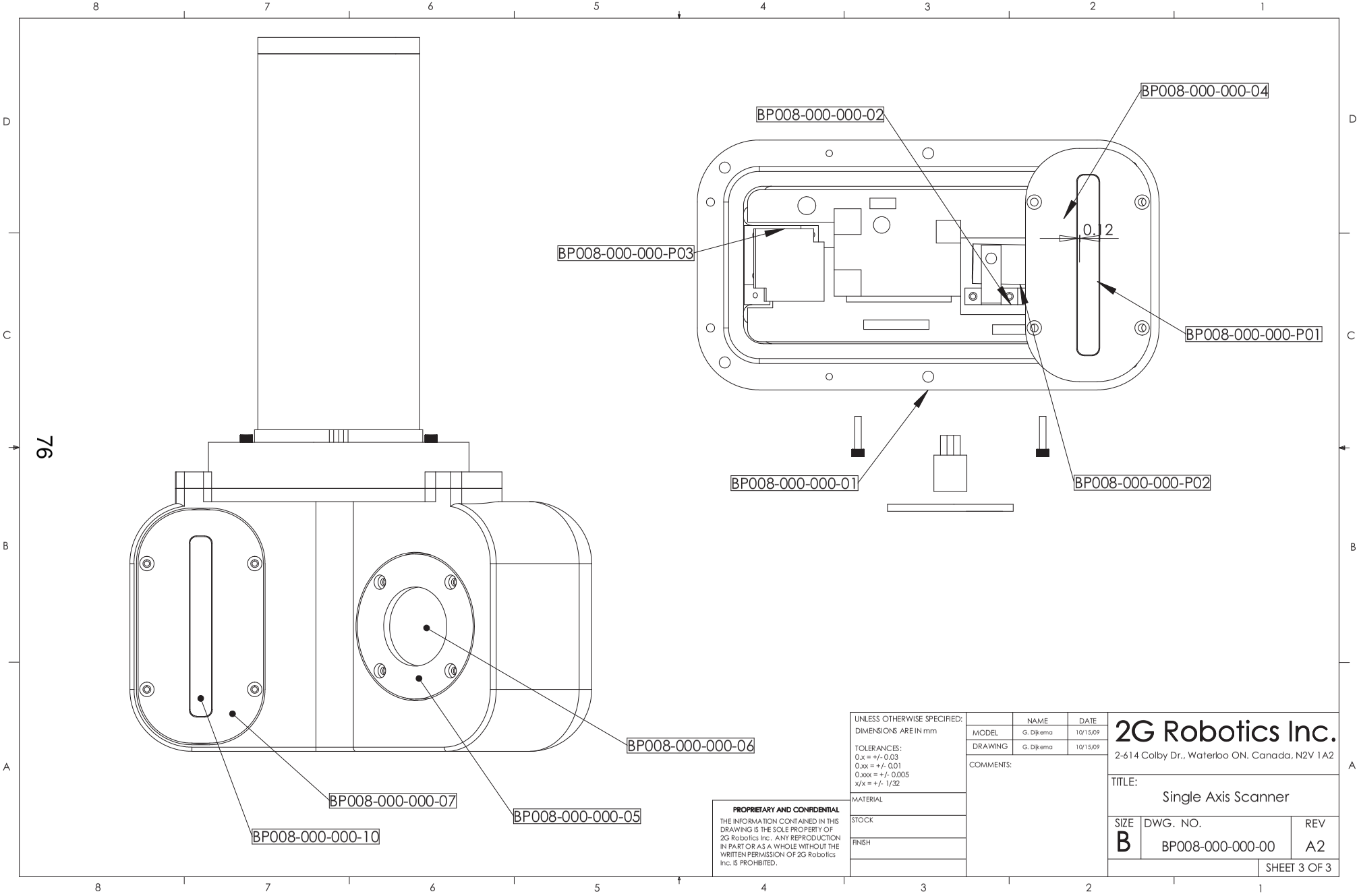




UNLESS OTHERWISE SPECIFIED:
DIMENSIONS ARE IN mm

TOLERANCES:
0.x = +/- 0.03
0.xx = +/- 0.01
0.xxx = +/- 0.005
x/x = +/- 1/32

MATERIAL

STOCK

FINISH

| | NAME | DATE |
|---|---|---|
| MODEL | G. Dijkema | 10/15/09 |
| DRAWING | G. Dijkema | 10/15/09 |

COMMENTS:

2G Robotics Inc.
2-614 Colby Dr., Waterloo ON. Canada, N2V 1A2

TITLE:
Single Axis Scanner

| SIZE | DWG. NO. | REV |
|---|---|---|
| B | BP008-000-000-00 | A2 |

SHEET 3 OF 3

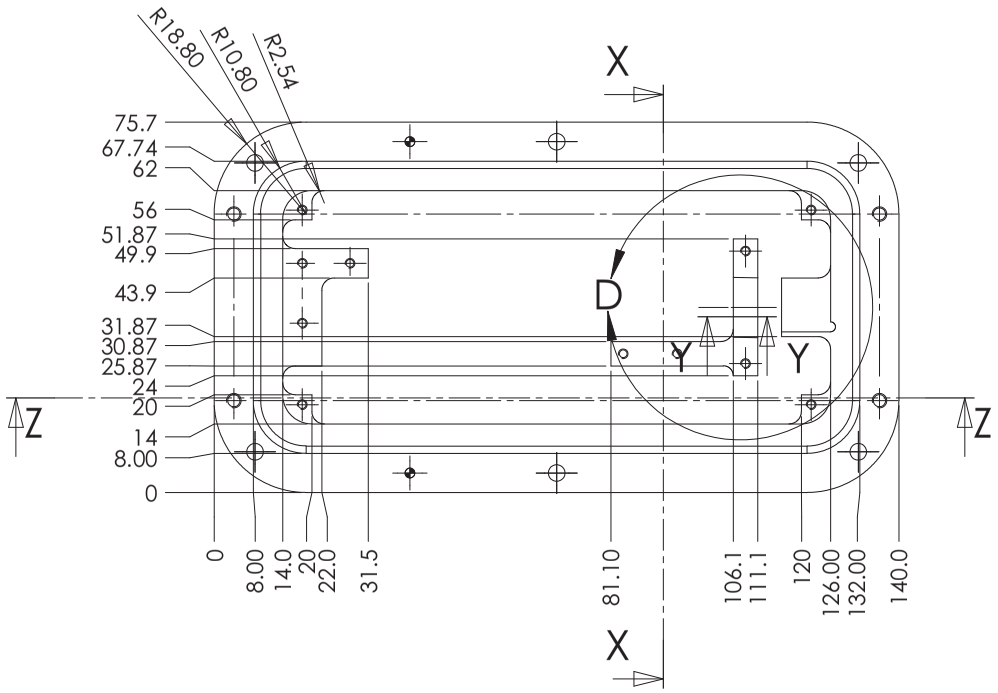


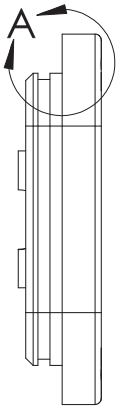


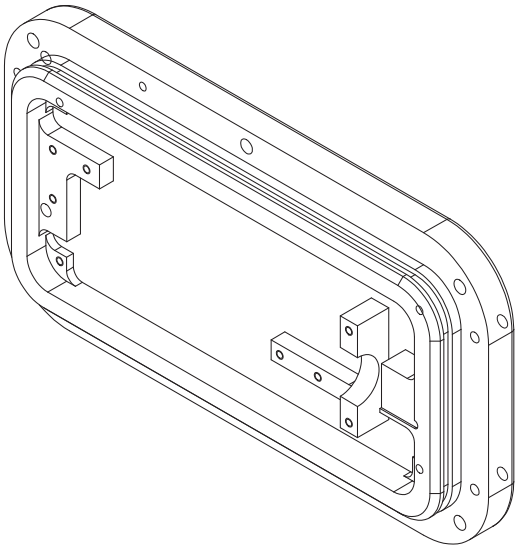

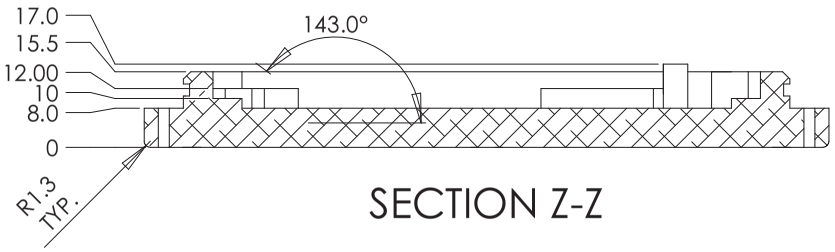


SECTION Z-Z

77



UNLESS OTHERWISE SPECIFIED:
DIMENSIONS ARE IN mm

TOLERANCES:
x = ± 0.75
x.x = ± 0.25
x.xx = ± 0.13
x.xxx = ±0.01

ANGULAR
x = ± 1 DEG.
x.x = ± 0.5 DEG.

MATERIAL
6061-T6

STOCK

FINISH
Clear Anodized

| | NAME | DATE |
|---|---|---|
| MODEL | G. Dijkema | 10/15/09 |
| DRAWING | G. Dijkema | 10/15/09 |

COMMENTS:

2G Robotics Inc.
2-614 Colby Dr., Waterloo ON. Canada, N2V 1A2

TITLE:
Scanner Base

| SIZE | DWG. NO. | REV |
|---|---|---|
| B | BP008-000-000-01 | A6 |

SHEET 1 OF 4

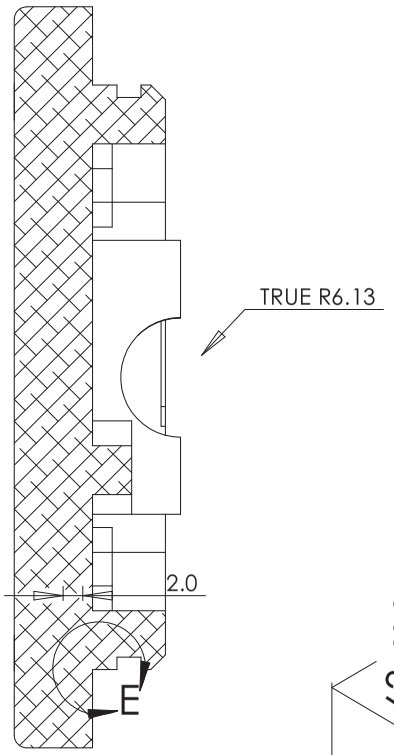


SECTION X-X
SCALE 2 : 1

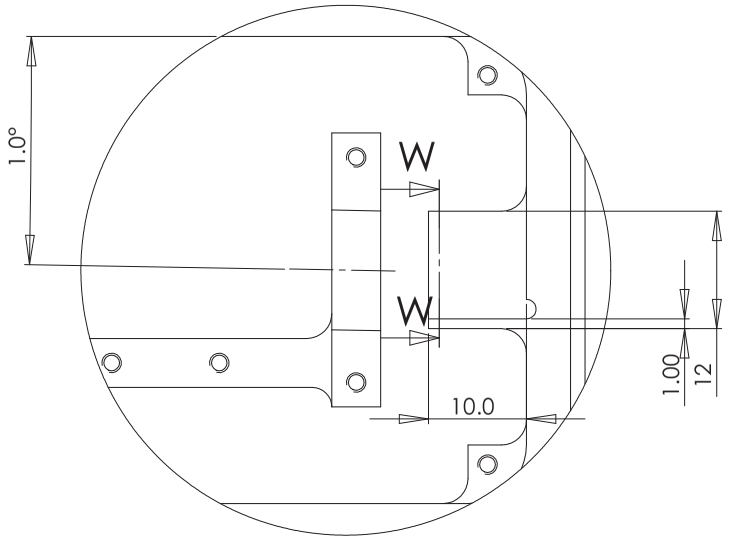


DETAIL D
SCALE 2 : 1

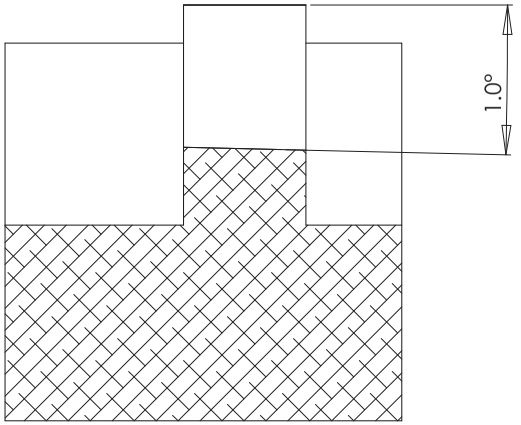


SECTION Y-Y
SCALE 5 : 1

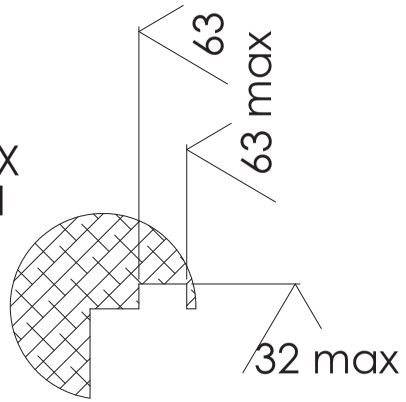


DETAIL E
SCALE 4 : 1

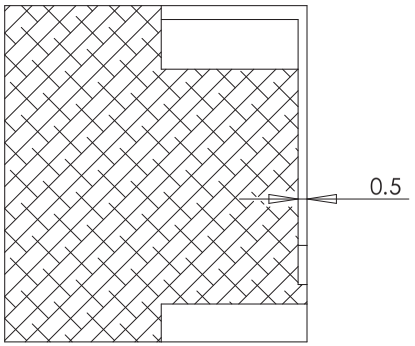


SECTION W-W
SCALE 4 : 1

78



UNLESS OTHERWISE SPECIFIED:
DIMENSIONS ARE IN mm
TOLERANCES:
x = ± 0.75
x.x = ± 0.25
x.xx = ± 0.13
x.xxx = ±0.01
ANGULAR
x = ± 1 DEG.
x.x = ± 0.5 DEG.
MATERIAL
6061-T6
STOCK
FINISH
Clear Anodized

| | NAME | DATE |
|---|---|---|
| MODEL | G. Dijkema | 10/15/09 |
| DRAWING | G. Dijkema | 10/15/09 |

COMMENTS:
Surface finishes are maximum acceptable. Very smooth surfaces are ideal.

2G Robotics Inc.
2-614 Colby Dr., Waterloo ON. Canada, N2V 1A2

TITLE:
Scanner Base

| SIZE | DWG. NO. | REV |
|---|---|---|
| B | BP008-000-000-01 | A6 |

SHEET 2 OF 4

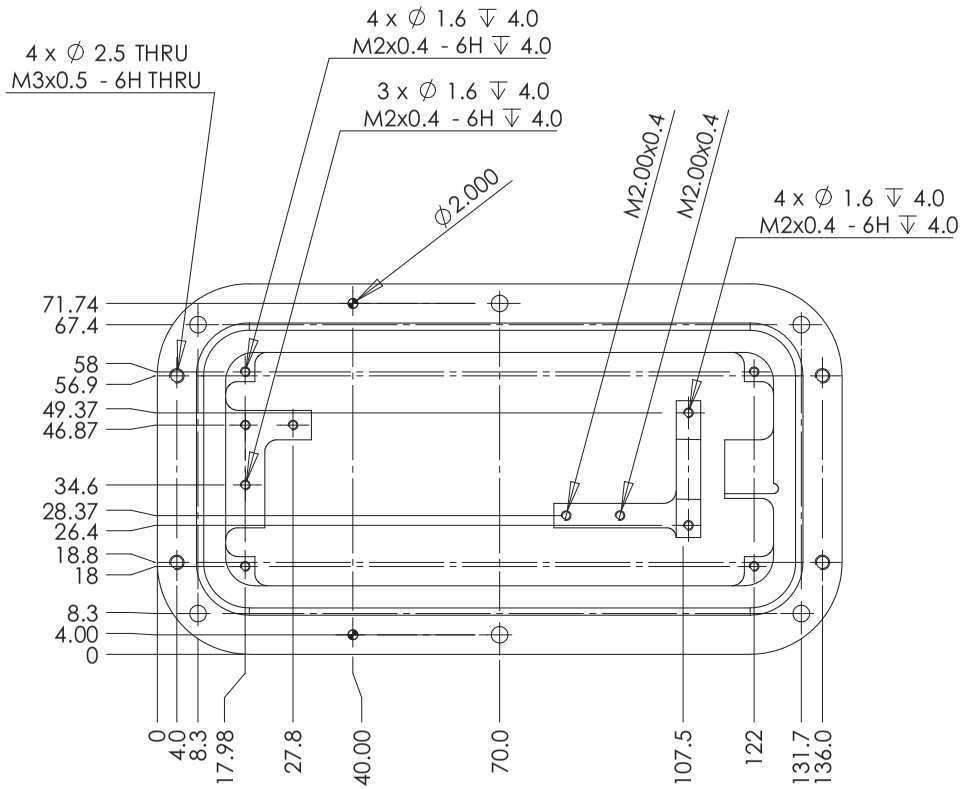


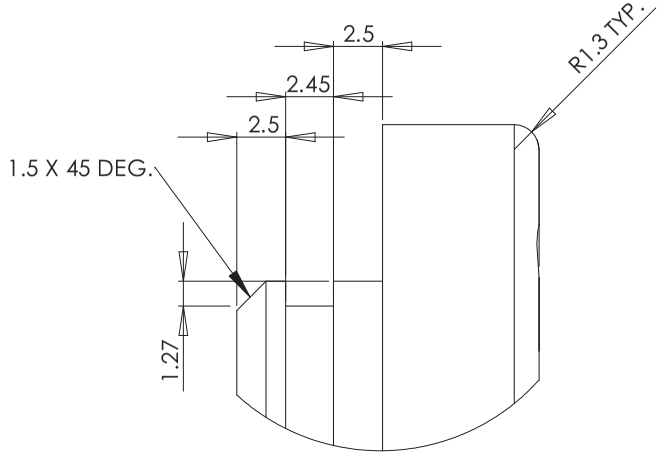


DETAIL A
SCALE 4 : 1

79



UNLESS OTHERWISE SPECIFIED:
DIMENSIONS ARE IN mm
TOLERANCES:
x = ± 0.75
x.x = ± 0.25
x.xx = ± 0.13
x.xxx = ±0.01
ANGULAR
x = ± 1 DEG.
x.x = ± 0.5 DEG.
MATERIAL
6061-T6
STOCK
FINISH
Clear Anodized

| | NAME | DATE |
|---|---|---|
| MODEL | G. Dijkema | 10/15/09 |
| DRAWING | G. Dijkema | 10/15/09 |

COMMENTS:

2G Robotics Inc.
2-614 Colby Dr., Waterloo ON. Canada, N2V 1A2

TITLE: Scanner Base

| SIZE | DWG. NO. | REV |
|---|---|---|
| B | BP008-000-000-01 | A6 |

SHEET 3 OF 4

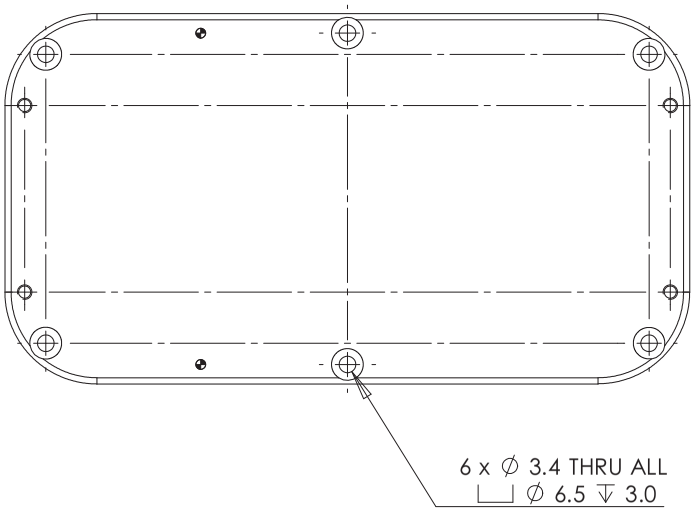


80

| | NAME | DATE |
|---|---|---|
| MODEL | G. Dijkema | 10/15/09 |
| DRAWING | G. Dijkema | 10/15/09 |

UNLESS OTHERWISE SPECIFIED:
DIMENSIONS ARE IN mm

TOLERANCES:
x = ± 0.75
x.x = ± 0.25
x.xx = ± 0.13
x.xxx = ±0.01

ANGULAR
x = ± 1 DEG.
x.x = ± 0.5 DEG.

MATERIAL
6061-T6

STOCK

FINISH
Clear Anodized

COMMENTS:



2G Robotics Inc.
2-614 Colby Dr., Waterloo ON. Canada, N2V 1A2

TITLE:
Scanner Base

| SIZE | DWG. NO. | REV |
|---|---|---|
| B | BP008-000-000-01 | A6 |

SHEET 4 OF 4

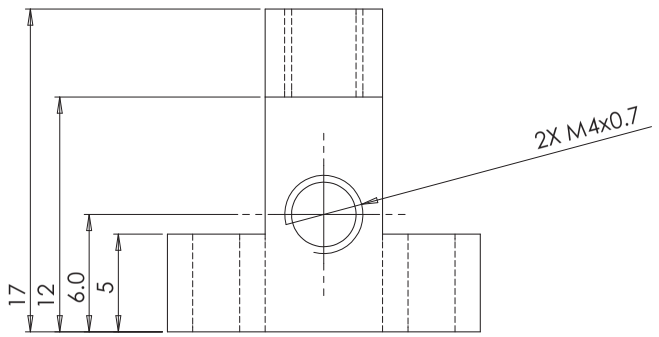


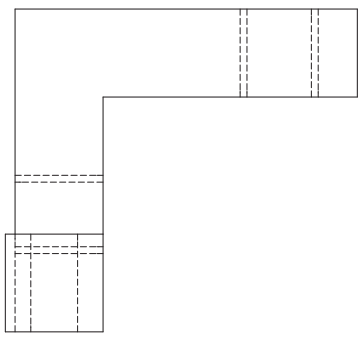

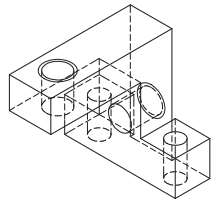

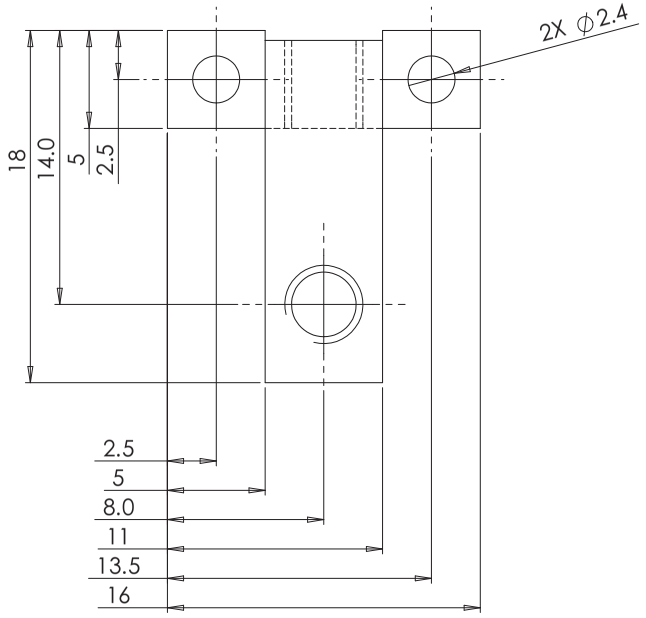


81



UNLESS OTHERWISE SPECIFIED:

DIMENSIONS ARE IN mm

TOLERANCES:
0.x = +/- 0.03
0.xx = +/- 0.01
0.xxx = +/- 0.005
x/x = +/- 1/32

MATERIAL: 6061-T6

STOCK:

FINISH: Clear Anodize

| | NAME | DATE |
|---|---|---|
| MODEL | G. Dijkema | 10/14/09 |
| DRAWING | G. Dijkema | 10/15/09 |

COMMENTS:

2G Robotics Inc.
2-614 Colby Dr., Waterloo ON. Canada, N2V 1A2

TITLE: Set Collar

| SIZE | DWG. NO. | REV |
|---|---|---|
| B | BP008-000-000-02 | A2 |

SHEET 1 OF 1

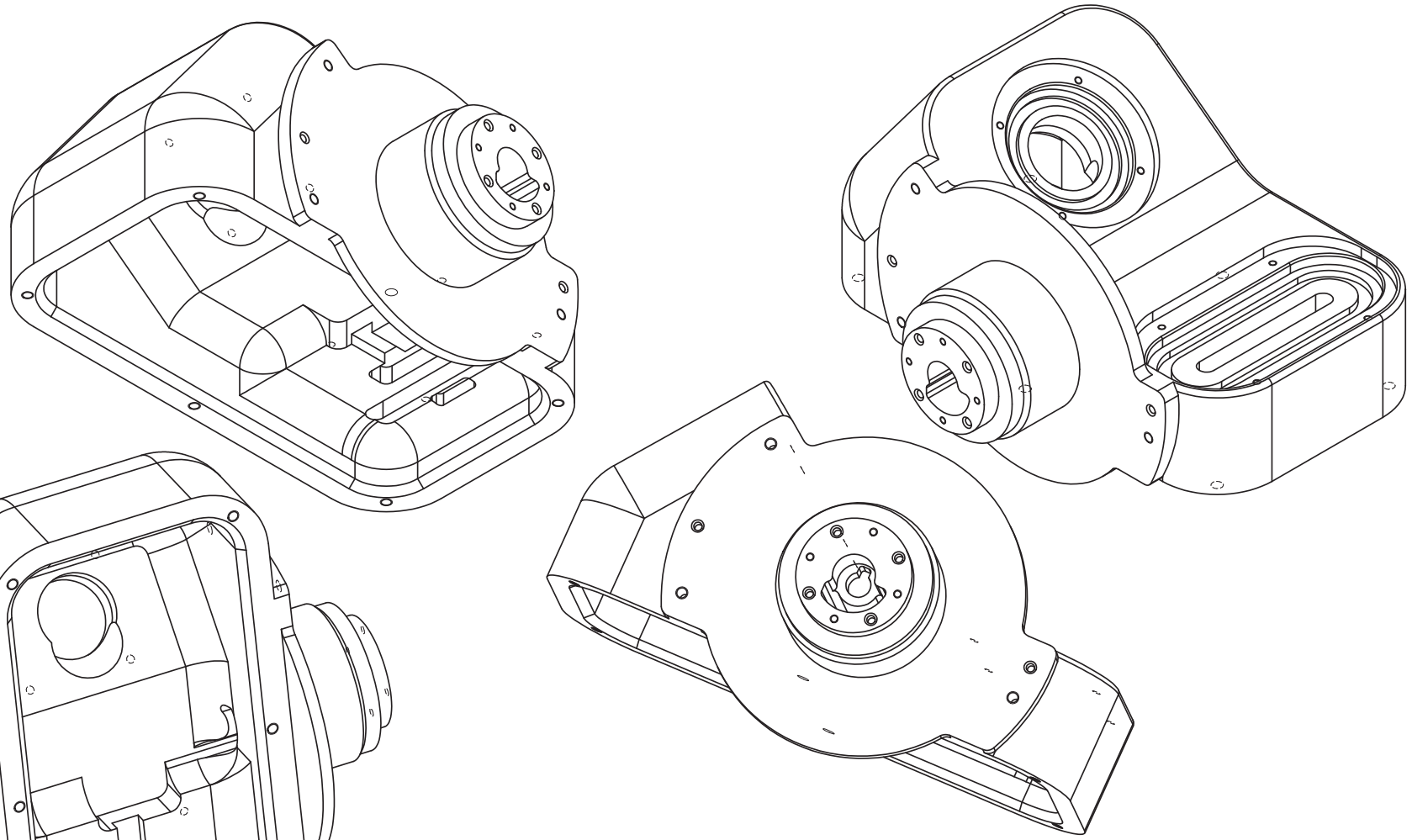

82

| UNLESS OTHERWISE SPECIFIED: | | NAME | DATE |
|---|---|---|---|
| DIMENSIONS ARE IN mm | MODEL | G. Dijkema | 10/15/2009 |
| TOLERANCES:<br>x = ± 0.75<br>x.x = ± 0.25<br>x.xx = ± 0.13<br>x.xxx = ±0.01 | DRAWING | G. Dijkema | 10/15/2009 |
| ANGULAR<br>x = ± 1 DEG.<br>x.x = ± 0.5 DEG. | COMMENTS: | | |
| MATERIAL<br>6061-T6 | | | |
| STOCK | | | |
| FINISH<br>Clear Anodize | | | |



2G Robotics Inc.

2-614 Colby Dr., Waterloo ON. Canada, N2V 1A2

TITLE: Scanner Case

| SIZE | DWG. NO. | REV |
|---|---|---|
| B | BP008-000-000-03 | A4 |

SHEET 1 OF 8

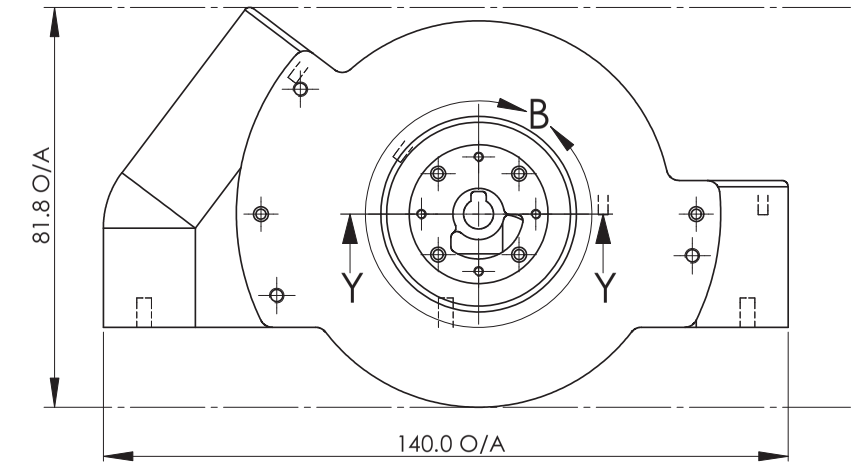


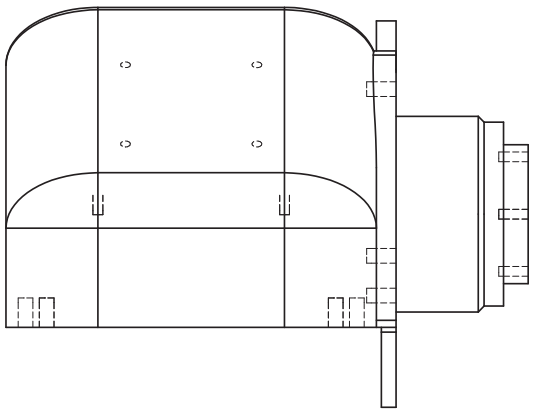

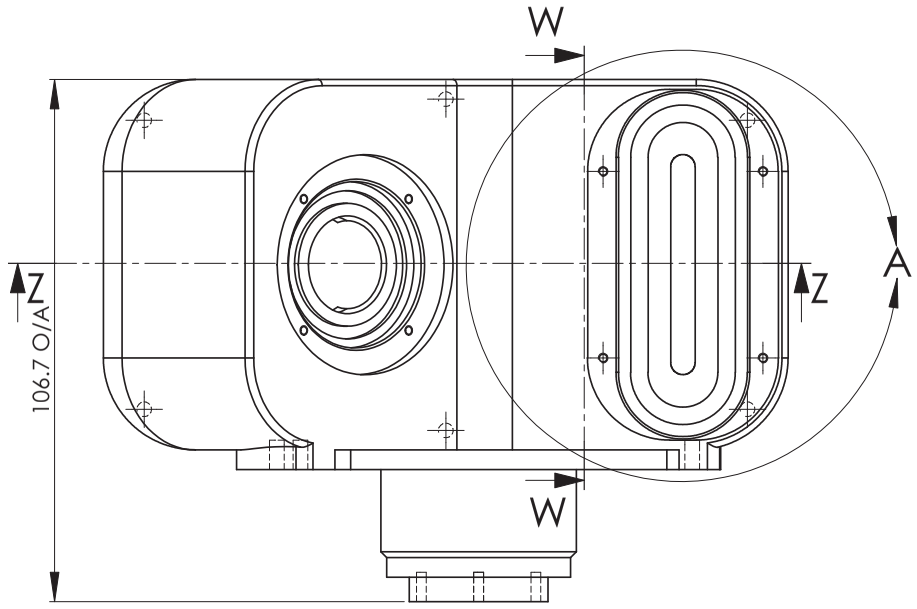


SECTION W-W
SCALE 1 : 1

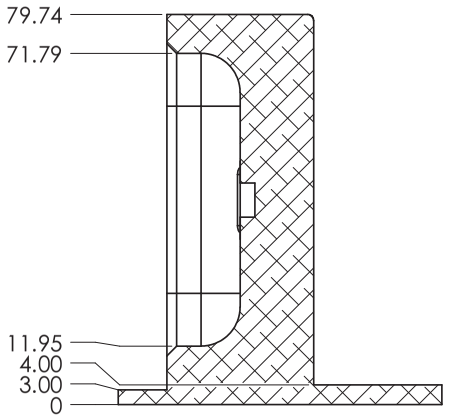


83

| | | |
|---|---|---|
| UNLESS OTHERWISE SPECIFIED: | | |
| DIMENSIONS ARE IN mm | | |
| TOLERANCES:<br>x = ± 0.75<br>x.x = ± 0.25<br>x.xx = ± 0.13<br>x.xxx = ±0.01 | | |
| ANGULAR<br>x = ± 1 DEG.<br>x.x = ± 0.5 DEG. | | |
| MATERIAL<br>6061-T6 | | |
| STOCK | | |
| FINISH<br>Clear Anodize | | |

| | NAME | DATE |
|---|---|---|
| MODEL | G. Dijkema | 10/16/2009 |
| DRAWING | G. Dijkema | 10/16/2009 |

COMMENTS:



2G Robotics Inc.
2-614 Colby Dr., Waterloo ON. Canada, N2V 1A2

TITLE: Scanner Case

| SIZE | DWG. NO. | REV |
|---|---|---|
| B | BP008-000-000-03 | A4 |

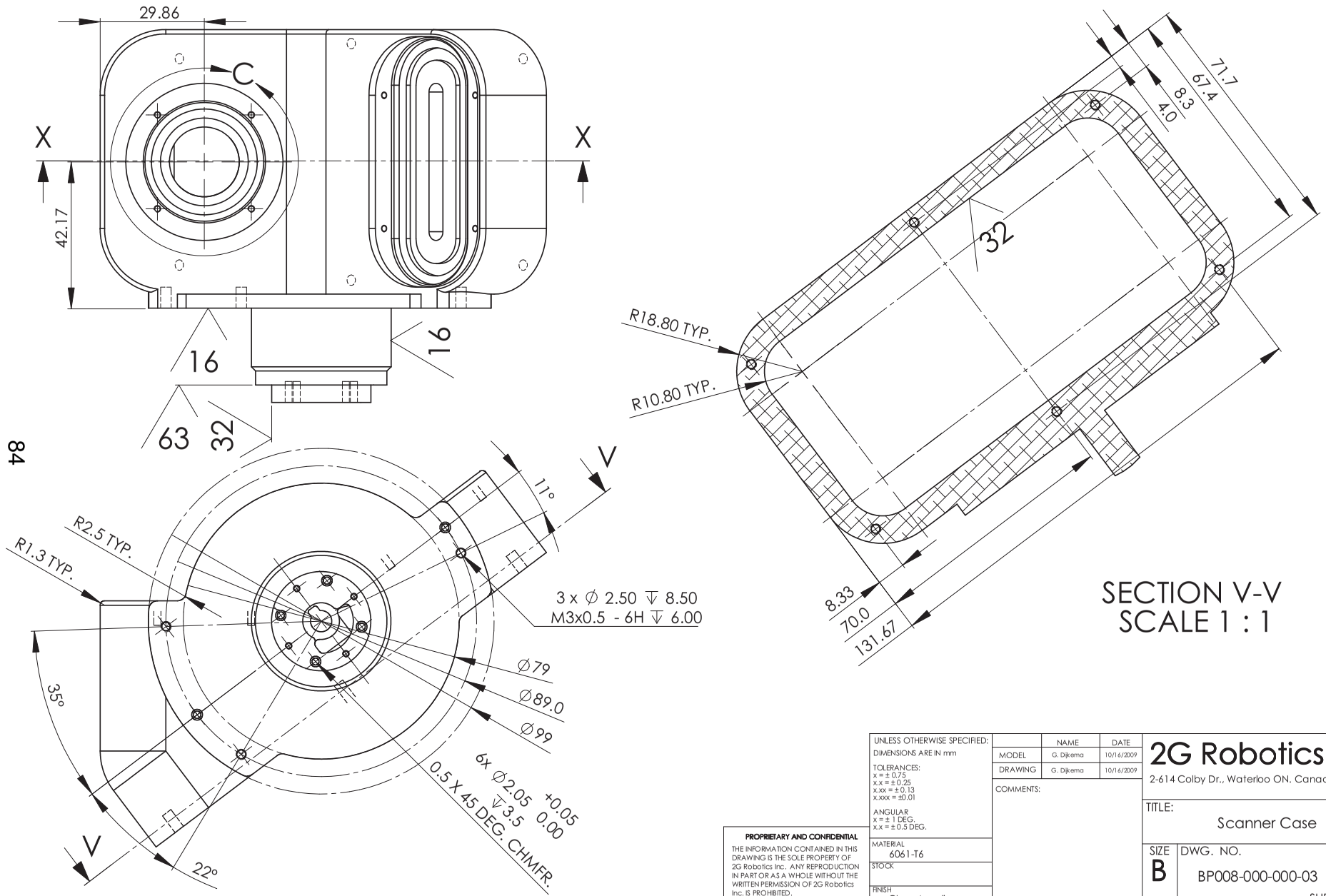


SECTION V-V
SCALE 1 : 1



UNLESS OTHERWISE SPECIFIED:
DIMENSIONS ARE IN mm

TOLERANCES:
x = ± 0.75
x.x = ± 0.25
x.xx = ± 0.13
x.xxx = ±0.01

ANGULAR
x = ± 1 DEG.
x.x = ± 0.5 DEG.

MATERIAL: 6061-T6
STOCK:
FINISH: Clear Anodize

| | NAME | DATE |
|---|---|---|
| MODEL | G. Dijkema | 10/16/2009 |
| DRAWING | G. Dijkema | 10/16/2009 |

COMMENTS:


2G Robotics Inc.
2-614 Colby Dr., Waterloo ON. Canada, N2V 1A2


TITLE: Scanner Case

| SIZE | DWG. NO. | REV |
|---|---|---|
| B | BP008-000-000-03 | A4 |

SHEET 3 OF 8

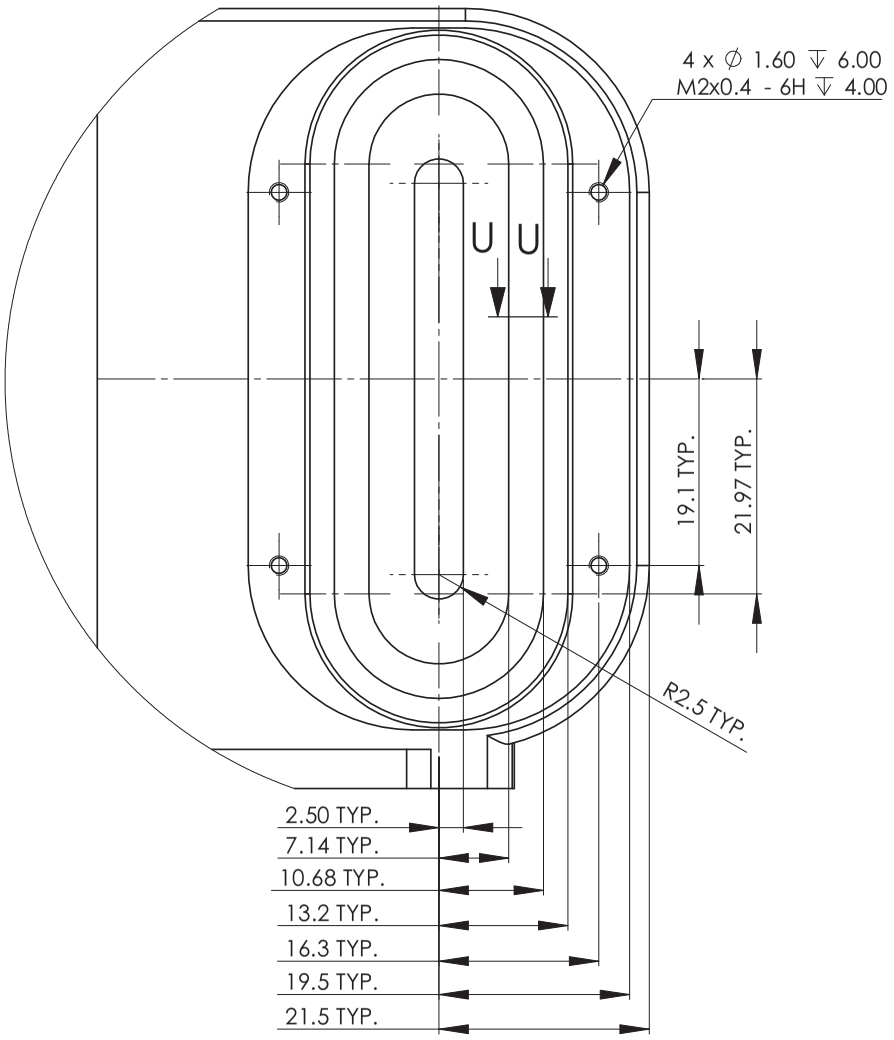


DETAIL A
SCALE 2 : 1

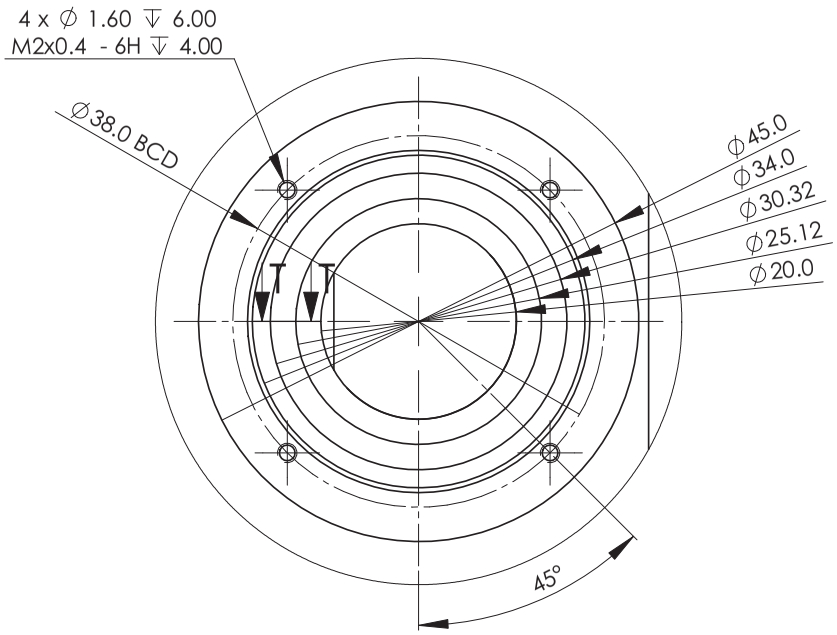


DETAIL C
SCALE 2 : 1

85



UNLESS OTHERWISE SPECIFIED:
DIMENSIONS ARE IN mm

TOLERANCES:
x = ± 0.75
x.x = ± 0.25
x.xx = ± 0.13
x.xxx = ±0.01

ANGULAR
x = ± 1 DEG.
x.x = ± 0.5 DEG.

MATERIAL: 6061-T6
STOCK:
FINISH: Clear Anodize

| | NAME | DATE |
|---|---|---|
| MODEL | G. Dijkema | 10/16/2009 |
| DRAWING | G. Dijkema | 10/16/2009 |

COMMENTS:

2G Robotics Inc.
2-614 Colby Dr., Waterloo ON. Canada, N2V 1A2

TITLE: Scanner Case

| SIZE | DWG. NO. | REV |
|---|---|---|
| B | BP008-000-000-03 | A4 |

SHEET 4 OF 8

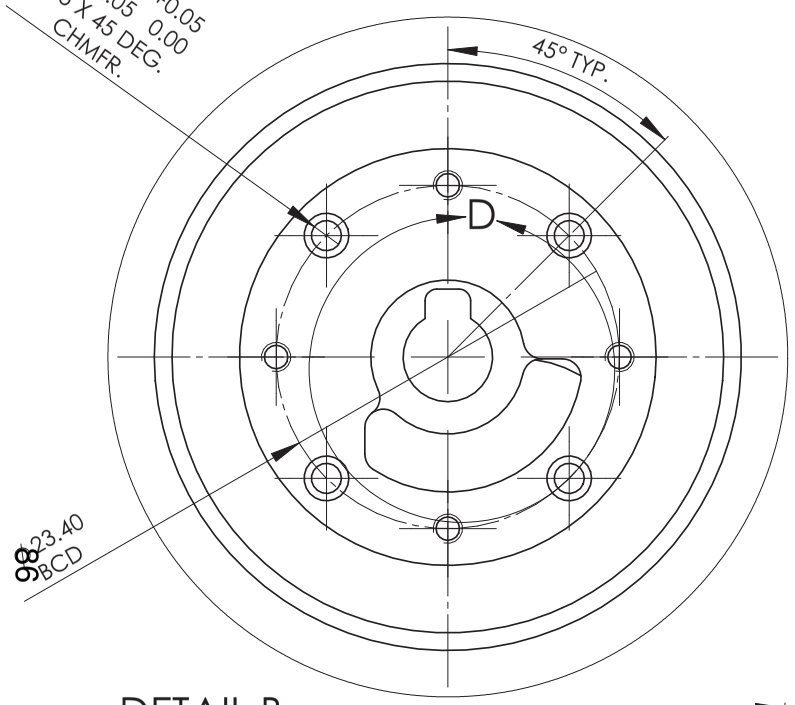


DETAIL B
SCALE 3 : 1

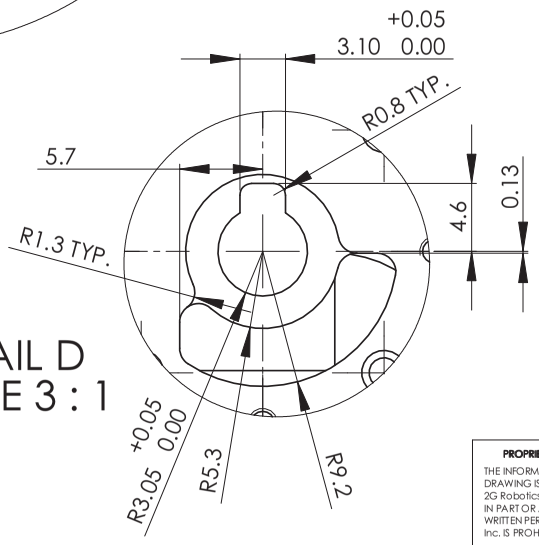


DETAIL D
SCALE 3 : 1

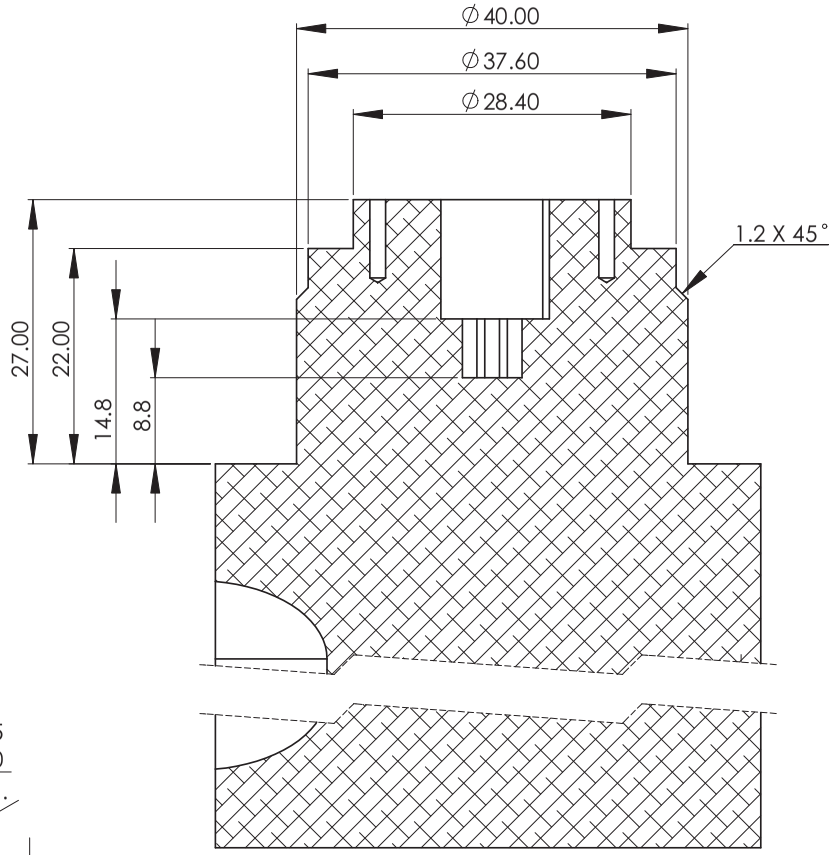


SECTION Y-Y
SCALE 2 : 1

| | | |
|---|---|---|
| UNLESS OTHERWISE SPECIFIED: | | |
| DIMENSIONS ARE IN mm | | |
| TOLERANCES: x = ± 0.75, x.x = ± 0.25, x.xx = ± 0.13, x.xxx = ±0.01 | | |
| ANGULAR x = ± 1 DEG., x.x = ± 0.5 DEG. | | |
| MATERIAL 6061-T6 | | |
| STOCK | | |
| FINISH Clear Anodize | | |

| | NAME | DATE |
|---|---|---|
| MODEL | G. Dijkema | 10/16/2009 |
| DRAWING | G. Dijkema | 10/16/2009 |

COMMENTS:



**2G Robotics Inc.**
2-614 Colby Dr., Waterloo ON. Canada, N2V 1A2

TITLE: Scanner Case

| SIZE | DWG. NO. | REV |
|---|---|---|
| B | BP008-000-000-03 | A4 |

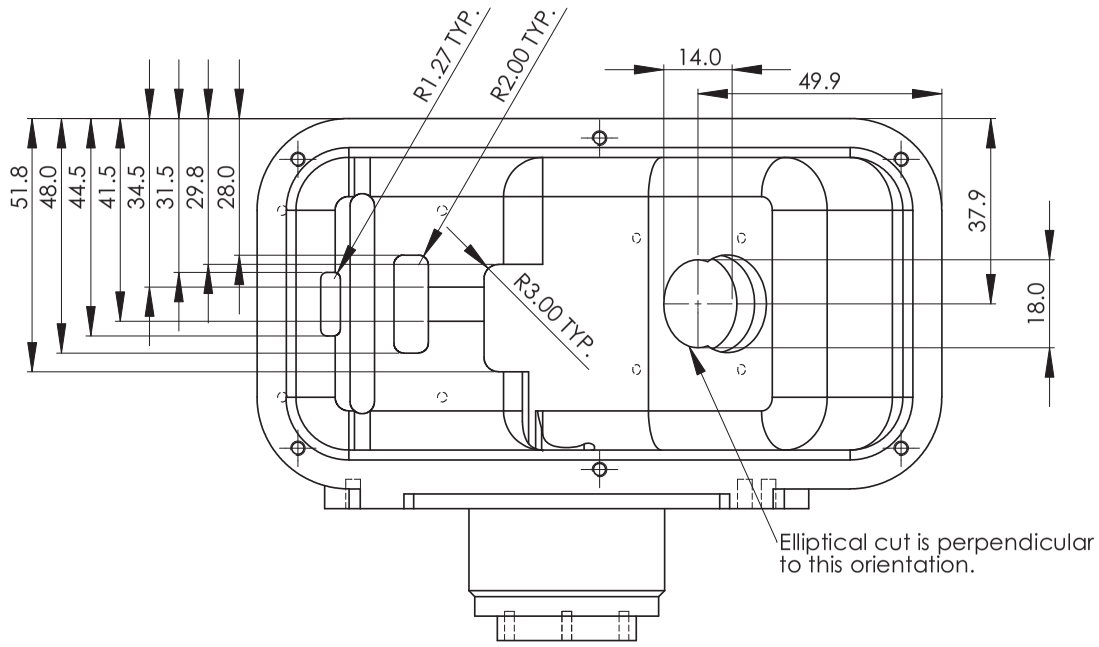


87

| | | |
|---|---|---|
| UNLESS OTHERWISE SPECIFIED: | | |
| DIMENSIONS ARE IN mm | | |
| TOLERANCES:<br>x = ± 0.75<br>x.x = ± 0.25<br>x.xx = ± 0.13<br>x.xxx = ±0.01 | | |
| ANGULAR<br>x = ± 1 DEG.<br>x.x = ± 0.5 DEG. | | |
| MATERIAL<br>6061-T6 | | |
| STOCK | | |
| FINISH<br>Clear Anodize | | |

| | NAME | DATE |
|---|---|---|
| MODEL | G. Dijkema | 10/16/2009 |
| DRAWING | G. Dijkema | 10/16/2009 |

COMMENTS:



2G Robotics Inc.
2-614 Colby Dr., Waterloo ON. Canada, N2V 1A2

TITLE: Scanner Case

| SIZE | DWG. NO. | REV |
|---|---|---|
| B | BP008-000-000-03 | A4 |

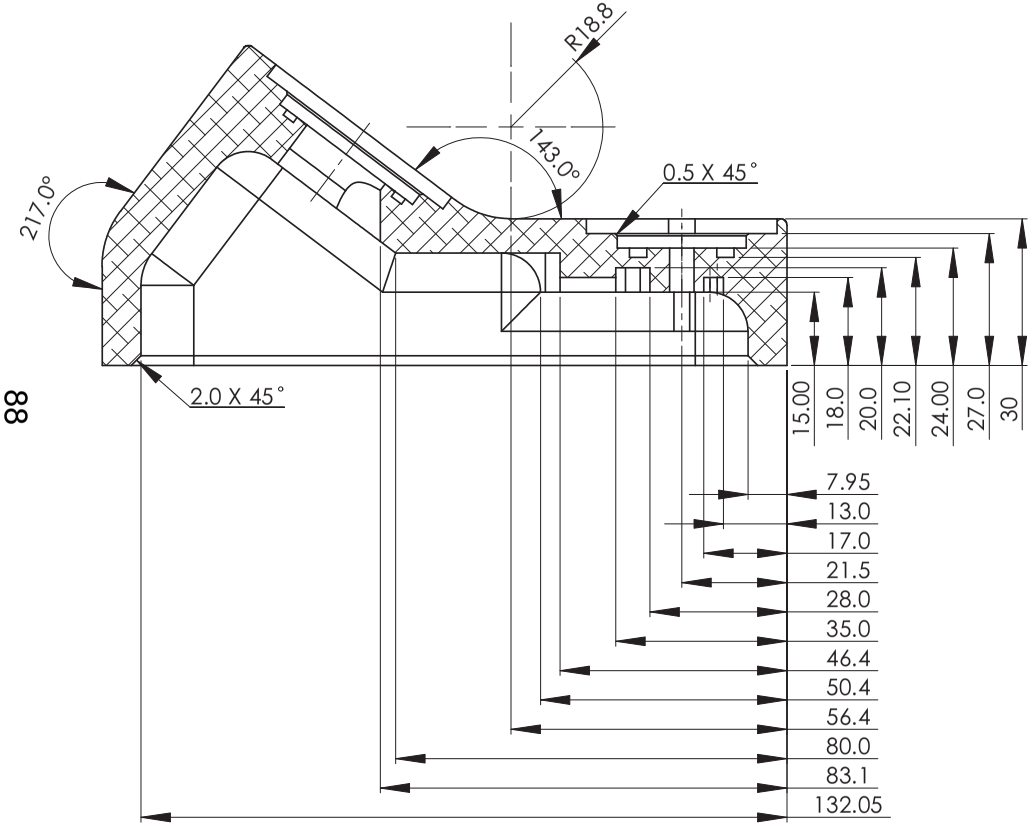


SECTION Z-Z
SCALE 1 : 1

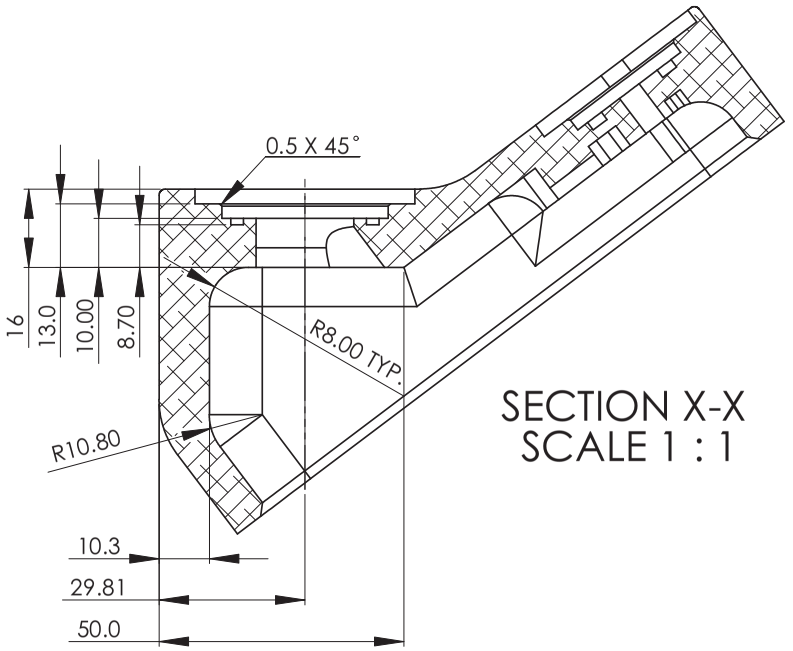


SECTION X-X
SCALE 1 : 1

88



UNLESS OTHERWISE SPECIFIED:
DIMENSIONS ARE IN mm
TOLERANCES:
x = ± 0.75
x.x = ± 0.25
x.xx = ± 0.13
x.xxx = ±0.01
ANGULAR
x = ± 1 DEG.
x.x = ± 0.5 DEG.
MATERIAL
6061-T6
STOCK
FINISH
Clear Anodize

| | NAME | DATE |
|---|---|---|
| MODEL | G. Dijkema | 10/16/2009 |
| DRAWING | G. Dijkema | 10/16/2009 |

COMMENTS:

2G Robotics Inc.
2-614 Colby Dr., Waterloo ON. Canada, N2V 1A2

TITLE:
Scanner Case

| SIZE | DWG. NO. | REV |
|---|---|---|
| B | BP008-000-000-03 | A4 |

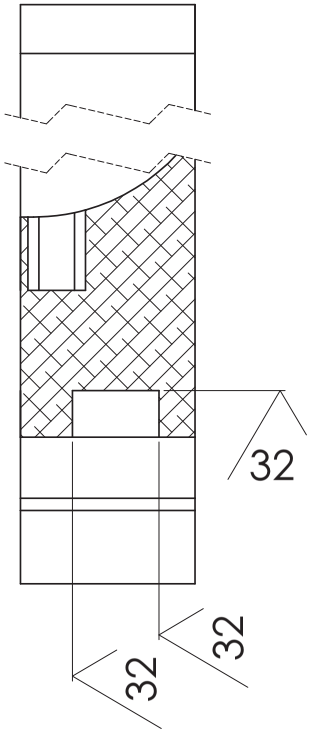


SECTION U-U
SCALE 5 : 1

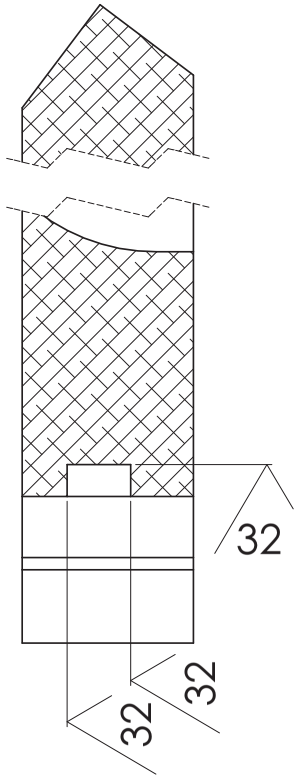


SECTION T-T
SCALE 5 : 1

68



UNLESS OTHERWISE SPECIFIED:
DIMENSIONS ARE IN mm

TOLERANCES:
x = ± 0.75
x.x = ± 0.25
x.xx = ± 0.13
x.xxx = ±0.01

ANGULAR
x = ± 1 DEG.
x.x = ± 0.5 DEG.

MATERIAL: 6061-T6

STOCK:

FINISH: Clear Anodize

| | NAME | DATE |
|---|---|---|
| MODEL | G. Dijkema | 10/16/2009 |
| DRAWING | G. Dijkema | 10/16/2009 |

COMMENTS:

2G Robotics Inc.
2-614 Colby Dr., Waterloo ON. Canada, N2V 1A2

TITLE: Scanner Case

| SIZE | DWG. NO. | REV |
|---|---|---|
| B | BP008-000-000-03 | A4 |

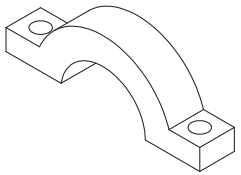

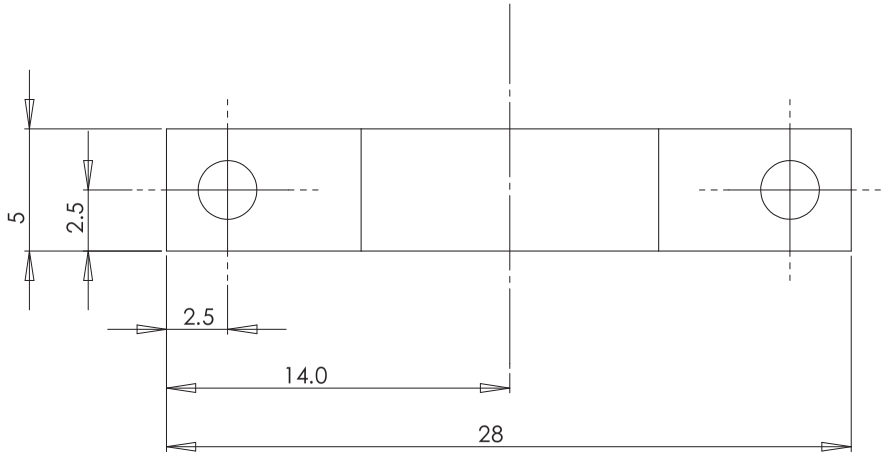


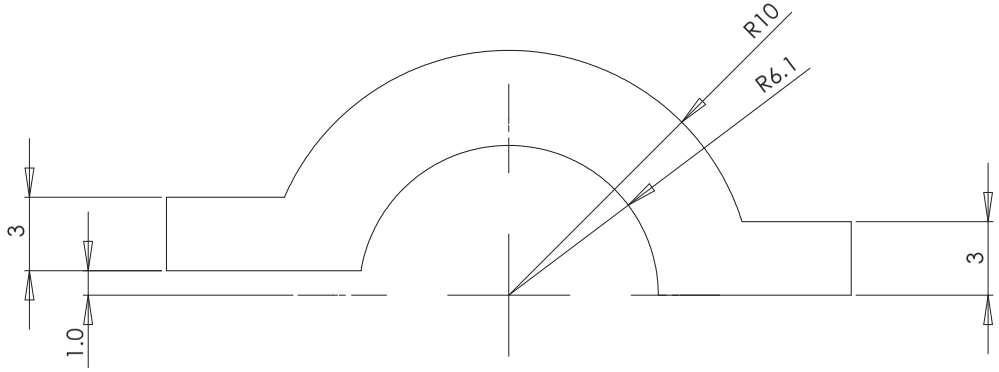


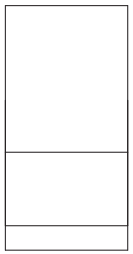

06

| UNLESS OTHERWISE SPECIFIED: | | NAME | DATE |
|---|---|---|---|
| DIMENSIONS ARE IN mm | MODEL | T. Ciochan | 2/23/2009 |
| TOLERANCES:<br>x = ± 0.75<br>x.x = ± 0.25<br>x.xx = ± 0.13<br>x.xxx = ±0.01 | DRAWING | T. Ciochan | 10/15/2009 |
| ANGULAR<br>x = ± 1 DEG.<br>x.x = ± 0.5 DEG. | COMMENTS: | | |
| MATERIAL<br>6061-T6 | | | |
| STOCK | | | |
| FINISH<br>Clear Anodize | | | |



2G Robotics Inc.
2-614 Colby Dr., Waterloo ON. Canada, N2V 1A2

TITLE: Collar

| SIZE | DWG. NO. | REV |
|---|---|---|
| B | BP008-000-000-04 | B1 |

SHEET 1 OF 1

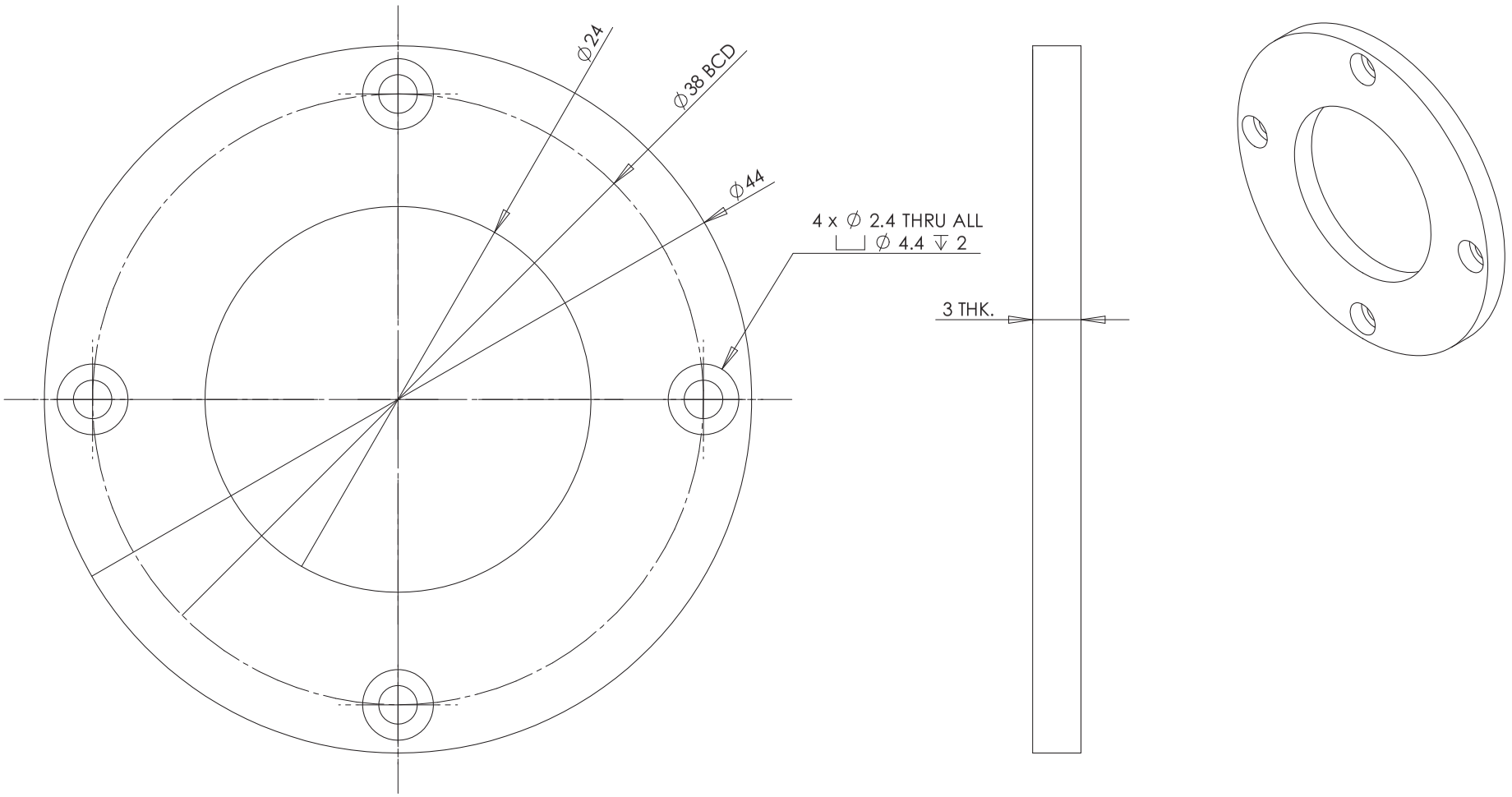






UNLESS OTHERWISE SPECIFIED:

DIMENSIONS ARE IN mm

TOLERANCES:
0.x = +/- 0.03
0.xx = +/- 0.01
0.xxx = +/- 0.005
x/x = +/- 1/32

MATERIAL: 6061-T6

STOCK:

FINISH: Black Anodized

| | NAME | DATE |
|---|---|---|
| MODEL | T. Ciochan | 01/23/09 |
| DRAWING | T. Ciochan | 01/23/09 |

COMMENTS:

2G Robotics Inc.
2-614 Colby Dr., Waterloo ON. Canada, N2V 1A2

TITLE: Camera Seal Clamp

| SIZE | DWG. NO. | REV |
|---|---|---|
| B | BP008-000-000-05 | A1 |

SHEET 1 OF 1

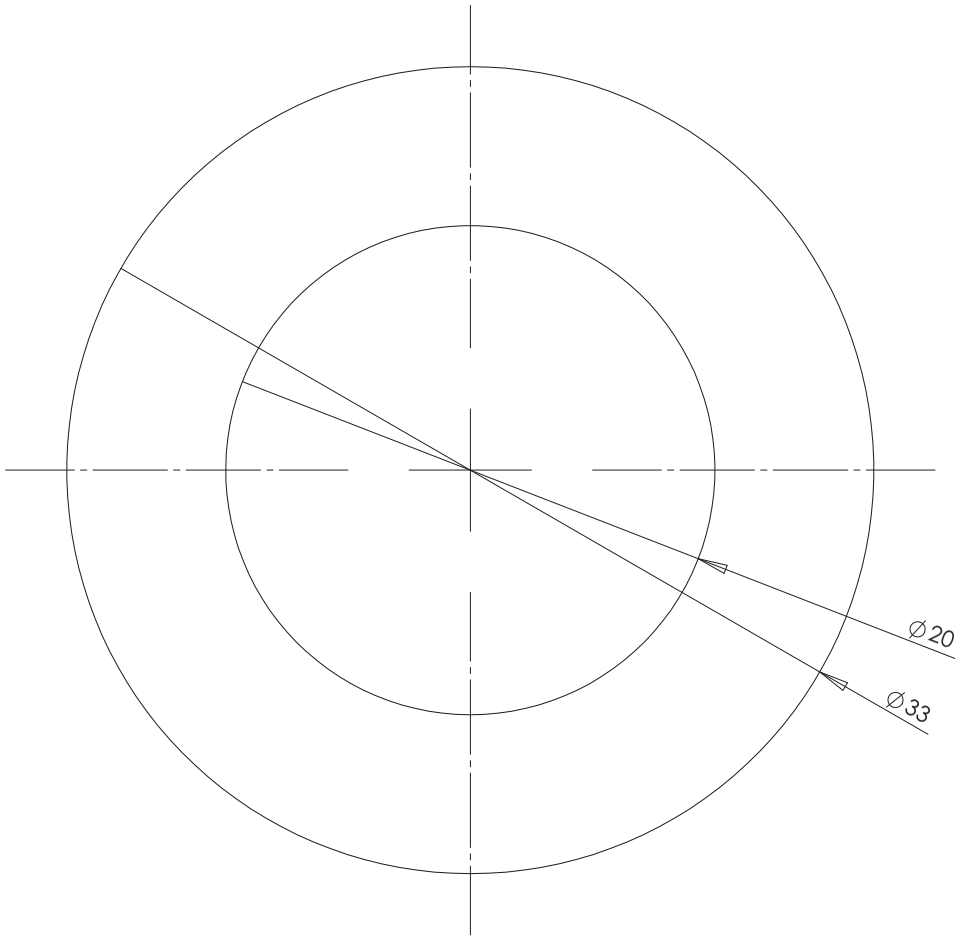


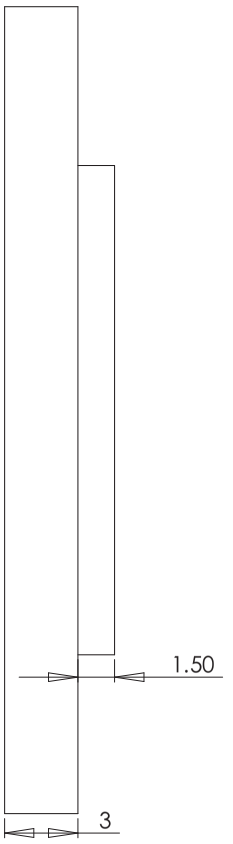


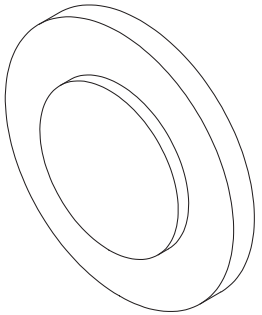

92

| UNLESS OTHERWISE SPECIFIED: | | NAME | DATE |
|---|---|---|---|
| DIMENSIONS ARE IN mm | MODEL | G. Dijkema | 10/15/09 |
| TOLERANCES:<br>x = ± 0.75<br>x.x = ± 0.25<br>x.xx = ± 0.13<br>x.xxx = ±0.01 | DRAWING | G. Dijkema | 10/15/09 |
| ANGULAR<br>x = ± 1 DEG.<br>x.x = ± 0.5 DEG. | COMMENTS: Two outermost parallel faces to be optically transparent. | | |
| MATERIAL: Clear Lexan | | | |
| STOCK | | | |
| FINISH: - | | | |



2G Robotics Inc.
2-614 Colby Dr., Waterloo ON. Canada, N2V 1A2

TITLE: Camera Glass

| SIZE | DWG. NO. | REV |
|---|---|---|
| B | BP008-000-000-06 | A2 |

SHEET 1 OF 1

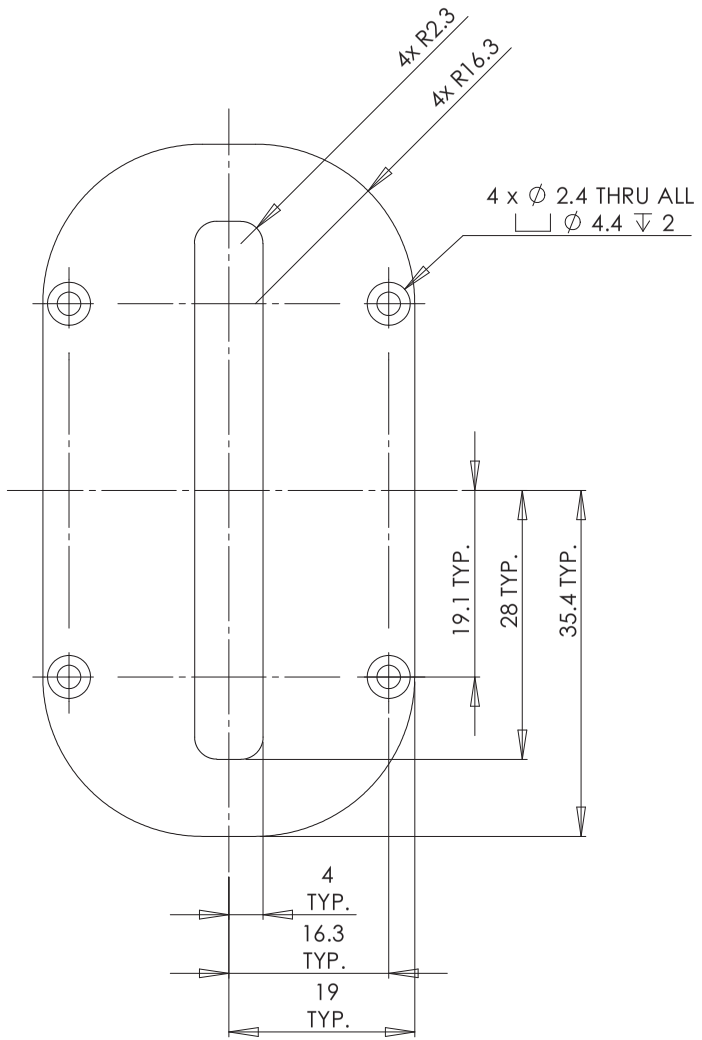


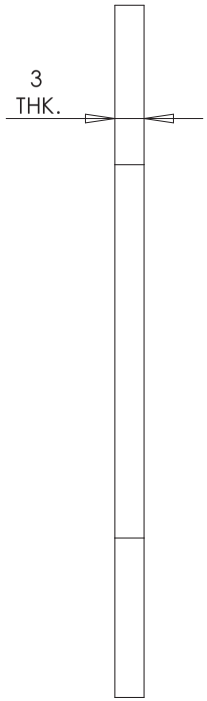


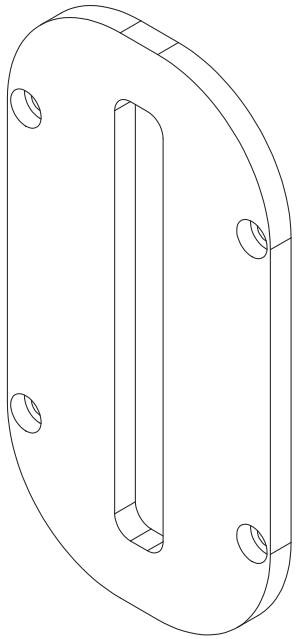

93

| UNLESS OTHERWISE SPECIFIED: | | NAME | DATE |
|---|---|---|---|
| DIMENSIONS ARE IN mm | MODEL | T. Ciochan | 01/14/09 |
| TOLERANCES:<br>x = ± 0.75<br>x.x = ± 0.25<br>x.xx = ± 0.13<br>x.xxx = ±0.01 | DRAWING | T. Ciochan | 01/14/09 |
| ANGULAR<br>x = ± 1 DEG.<br>x.x = ± 0.5 DEG. | COMMENTS: | | |
| MATERIAL<br>6061-T6 | | | |
| STOCK | | | |
| FINISH<br>Black Anodized | | | |



2G Robotics Inc.
2-614 Colby Dr., Waterloo ON. Canada, N2V 1A2

TITLE: Laser Window Clamp

| SIZE | DWG. NO. | REV |
|---|---|---|
| B | BP008-000-000-07 | A1 |

SHEET 1 OF 1

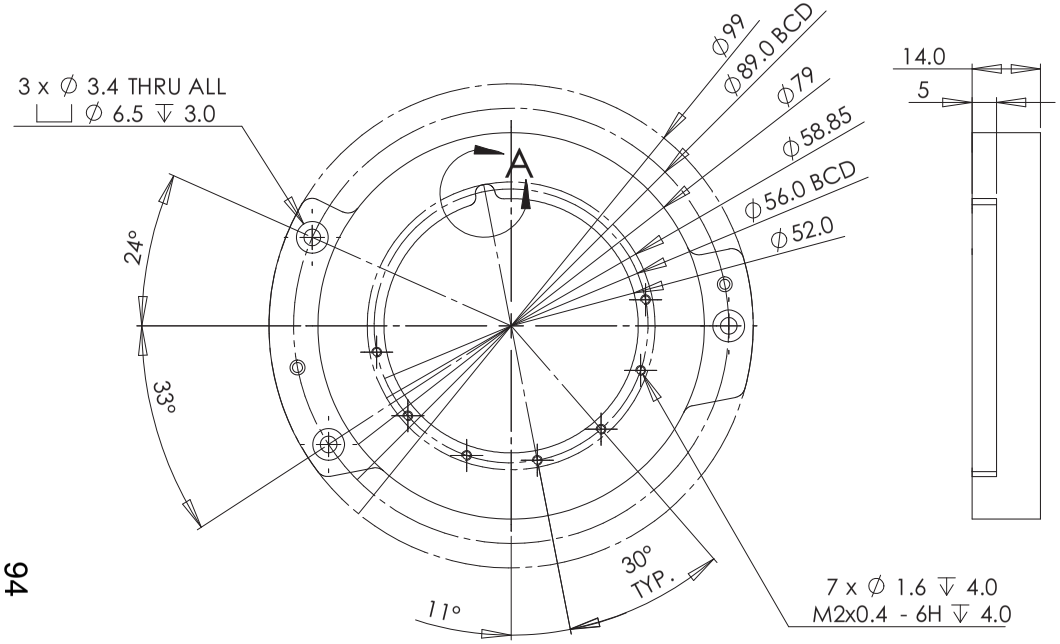





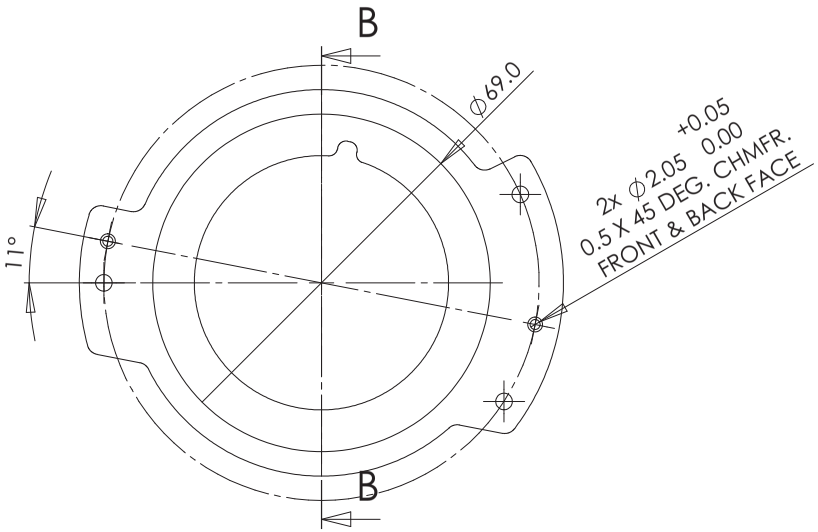


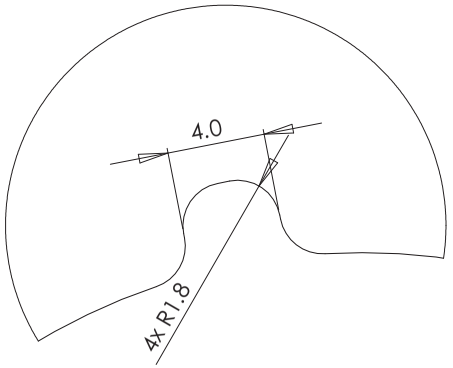


DETAIL A
SCALE 5 : 1

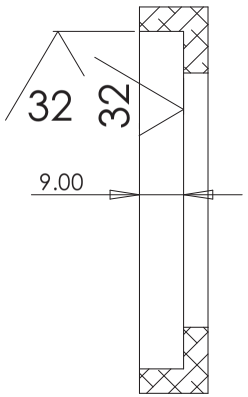


SECTION B-B

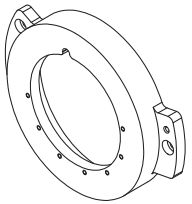

94



UNLESS OTHERWISE SPECIFIED:
DIMENSIONS ARE IN mm
TOLERANCES:
x = ± 0.75
x.x = ± 0.25
x.xx = ± 0.13
x.xxx = ±0.01
ANGULAR
x = ± 1 DEG.
x.x = ± 0.5 DEG.
MATERIAL: 6061-T6
STOCK:
FINISH: Black Anodized

| | NAME | DATE |
|---|---|---|
| MODEL | T. Ciochan | 01/16/09 |
| DRAWING | T. Ciochan | 01/16/09 |

COMMENTS:

2G Robotics Inc.
2-614 Colby Dr., Waterloo ON. Canada, N2V 1A2

TITLE: Joining Bracket

| SIZE | DWG. NO. | REV |
|---|---|---|
| B | BP008-000-000-08 | A2 |

SHEET 1 OF 1

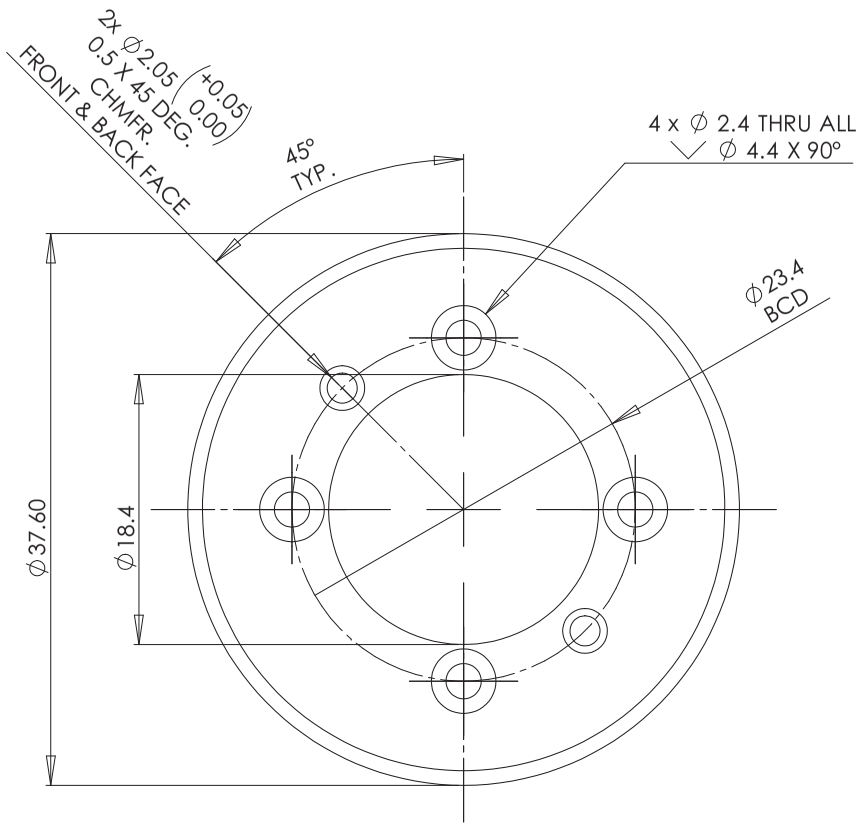


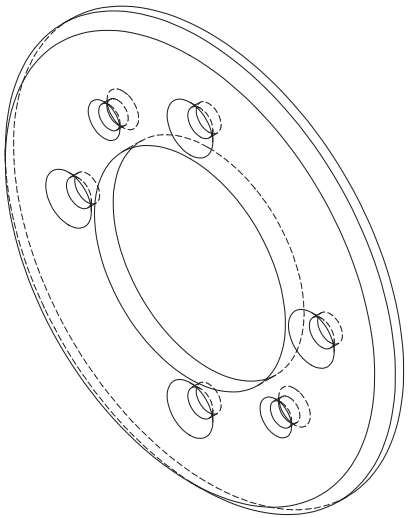

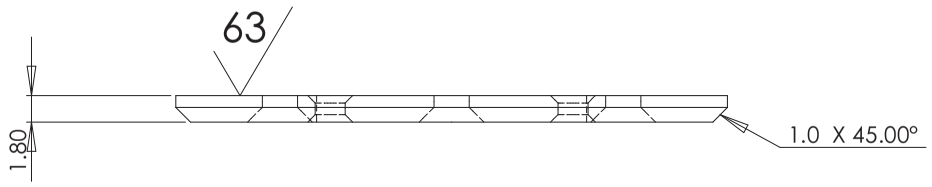


95

| UNLESS OTHERWISE SPECIFIED: | | NAME | DATE |
|---|---|---|---|
| DIMENSIONS ARE IN mm | MODEL | G. Dijkema | 10/15/09 |
| TOLERANCES: 0.x = +/- 0.03, 0.xx = +/- 0.01, 0.xxx = +/- 0.005, x/x = +/- 1/32 | DRAWING | G. Dijkema | 10/15/09 |
| MATERIAL: 6061-T6 | COMMENTS: Surface finishes are maximum acceptable. Very smooth surfaces are ideal. | | |
| STOCK: | | | |
| FINISH: Clear Anodize | | | |



2G Robotics Inc.
2-614 Colby Dr., Waterloo ON. Canada, N2V 1A2

TITLE: Dynamic Seal Cap

| SIZE | DWG. NO. | REV |
|---|---|---|
| B | BP008-000-000-09 | A5 |

SHEET 1 OF 1

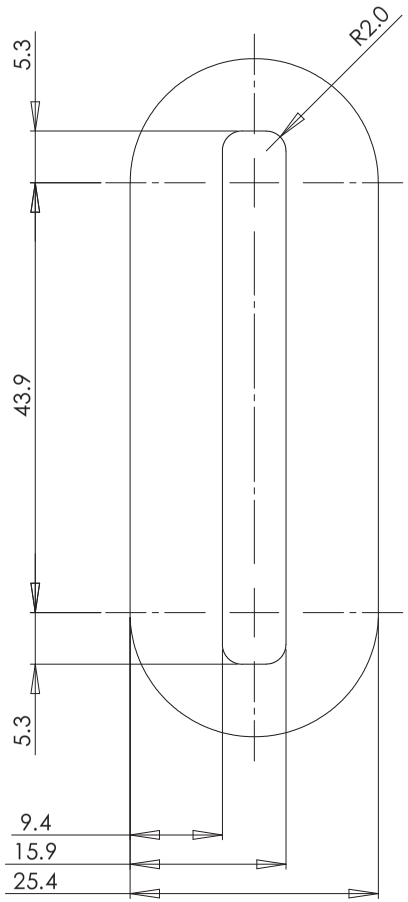


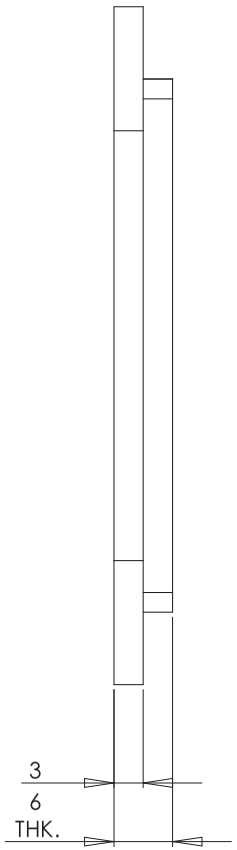


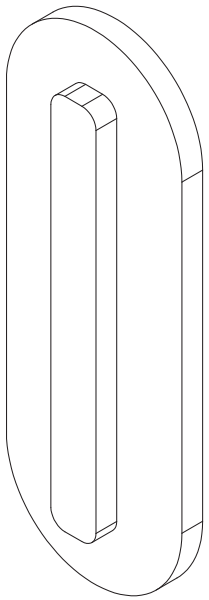

96



UNLESS OTHERWISE SPECIFIED:
DIMENSIONS ARE IN mm

TOLERANCES:
x = ± 0.75
x.x = ± 0.25
x.xx = ± 0.13
x.xxx = ±0.01

ANGULAR
x = ± 1 DEG.
x.x = ± 0.5 DEG.

MATERIAL
Clear Lexan

STOCK

FINISH
-

| | NAME | DATE |
|---|---|---|
| MODEL | T. Ciochan | 03/10/09 |
| DRAWING | T. Ciochan | 03/10/09 |

COMMENTS:
Two outermost parallel faces to be optically transparent.

2G Robotics Inc.
2-614 Colby Dr., Waterloo ON. Canada, N2V 1A2

TITLE:

| SIZE | DWG. NO. | REV |
|---|---|---|
| B | BP008-000-000-10 | A2 |

SHEET 1 OF 1

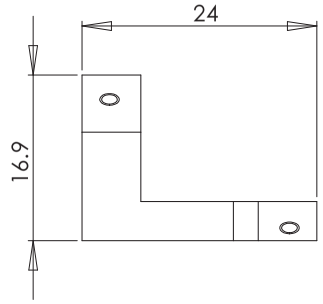


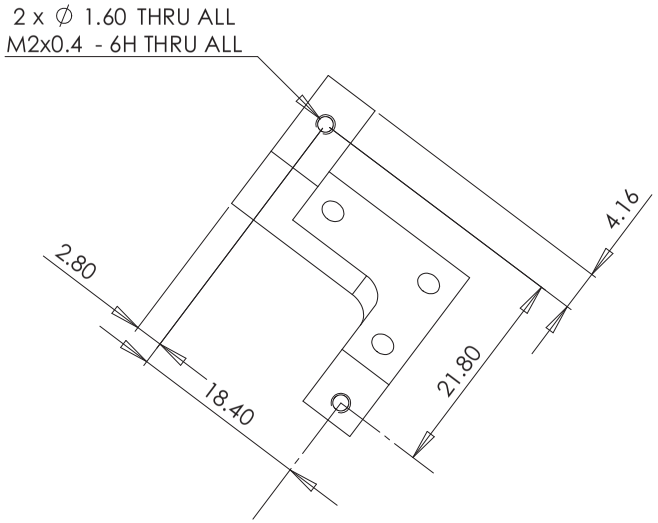


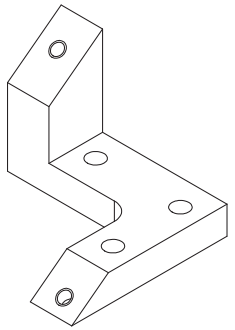

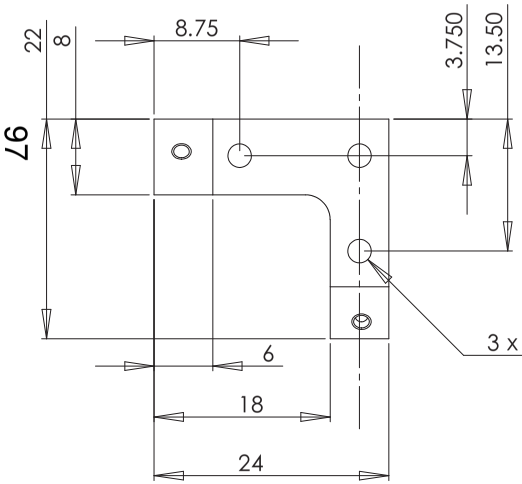


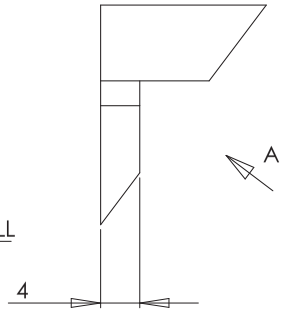


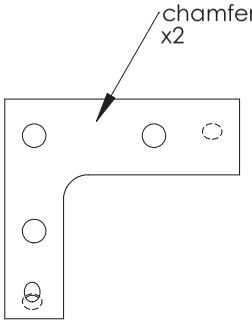


| UNLESS OTHERWISE SPECIFIED: | | NAME | DATE |
|---|---|---|---|
| DIMENSIONS ARE IN mm | MODEL | J. Gillham | 08/17/09 |
| TOLERANCES: x = ± 0.75, x.x = ± 0.25, x.xx = ± 0.13, x.xxx = ±0.01 | DRAWING | J. Gillham | 08/17/09 |
| ANGULAR x = ± 1 DEG., x.x = ± 0.5 DEG. | COMMENTS: | | |
| MATERIAL 6061-T6 | | | |
| STOCK | | | |
| FINISH - | | | |



2G Robotics Inc.
2-614 Colby Dr., Waterloo ON. Canada, N2V 1A2

TITLE: Camera Stand

| SIZE | DWG. NO. | REV |
|---|---|---|
| B | BP008-000-000-14 | A4 |

SHEET 1 OF 1

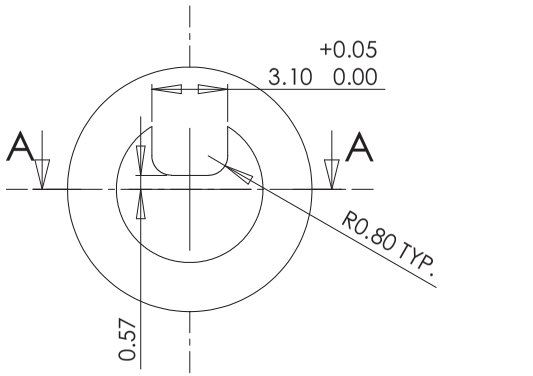


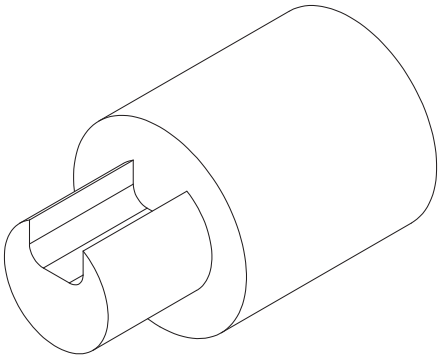

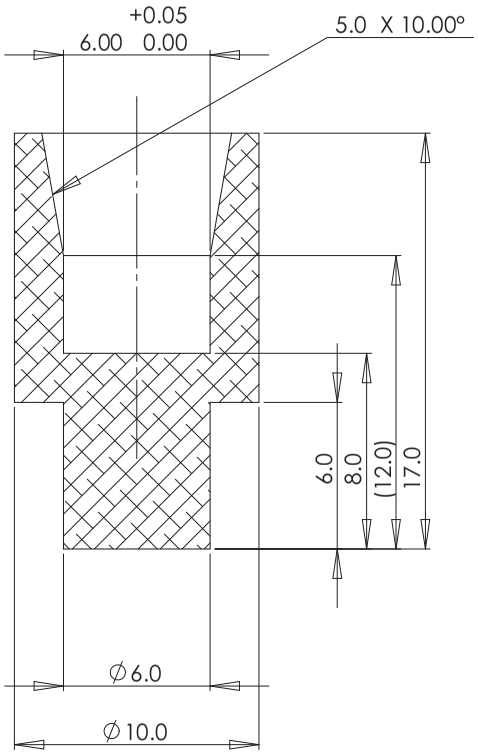


SECTION A-A

86



UNLESS OTHERWISE SPECIFIED:
DIMENSIONS ARE IN mm

TOLERANCES:
x = ± 0.75
x.x = ± 0.25
x.xx = ± 0.13
x.xxx = ±0.01

ANGULAR
x = ± 1 DEG.
x.x = ± 0.5 DEG.

MATERIAL
6061-T6

STOCK

FINISH
Clear Anodize

| | NAME | DATE |
|---|---|---|
| MODEL | G. Dijkema | 10/15/09 |
| DRAWING | G. Dijkema | 10/15/09 |

COMMENTS:

2G Robotics Inc.
2-614 Colby Dr., Waterloo ON. Canada, N2V 1A2

TITLE:

| SIZE | DWG. NO. | REV |
|---|---|---|
| B | BP008-000-001-003 | A2 |

SHEET 1 OF 1

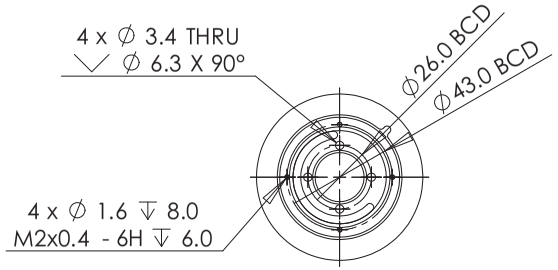


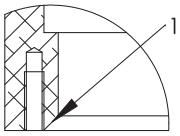


DETAIL F
SCALE 2 : 1

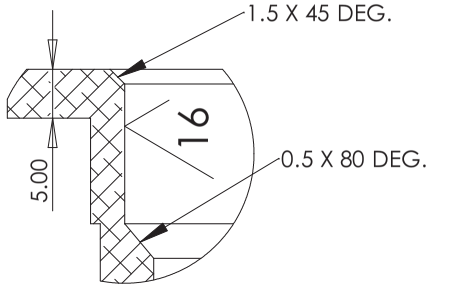


DETAIL D
SCALE 2 : 1

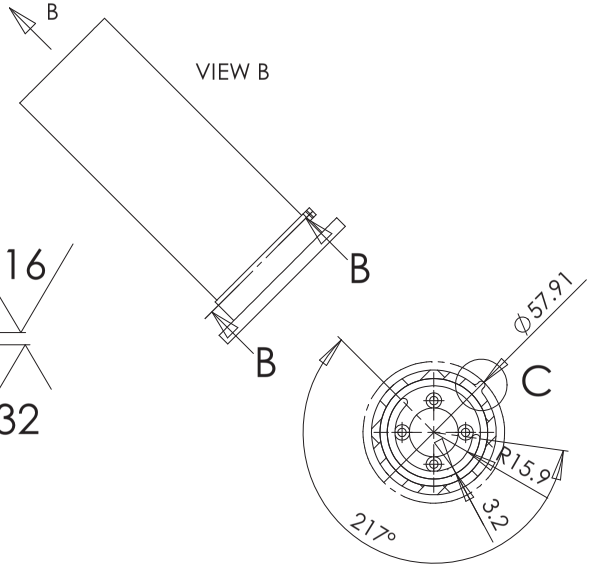


SECTION B-B

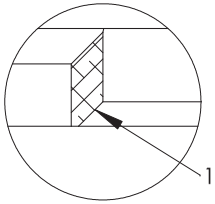


DETAIL E
SCALE 5 : 1

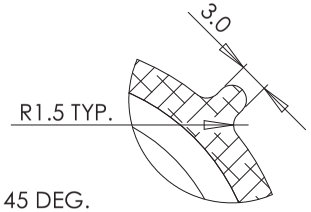


DETAIL C
SCALE 2 : 1

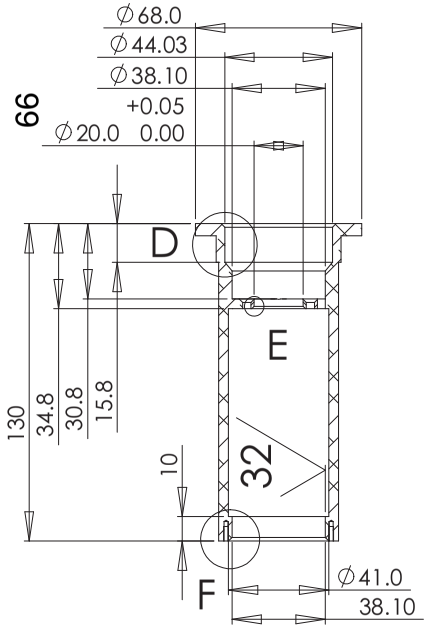


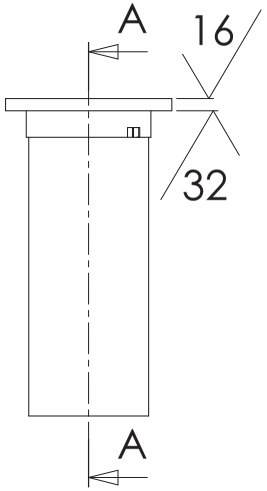


SECTION A-A



UNLESS OTHERWISE SPECIFIED:
DIMENSIONS ARE IN mm

TOLERANCES:
x = ± 0.75
x.x = ± 0.25
x.xx = ± 0.13
x.xxx = ±0.01

ANGULAR
x = ± 1 DEG.
x.x = ± 0.5 DEG.

MATERIAL
6061-T6

STOCK

FINISH
Clear Anodize

| | NAME | DATE |
|---|---|---|
| MODEL | T. Ciochon | 01/26/09 |
| DRAWING | T. Ciochon | 01/26/09 |

COMMENTS:

2G Robotics Inc.
2-614 Colby Dr., Waterloo ON. Canada, N2V 1A2

TITLE:
Motor Casement

| SIZE | DWG. NO. | REV |
|---|---|---|
| B | BP008-000-001-01 | A3 |

SHEET 1 OF 1

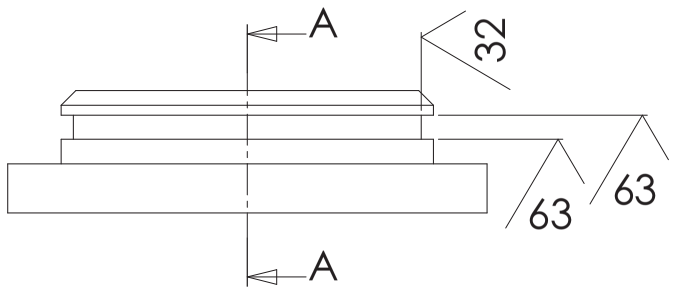


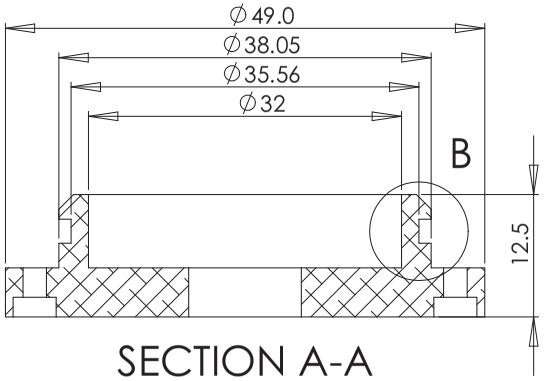


SECTION A-A

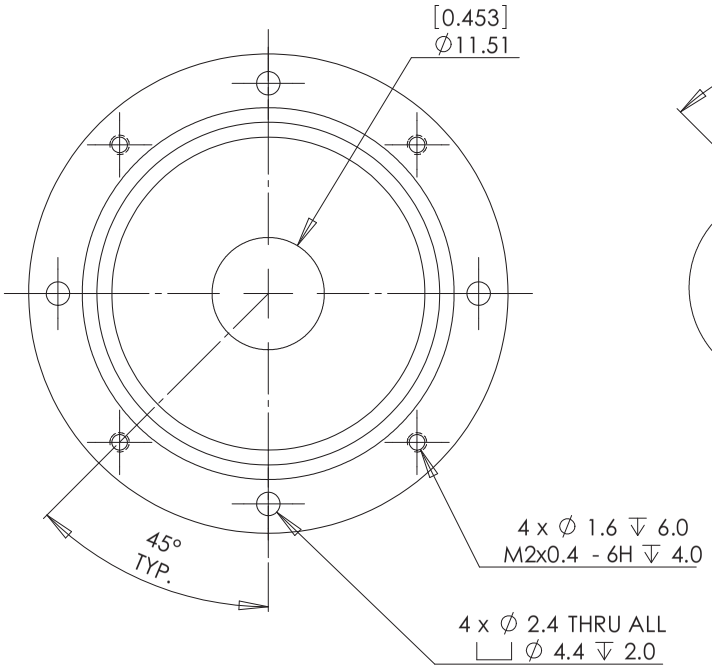


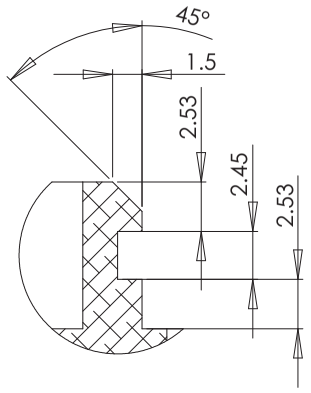


DETAIL B
SCALE 4 : 1

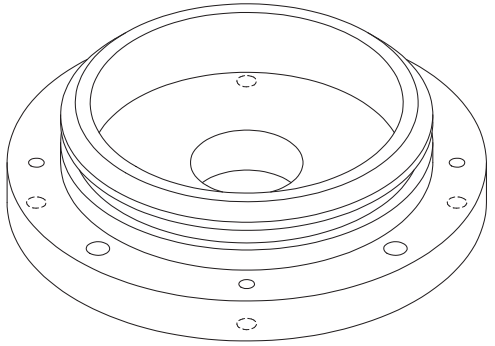

100

| | NAME | DATE |
|---|---|---|
| MODEL | T. Ciochan | 01/26/09 |
| DRAWING | T. Ciochan | 01/26/09 |

UNLESS OTHERWISE SPECIFIED:
DIMENSIONS ARE IN mm
TOLERANCES:
0.x = +/- 0.03
0.xx = +/- 0.01
0.xxx = +/- 0.005
x/x = +/- 1/32

COMMENTS:

MATERIAL: 6061-T6
STOCK:
FINISH: Clear Anodize



2G Robotics Inc.
2-614 Colby Dr., Waterloo ON. Canada, N2V 1A2

TITLE: Motor Casement End Cap

| SIZE | DWG. NO. | REV |
|---|---|---|
| B | BP008-000-001-02 | A3 |

SHEET 1 OF 1

# Appendix C

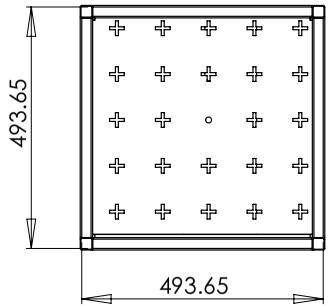


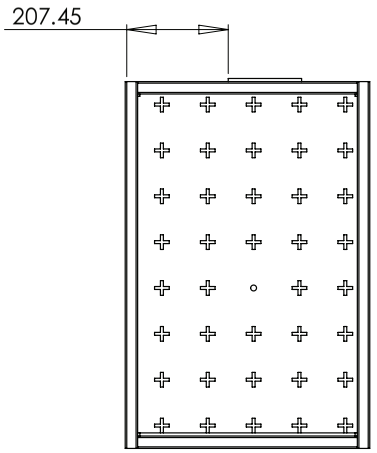


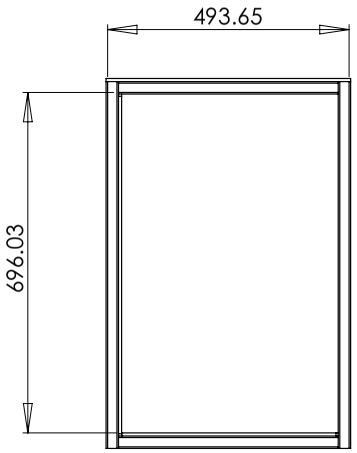


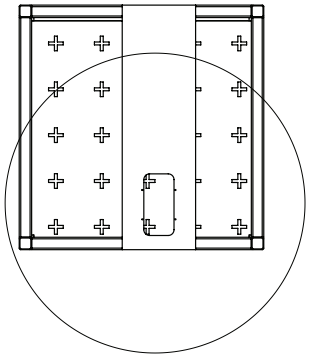


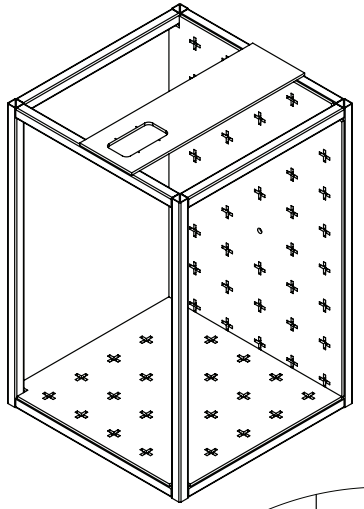

DETAIL A
SCALE 1 : 5

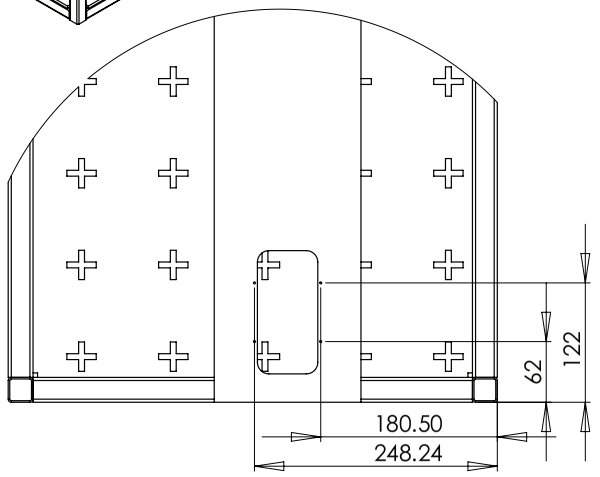


102



UNLESS OTHERWISE SPECIFIED:
DIMENSIONS ARE IN mm
TOLERANCES:
x = ± 0.75
x.x = ± 0.25
x.xx = ± 0.13
x.xxx = ±0.01
ANGULAR
x = ± 1 DEG.
x.x = ± 0.5 DEG.
MATERIAL
STOCK
FINISH

| | NAME | DATE |
|---|---|---|
| MODEL | | 8/9/2011 |
| DRAWING | J.G. GILLHAM | 8/9/2011 |

COMMENTS:
Rectangular weldement to hold flat plates

2G Robotics Inc.
2-614 Colby Dr., Waterloo ON. Canada, N2V 1A2

TITLE:

| SIZE | DWG. NO. | REV |
|---|---|---|
| B | Calibration Rig Overall | A1 |

SHEET 1 OF 1

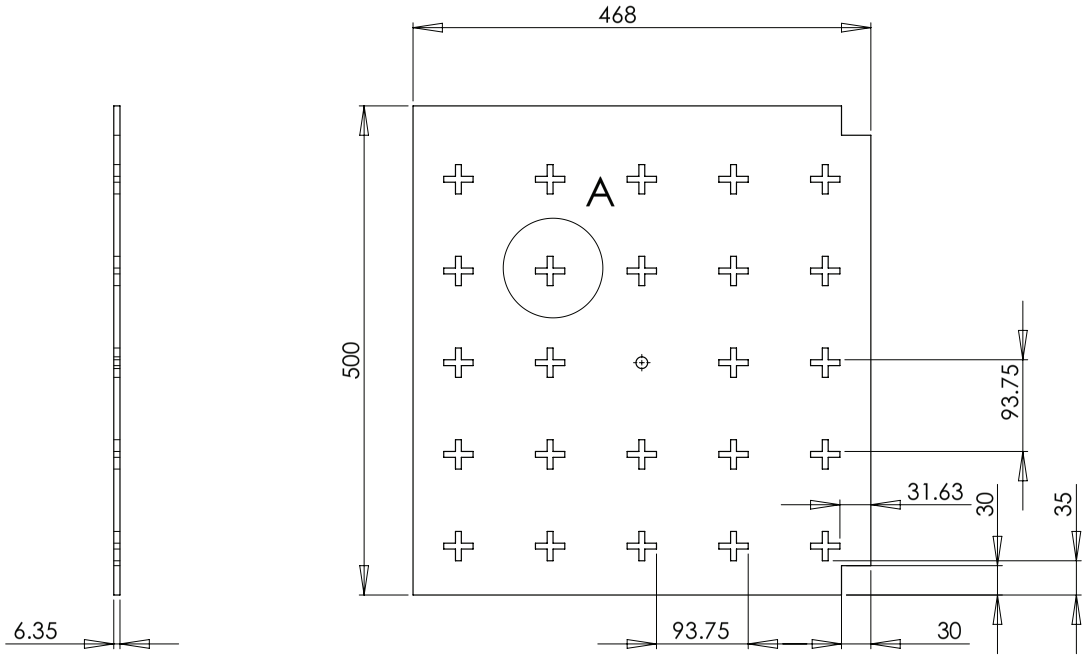


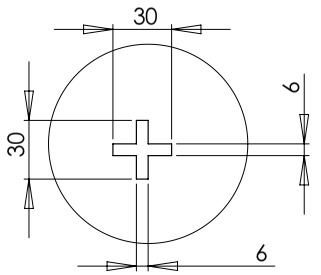


DETAIL A
SCALE 2 : 5



UNLESS OTHERWISE SPECIFIED:
DIMENSIONS ARE IN mm
TOLERANCES:
x = ± 0.75
x.x = ± 0.25
x.xx = ± 0.13
x.xxx = ±0.01
ANGULAR
x = ± 1 DEG.
x.x = ± 0.5 DEG.
MATERIAL
STOCK
FINISH

| | NAME | DATE |
|---|---|---|
| MODEL | | 3/27/2009 |
| DRAWING | J.G. GILLHAM | 8/9/2011 |

COMMENTS:

2G Robotics Inc.
2-614 Colby Dr., Waterloo ON. Canada, N2V 1A2

TITLE:

| SIZE | DWG. NO. | REV |
|---|---|---|
| B | Bottom Pattern Plate | A1 |

SHEET 1 OF 1

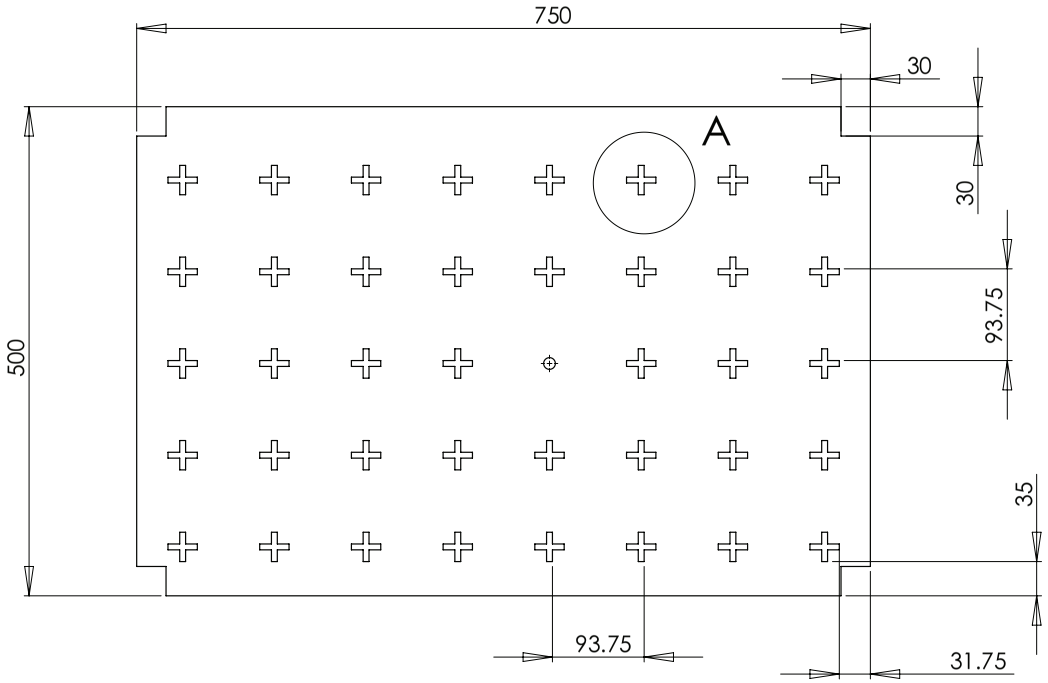


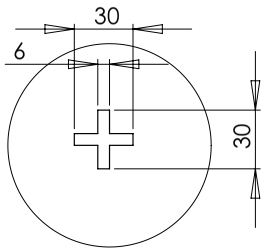


DETAIL A
SCALE 2 : 5

104



UNLESS OTHERWISE SPECIFIED:
DIMENSIONS ARE IN mm

TOLERANCES:
x = ± 0.75
x.x = ± 0.25
x.xx = ± 0.13
x.xxx = ±0.01

ANGULAR
x = ± 1 DEG.
x.x = ± 0.5 DEG.

MATERIAL

STOCK

FINISH

| | NAME | DATE |
|---|---|---|
| MODEL | | 3/27/2009 |
| DRAWING | J.G. GILLHAM | 8/9/2011 |

COMMENTS:

2G Robotics Inc.
2-614 Colby Dr., Waterloo ON. Canada, N2V 1A2

TITLE:

| SIZE | DWG. NO. | REV |
|---|---|---|
| B | Side Pattern Plate | A1 |

SHEET 1 OF 1

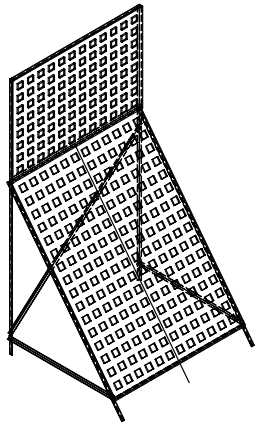

VIEW A

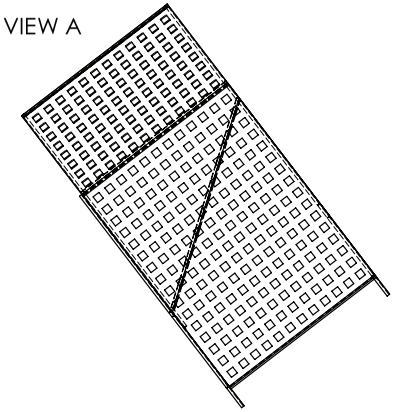

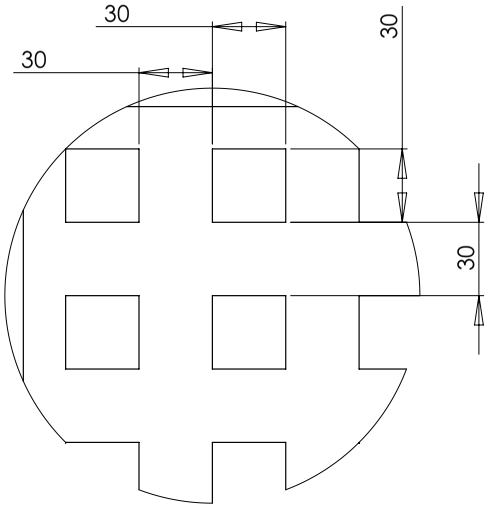


DETAIL B
SCALE 1 : 2

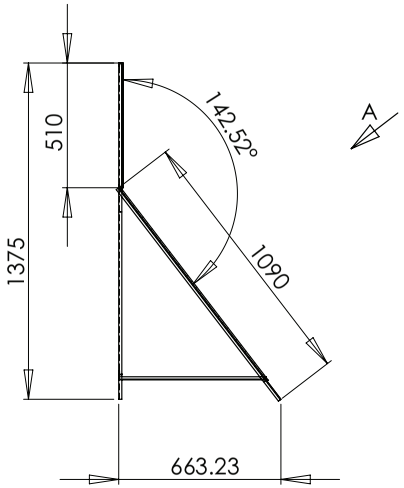


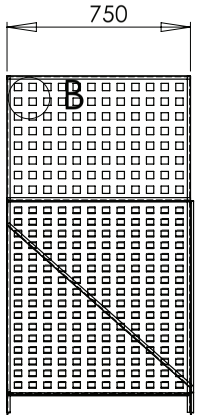


105

| | | |
|---|---|---|
| UNLESS OTHERWISE SPECIFIED: | | |
| DIMENSIONS ARE IN mm | | |
| TOLERANCES:<br>x = ± 0.75<br>x.x = ± 0.25<br>x.xx = ± 0.13<br>x.xxx = ±0.01 | | |
| ANGULAR<br>x = ± 1 DEG.<br>x.x = ± 0.5 DEG. | | |
| MATERIAL | | |
| STOCK | | |
| FINISH | | |

| | NAME | DATE |
|---|---|---|
| MODEL | | 8/9/2011 |
| DRAWING | J.G. GILLHAM | 8/9/2011 |

COMMENTS:



2G Robotics Inc.
2-614 Colby Dr., Waterloo ON. Canada, N2V 1A2

TITLE:

| SIZE | DWG. NO. | REV |
|---|---|---|
| B | Testing Rig | A1 |
| | | SHEET 1 OF 1 |

# Appendix D

# Underwater Laser Scanner Specifications Sheet

## Scan Specifications

Adjustable Step Size (0.018 degree minimum step size)
Adjustable Sector Scan (170degree maximum range)
Measurement Range: 0.1m minimum, 1m ideal, 3m maximum
Scan Swath Angle: 50 degrees in water
Swath Resolution: 0.104 degrees per sample

## Mechanical

Body: Anodized Aluminium Housing
Depth Rating: 350m
Weight: 0.9kg in water

## Electrical

Power: 12VDC to 24VDC, 1A max
Telemetry: RS-232 or RS-485